THE UNIVERSITY OF MANITOBA

Ultrastructure and Morphogenesis of the Female Accessory Gland in the insect Rhodnius prolixus

by

Donald Lococo

A Thesis

Submitted to the Faculty of Graduate Studies

in Partial Fulfillment of the Requirements for the Degree

of Master of Science

Department of Zoology

Winnipeg, Manitoba

July, 1979

Ultrastructure and Morphogenesis of the Female Accessory Gland in the insect *Rhodnius prolixus*

BY

DONALD JOSEPH LOCOCO

A dissertation submitted to the Faculty of Graduate Studies of the University of Manitoba in partial fulfillment of the requirements of the degree of

MASTER OF SCIENCE

TABLE OF CONTENTS

ABSTRACT

The cement gland of Rhodnius prolixus is an epidermally derived tubular gland consisting of a distal synthetic region and a proximal muscular duct region. The synthetic region consists of numerous secretory units joined to a central chitinous duct via cuticular ductules. Proteinaceous secretion, synthesized by the goblet-shaped secretory cell, passes through the delicate cuticular lattice of a ductule-end apparatus and out through the delicate cuticular lattice of a ductule-end apparatus and out through fine ductules to the central duct. Secretory cells are rich in rough endoplasmic reticulum and mitochondria. Light microscopy, SEM and TEM reveal the delicate lattice-like end apparatus structure, its formation and relationship to the secretory cell. The secretory cell associates via septate junctions with a tubular ductule cell that encloses a cuticle-lined ductule by forming an elaborate septate junction with itself. The ductules are continuous with the cuticle lining of the large central duct that conveys secretion to the proximal area.

The proximal muscular duct has a corrugated cuticular lining, a thin epithelium rich in microtubules and thick longitudinal, striated muscles which contract during oviposition, forcing the secretion out. Histochemistry and electrophoresis reveal the secretion as proteinaceous, consisting of three components with basic isoelectric points.

The complex adult cement gland differentiates from a simple epithelial tube in the unfed fifth instar. A blood meal initiates rapid proliferative cell divisions characterized by a spindle-oriented parallel to the gland's long axis. A 90^{o} rotation of the spindle gives rise to differentiative divisions that result in morphogenetic events producing ductules and presumptive gland cells. Morphogenesis differs significantly from other insect glands in the lack of a ciliary structure associated with the formation of the secretory unit and ductules. The morphogenesis of the adult secretory unit involves a complex interaction of cells requiring changing contacts and shape. The secretory cell and end apparatus develop from a double cell unit at the base of the elongating ductules. The inner cell produces the end apparatus and then undergoes autolysis while the outer becomes the adult secretory cell. The cellular changes during the differentiation of the ductules and secretory cell unit were determined by electron microscopic analysis.

Cuticulin and inner epicuticle are deposited in the ductules. The end apparatus is constructed of inner epicuticle, deposited at the tips of polygonally arranged microvilli. The main duct, in addition to cuticulin and epicuticle, has a thick endocuticle. When the end apparatus synthetic cell degenerates, the adult gland structure is complete.

ACKNOWLEDGMENTS

I wish to thank several people that have given me enormous help in my research and writing of this thesis, but I am incapable of it. Words are insufficient to express my gratitude. But since hugs and kisses are not easily translated into writing, I will compromise.

Thanks, to Dr. Erwin Huebner, for extreme patience and enthusiastic encouragement during my invasion of his lab, where I learned much, about science, as well as pain, suffering, agony, and how to gnash one's teeth, all by-products of electron microscopy. In addition, I aquired a genuine joy of discovery through close association with him, that I hope to always retain.

Thanks to Douglas Lutz, for a myriad of discussions; technical, intellectual, and silly, as well as great assistance in many exacting and extremely mundane preparations that would drive any sensible person to the brink of insanity.

Thanks to Diane Hill, for her extremely rapid typing of the thesis under less than ideal conditions, and Jody Hill, for various excretory and auditory contributions.

Thanks to Dr. J. Jamieson, for use of his lab and equipment for running cellulose acetate and polyacrylamide gel electrophoresis. and especially to Michael Woloski, for his amazing technical help with the gels.

Thanks to Ann Ismond, for use of equipment, materials and assistance in doing the isoelectric focusing.

Thanks to Bert Luit, for operating the scanning EM and taking the excellent micrographs, and to Dr. B. Dronzek for the use of the facillities.

Thanks to Wolf Heck, for copying the finished thesis plates, and expert photographic advice.

Thanks to Dr. C. Braekevelt and Dr. T. Weins for excellent critical evaluation of the thesis, and mercifully short oral exam.

Thanks to J. Douglas Prest, for help in proof reading the thesis, and his incredible loyalty and friendship.

Thanks to my mother Rose Lococo, for covering the typing fees, and for constant love and encouragment.

I would like to acknowledge financial assistance from a Sigma Xi, Grant-in-Aid of research and NSERC research grant to Dr. E Huebner.

Special thanks to Merlin, who occasionally left his wizard's hat and staff behind. They came in handy.

INTRODUCTION

The morphology of cells and tissues that comprise an organ is often an excellent indicator of function. Generally, secretion is a fundamental biological function occurring to some degree, in most cell types. However, functional specialization invariably results in cells accentuating some of their morphology to enhance one function over another, thus creating not only special cell types, but also organs specialized for specific functions. Invariably, this involves complex morphological and functional integration of cell communities, specialized for secretion production and extracellular release, with others functioning in secretion modification and conduction along a transport route.

The elegant studies of Palade and co-workers on the vertebrate exocrine pancreas, have demonstrated the importance of the study of secretory systems in providing insight into fundamental aspects of cell biology. Their investigations of protein synthesis, packaging, and transport depended, in part, on the judicious selection of an appropriate experimental system.

Insects are evolutionarily the most successful of all organisms. Evolutionary diversity has resulted in a myriad of highly advanced organisms with countless internal and external morphological specializations linked to special behavioural, ecological and physiological functions. Thus, besides being interesting in their own right for medical, economic, artistic and other reasons, the insects provide an enormous wealth of exploitable experimental systems for elucidating fundamental

biological problems. Basic biological advances such as the first microscopic descriptions of striated muscle (Altmann, 1890; Veratti, 1902; from Smith, 1972), early investigations on sensory physiology by Roeder,von Frisch and Dethier, the first descriptions of the segregation of primordial germ cells by Weismann and Metschinkoff, early investigations of spermatogenesis (see Wilson, 1928), and more recently, the first study on the mechanics and ultrastructure of pinocytosis (Anderson, 1964; Roth and Porter, 1964), the first description of nuclear extrusion (Anderson and Beams, 1956), ion regulation in Malpighian tubules (Berridge and Oschman, 1969) and others have come from the selection and experimental exploitation of insect tissues. Advances over the past thirty years in our understanding of physiological controls in insects now makes it possible to more readily determine structure-function correlates, as well as their modulations.

The development of a variety of secretory glands for highly varied functions has occurred in insects. Secretion phenomena play roles in communication, defence, anticoagulation, digestion, hormone production and reproduction. Many of the secretory glands are epithelial structures and, more specifically, often epidermal derivatives. Although current literature has merely begun to describe the great diversity of insect glands, certain similarities in general cellular organization are seen (Mercer and Brunet, 1959; Stein, 1967; Happ, 1968; Berry, 1968; Noirot and Quennedey, 1974). However, the interesting and important aspect is that structural specializations possible within a

relatively simple basic framework have permitted a broad diversity of function.

The female accessory glands comprise a general category, clearly exemplifying a broad functional diversity. In many insects, these glands produce a secretion which sticks the oviposited eggs to a substrate. Such a function exists in species from Hemiptera, Neuroptera, Lepidoptera and Hymenoptera (Galliard, 1935; Berry, 1968; Barbier, 1974; Adiyodi and Adiyodi, 1975). A functional variation occurs in Dictyoptera, where the eggs are retained in the vagina and enclosed within an ootheca produced by the accessory glands (Stay and Roth, 1962). Mantid accessory glands produce a frothy secretion that hardens, forming a protective sheath encasing the eggs. The Acridiids produce a similar frothy secretion that forms a protective plug, sealing the buried eggs from the air (Wigglesworth, 1972).

Functional modifications in the accessory glands of some insects result in remote functional specializations. Glossina accessory glands produce a secretion that is released to feed intrauterine larva (Buxton, 1955; Tobe et al., 1973). In some Hymenopterans (Pompilids and Sphecids), the accessory glands are modified into poison glands (Wigglesworth, 1972). The alkaline or Dufour's gland of bees are accessory glands which produce a natural polyester from macrocyclic lactones, used as a waterproof lining of brood cells (Hefetz et al., 1979). However, accessory glands, in most insects, are in some way involved in reproduction.

Female accessory glands are useful for study because the adult gland synthesis, and secretion functions in concert with ovarian and ovulation events. Thus they are presumably directly or indirectly under similar physiological control, thereby facilitating the correlation of timing and functional changes with morphological changes. As will become evident in the text, even with these correlations, understanding of the complex, fully differentiated adult tissue is more fully realized by analysis of the development of the component cells and their interrelationships. The nature of insect life cycles makes the developmental analysis of differentiation experimentally attractive.

Insect life cycles consist of hormonally regulated sequential intermolt, apolysis and molt stages. In the paurometabolous insects such as Rhodnius prolixus and Oncopeltus faciatus, this involves a gradual development through a series of juvenile molts, superficially resembling the adult (Wigglesworth, 1972). Early molts characteristically involve, primarily, body growth, and the slow development of presumptive adult organs such as the functioning reproductive tract, in early primordial phases. Altered hormone titres, initiating the final molt, trigger differentiative events, resulting in adult morphology. Thus, with knowledge of the environmental or nutritional cues necessary to initiate the neuroendocrine trigger, it is possible to precisely time and analyse the activation and progression of differentiation.

Rhodnius prolixus is an ideal species for analysis of accessory gland structure and differentiation, because of the wealth of background physiological information. Normal adult reproductive processes are triggered by a blood meal that is known to activate the release of the gonadotropin, juvenile hormone (JH), from the corpus allatum (Wigglesworth, 1972; Pratt and Davey, 1972). Furthermore, each life cycle molt is initiated by a single blood meal. Differentiation events in the final molt are linked to a molt activation in the presence of an inactive corpus allatum, and hence presumably a low JH level (as opposed to earlier molts, when the corpus allatum was active). Thus, the timing of cellular events is possible.

The value of the Rhodnius system was recognized in the 1930's by V.B. Wigglesworth, who provided some of the classic evidence for corpus allatum control of ovarian function and adult differentiation. Galliard (1935) did a comparative study of the reproductive physiology of various reduviids including Rhodnius and presented some preliminary histological data (elaborated below) on the female accessory gland.

Along with these life cycle and physiological advantages, although small in size, the accessory glands can easily be dissected in total, and are suitable for analysis by a variety of techniques including light microscopy, transmission and scanning electron microscopy, and various electrophoretic techniques. Summarizing the results of investigators that have utilized these techniques on insect glands in the past fifteen years allows one to review the functional morphology of accessory glands.

The secretion of accessory glands is produced in a highly complex organ system, involving cellular components specialized for the production of the secretion and a cuticular component, that acts as a conduit system, relaying the secretion out. The interaction of the secretory cells and the cuticular ductule system, as well as supporting cells, defines a highly complicated three-dimensional cytoarchitecture (Berry, 1968; Barbier, 1974). The adult structure of accessory glands is the result of complex cell-division patterns, coupled with intricate cellular morphogenetic movements of a simple epithelium lining the tubular accessory gland during the last juvenile stadium (Johnson and Berry, 1977; Happ and Happ, 1977).

Using light microscopic methods of limited resolution, Galliard's (1935) early study revealed the Rhodnius accessory gland as a cylindrical, blind ending tube, with two regions, a shorter duct region and a longer gland region. Enclosed by a basal lamina, they contain a great number of gland cells, with a large, centrally located vesicle, that stains violet with Mallory's stain. A ductule leaves each gland cell, travels in a meandering fashion and attaches to the central duct cuticle. The ductule originates in the form of a funnel, in a central zone within the vesicle, that stains a lighter violet. The ductule dilates as it leaves the gland cell, then takes on a narrower calibre. The duct region of the gland is lined by a ribbed cuticle that is lined by a thin epithelium and a layer of longitudinal muscle bundles.

My work re-examines the accessory gland, with the aid of a broad range of modern light and electron microscopic techniques, in order to clarify and clearly determine the cellular composition, organization and interaction present in the adult gland, as well as determining the differentiation of these structures. My results show the adult cement gland to consist of numerous secretory units, made up of a flask-shaped cell, enveloping a central reservoir. Within this reservoir is a cuticular end apparatus, connected to a cuticular ductule. This ductule is surrounded by a cell that accompanies it to its insertion at the central cuticular duct. This central lumen, which is continuous with the lumens of the ductules and ultimately the reservoirs, is surrounded by a squamous epithelium. These cellular and cuticular components interact in a highly complex fashion, by various cell junctions and connective tissue elements, revealing a structure well suited to the synthesis and mobilization of a secretory product. The secretion produced by this gland is an adhesive protein, which adheres the oviposited eggs to the substrate.

During the 5th instar, the cement gland increases greatly in size and undergoes a complex cellular reconstruction. The initial simple epithelial cells divide and undergo complex elongation and shape changes, forming ductules and gland cells. Cuticulogenesis gives rise to the cuticular duct, ductules and end apparati present in adult glands.

The complex restructuring of the cellular components is traced in a sequential fashion throughout the 5th instar and a detailed study of the adult ultrastructure is made, as well as

preliminary electrophoretic analysis of the adult secretion.

MATERIALS AND METHODS

Rearing Methods

Rhodnius were maintained in a Controlled Environments incubator at 26°C and a relative humidity of 70%, in constant darkness. Approximately 20 adults were housed in 9 cm diameter glass jars. Fluted chromatography paper provided a substrate for egg laying and absorption of excretory material.

After oviposition, the papers were removed and placed in empty jars in order to keep the larval instars separate from the adults. The fifth instars were separated into males and females prior to use in experiments and fixations.

Feeding

The colony was maintained by periodic blood feeding on rabbits. The rabbits were strapped down on their backs, held in place by a heavy fabric strip with holes cut in it for their legs. Wire mesh topped jars were placed on the shaven abdomens of the rabbits and the insects allowed to feed for approximately 10-15 minutes.

Enough fifth instars were fed each time to maintain the breeding colony. The rest were accumulated unfed. All fifth instars used in this study were left no longer than two months in the unfed state before they were fed for experimental purposes, to ensure a uniformity of nutritional state.

Dissection Techniques

The cement glands were dissected out by removing the dorsal cuticle, flooding the abdomen with saline, or fixative, removing the gut and exposing the cement gland. The gland was then removed either by grasping it with fine forceps at its junction at the ovipositor, or by cutting at the same location with iris scissors. To prevent distortion of the gland structure, all transfers were made in saline.

At first, all dissections for non-fixation use were done under Yeager's Ringer's. This medium caused the delicate basal lining of the gland to burst and spill the gland contents into the medium. Cockroach Heart Ringer's proved a better saline for routine dissections.

To assess the change in fifth instar development, glands were removed at 8:00 - 9:00 a.m. from unfed animals, at day 2 and every second day to day 8 and daily after that to day 21. The adult molt usually took place between day 20 and day 22, with most occurring by day 21. Adult glands were taken from unfed animals, and various times after feed as described in the text.

Microscopy

Live Preparations

Cement glands were dissected under saline, placed on a microscope slide, and covered with a coverslip supported on the four corners by drops of vaseline, in order not to distort

the actual dimensions of the gland. The preparations were viewed with a Zeiss Photomicroscope II using Nomarski differential interference contrast and polarizing optics.

Tissue Preparations

For both light and electron microscopy, the glands were prefixed in a modification of Karnovsky's (1965) fixative containing 3% gluteraldehyde, 1% paraformaldehyde in 0.1 M sodium cacodylate buffer, plus 0.05% CaCl, pH 7.2. The tissue was prefixed for 1.5 hours (in the cold for the first 0.5 hour, allowed to come to room temperature for the second and returned to the cold for the third). Alternatively, some glands were prefixed with a microtubule fixative, (Luftig et al., 1977) containing 5% glutaraldehyde in 100 mM piperazine - N,N' - bis (2 ethane sulfonic acid) (PIPES) buffer, containing 1 mM $MgSO_4$, 2 mM ethylene glycol bis (aminoethylether) - N,N' - tetracetic acid (EGTS), 1 mM GTP at pH 6.9.

Subsequently, the tissues were washed for 0.5 - 1 hour in 0.1 M sodium cacodylate or 0.1 M PIPES buffer and post-fixed in 1% osmium tetroxide in 0.1 M sodium phosphate or 0.1 M sodium cacodylate. Since Maupin-Zamier and Pollard (1978) have shown that osmium destroys purified actin filaments, post-fixation time was reduced to 0.5 hour. The resulting inferior fixation quality prompted a return to 1 hour post-fixations. Rapid dehydration was done at $0^{\circ}C$ in a graded (70-100%) ethanol series. Once at 100% ethanol, they were allowed to come to room temperature. Four more 0.5 hour

changes of room temperature 100% ethanol were made. After a change to propylene oxide - alcohol (1:1) and three changes of propylene oxide, the tissue was infiltrated in a 1:1 mixture of propylene oxide and epoxy resin. The plastic used was a mixture of Epon 812, Araldite 502 and dodecenyl succinic anhydride (DDSA) in proportion of 2.5:2:6 respectively (Anderson and Ellis, 1965), with 3-4% tridimethyldiethylphenol (DMP 30). The propylene oxide/epoxy mixture was left open in a fume hood 24-36 hours to allow the propylene oxide to evaporate. The tissue was then embedded in flat molds in a fresh embedding medium.

Light Microscopy

Semi-thin (1 μm) light microscopy sections were cut on glass knives using a Sorval MT2B Ultratome, and stained with 0.1% toluidine blue in 0.1% sodium borate.

Histochemistry

To determine some of the chemical properties of the adult gland secretion, light histochemistry was done on glands fixed either in buffered formalin for three hours or Carnoy's fixative for three hours (Humason, 1972). The tissues were washed and dehydrated in a series of ethanol (50-100%), cleared in toluene, infiltrated and embedded in Tissue Prep[1] paraffin embedding medium (MP 61°F). The blocks were trimmed with a razor blade, and sectioned on a Leitz rotary microtome.

1 Fisher Scientific Co., Cat. No. T-610.

PAS Technique

Deparaffinized sections were treated with periodic acid for 5 minutes, washed in running water for 5 minutes, and treated with Schiff's reagent for 10 minutes. After transfer through three changes of 0.5% sodium metabisulfide solutions, the slides were washed in water, dehydrated, cleared and mounted in Histoclad[2] (Humason, 1972).

Nile Blue

Deparaffinized sections were stained in 0.5% Nile Blue A in 1% sulfuric acid for 20 minutes, washed in running water and mounted in glycerine (Humason, 1972).

Millon's Reaction

Deparaffinized sections were incubated in solution A (5% mercuric acetate in a 15% solution of trichloracetic acid) for 10 minutes and then transferred to solution B (sodium nitrite, 1% aq.). They were then dehydrated, cleared and mounted (Humason, 1972).

The Millon reaction was also tried on plastic sections that were de-eponized with alcoholic sodium hydroxide (Lane and Europa, 1965). The sections were then processed as above. Coomassie Brilliant Blue and Analine Blue-Black.

Some Epon sections were stained in 1% Analine Blue-Black in 7% acetic acid for 4-5 hours at 60°C and other sections in Coomassie Brilliant Blue 0.25% in 7% acetic acid at 60°C for 4-5 hours. Subsequently, the slides were dipped in 7% acetic acid, rinsed and air dried. The technique was also performed

2 Clay Adams No. A-1399 (3921).

on deparaffinized sections, except that the staining time was reduced to 10-15 minutes, and the slides were processed for mounting in Histoclad.

Electrophoresis

To support and verify the light microscopy histochemistry, some preliminary electrophoresis was performed as follows. Glands, taken from adult virgin females in both the unfed state and animals seven days after feeding, were dissected in a barbiturate buffer containing 8.3 mM dimethyl-barbituric acid and 41.6 mM sodium diethylbarbiturate at pH 8.6. Upon dissection, the glands were transferred to 3 ml cone-bottomed plastic vials containing 0.2 ml of buffer, sonicated in a Megason Sonic Disintegrator with a micro probe, transferred to 3 ml centrifuge tubes and centrifuged to remove insoluble substances from suspension.

Initially, electrophoresis of the contents of 20 glands was done on cellulose acetate strips (Cellogel, 5.5 cm/13.5 cm). The full 0.2 ml of the sample was applied to the centre of the gel in a 4 cm strip. The gels were run for 5 hours at 25 mA, on a COLAB electrophoresis chamber with a Heathkit Regulated H.V. Power Supply, and stained in saturated Napthalene Black 10B. They were de-stained in a solution containing methanol, water and acetic acid in proportion 55:35:7, examined and photographed.

On the basis of results from Cellogel runs, it was felt that a more detailed examination of the secretion was needed. Therefore, the gland preparations were run in 5 and 7.5% polyacrylamide for two hours at 4 mH/gel (Davis, 1964). The running buffer used contained 0.118 M glycine and 0.188 M Tris. Gels were run on a Bio-Rad Gel Electrophoresis Cell (Hoefler Scientific) with a Heathkit Regulated H.V. Power Supply.

The gels were stained using a double staining procedure. The gels are stained overnight in 0.03% Coomasse Brilliant Blue in 18% acetic acid and 25% isopropanol, and then stained in 0.0025% Coomasse Brilliant Blue in 10% acetic acid in 10% isopropanol for 4-6 hours. The gels were de-stained in 10% acetic acid in 10% isopropanol.

The 5% polyacrylamide gels were run with 0.1 ml of the buffer soluble extract of 30 glands from mated females and from day 17 fifth instars at 2 mA/gel for two hours and stained as above. The 7.5% polyacrylamide gels were scanned with a Gelman DCD-16 scanning desitomiter. The 5% gels were viewed and photographed.

For a more precise separation of the protein components of day 7 fed mated adult and day 17 fifth instar glands, isoelectric focussing was done on the buffer soluble extracts. Thirty cement glands of each type were dissected under barbiturate buffer and stored in 0.1 ml of the same buffer. The sample was run on a half 2.4% (W/V) ampholine 5% polyacrylamide gel (PAG) plate with a range of pH 3.5 - 9.6 on an LKB 2117 Multiphor chamber with a cooling plate. The

procedure was as follows. A grid was placed on the cooling stage on a thin kerosene film. The PAG plate was placed over it on a film of kerosene. Paper electrode strips were cut to fit the plate. The cathode electrode solution was 1M NaOH and the anode solution was 1M H_3PO_4, which was soaked into the electrodes. The samples were placed on the gel and run on an Electrophosis ISCO power unit, starting at 155 volts, increasing at increments every 5 minutes for a total of 90 minutes, reaching a final voltage of 485 volts. The gel was electro-focussed and run at 485 volts for another 0.5 hours. The gels were stained with the same stain used for polyacrylamide, except stain A was removed after 2 hours and stain B was not used.

Electron Microscopy

Thin transmission microscopy sections were cut on Sorval MT2B or Reihert UM1 ultramicrotomes. Sections were placed on naked 150, 300 or 400 mesh, or formvar-coated copper slot grids and stained in uranyl acetate for 30-45 minutes, and lead citrate for 1.5 minutes (Venable and Coggeshall, 1965), and viewed in AEI 6B and AEI 801S electron microscopes at 60 KV.

Cement glands were prepared for scanning EM using the same fixation and dehydration procedures used for TEM. Some glands were digested in a mixture of 1% EDTA and 5% trypsin in Ca+-free Roach ringers and then fixed (modified from Overton, 1977).

From 100% ethanol the specimens were placed in 2 changes of 100% acetone. The tissues were prepared for SEM using a Sorval Critical Point Dryer. Using acetone as the final solvent, liquid CO_2 was carefully bubbled into the chamber containing the specimens at 700-900 psi, 5 times to ensure complete substitution of the solvent. The chamber was brought to 1500 psi with warm water, and gradually lowered to atmospheric at 2-3 psi/second. The specimens were removed, mounted on stubs and gold-coated with a Balsers Sputter Coater. Specimens were viewed with a Cambridge Stereoscan scanning electron microscope. Micrographs of the prepared stubs were taken by Bert Luit, of areas and at appropriate magnifications, as directed.

Photomicrography

Light and scanning electron photo-micrographs were taken on Kodak Panatomic X135 film. The film was developed in Microdol X, in a 3:1 dilution with water, or Acufine developer and processed routinely.

Transmission electron micrographs were taken with either Kodak EM Image Film 4463 or Kodak Electron Microscope Film 4489 and routinely processed.

Routine photographic procedure, using a Besseler enlarger and an Ilford automatic print processor were performed and the final prints glossed on an Arkay rotary print dryer.

RESULTS

The Adult Cement Gland

Gross Anatomy

The cement gland of Rhodnius is a large tubular, epithelial structure located in the extreme posterior end of the abdominal cavity of the female (Fig. 1 and 2). It is approximately 9 mm long and consists of two morphologically distinct regions: the distal synthetic region (approximately 7 mm) and a proximal duct region (approximately 2 mm long) (Fig. 3 and 4). The extreme terminus of the gland is at the ovipositor, facilitating deposition of the secretion onto the eggs as they are laid. The gland folds back on itself in a random fashion that varies from individual to individual and almost always lies to the right of the midline, although its insertion is mid-dorsal.

The distal synthetic region varies in diameter from 120 μm at the tip, increasing to 150 μm near the transition to the duct region. A thin basal lamina (Fig. 7 and 8) surrounds it giving it a smooth surface, penetrated by few tracheoles as is evident in the scanning electron microscope (Fig. 19).

An abrupt transition occurs between the proximal and distal region as evident in the scanning electron micrographs and sections (Fig. 4, 44, 45, 46). At this transition, the gland narrows to 200 μm, decreasing to 34 μm at the terminus. The proximal region is surrounded by a layer of longitudinally

arranged muscle (Fig. 4), that contracts during oviposition, forcing the secretion out of the gland. The secretion coats the ventral egg surface as they are laid, firmly sticking them to the substrate.

Functional Morphology of the Adult Gland

Distal Secretory Region

Secretory Unit

The obvious anatomical differences between the two gland regions is reflected in their function and ultrastructure. The secretory part of the gland (Fig. 3) synthesizes and accumulates the stored secretion until it is transferred to the central duct and out during ovulation. The unique cellular components responsible for producing the secretion are clearly evident at the light microscope level.

Examination of the living gland with Nomarski interference (Fig. 5) reveals numerous globule-shaped secretory cells that are connected to a central lumen by long ductules. Each gland cell and its ductule is a separate gland unit and can be isolated either by teasing or freeze-drying the gland, fracturing it, followed by rehydration (Fig. 6 inset). The central lumen in the integrating structure acts to pool the secretion that is released into it. This section will focus, in detail, on each component of the synthetic region using various cytological techniques, beginning with the gland cell itself.

In sections of fixed embedded material, the gland cell units are arranged in a complex random fashion, sometimes closely opposed to each other, and sometimes with ductules between (Fig. 6, 21). Ultrastructurally, the intercellular space varies from fairly small to relatively large (Fig. 6, 21, 31).

The gland cell cytoplasm is thin yet extensive since it totally surrounds the large central extracellular reservoir. The reservoir is approximately 7 µm across when inactive and about 13 µm when active, while the cell cytoplasm is between 1 - 3 µm in thickness. Characteristically, the cytoplasm is rich in rough endoplasmic reticulum (RER), free ribosomes and mitochondria (Fig. 13 - 16). The abundance of RER and ribosomes is responsible for the highly basophilic nature of these cells in the light microscope (Fig. 13 and inset). In addition to the abundant protein synthetic components, there are some sparse Golgi, and a few dense multivesicular bodies (Fig. 16 and 18). These are probably autophagic in function, since they contain ribosomes. Microtubules are present only sparsely (Fig. 14). The nucleus is positioned randomly in the cytoplasm and can be either compressed or relatively ovoid shaped, containing one or two large nucleoli (Fig. 13 and 21). The outer plasmalemma is relatively smooth, with occasional interdigitations (Fig. 17), but adjacent to the inner reservoir, it has a few short microvilli with filamentous cores (Figs. 13, 14 and 17).

The prominent rough endoplasmic reticulum indicates that the gland cell secretory product must be highly proteinaceous. Histochemical analysis verifies this. Positive reactions for Analine Blue-Black and Coomassie Blue and negative reactions for PAS and Nile Blue sulfate suggest that the secretion is proteinaceous but not a glycoprotein, neutral lipid or a phospholipid. The negative Millon's reaction indicates that the secretion is not rich in tyrosine residues.

Simple experimental observations show that, if the gland is placed in buffer solution, and punctured so that the secretion spills out, it is easily soluble in the medium. However, if dried in air or freeze-dried, the solid form will not re-dissolve in either buffer, or distilled water. This property is consistent with a protein that changes its three dimensional conformation in the absence of water.

Preliminary electrophoresis runs with cellulose acetate (Cellogel), 5 and 7.5% polyacrylamide and isoelectric focussing also provide supporting evidence that the gland product is proteinaceous. Comparison of electrophoretic analysis of the barbiturate buffer-soluble contents of unfed virgin glands (containing no secretion) and glands 8 days post-feeding (rich in secretion) reveals band differences. In the cellulose acetate gels, a single band difference was observed between the two samples. In 7.5% polyacrylamide gels, approximately 70% of the sample did not migrate. Scans of the gels show that, of the two bands that migrated in the fed sample, one of them was not present in the unfed sample. A greater percentage of the

sample ran in the 5% gels, with only one essential band difference. The isoelectric focussing gels show a separation of over thirty bands. The one major band that migrated in both the cellulose acetate and the 5 and 7.5% polyacrylamide gels has an isoelectric point of 7.1. There are three prominent bands present in the sample containing secretion with isoelectric points of 9.2, 9.1 and 8.8, that are not present in the secretion-lacking sample. Other minor band differences may occur, but are only minor gland constituents and probably not part of the secretion.

In summary, the histochemistry and preliminary electrophoresis indicates the proteinaceous nature of the secretion. This secretion accumulates in the central extracellular reservoir as a dispersed flocculent material in fixed preparations (Fig. 13 - 16, 26 and 28). Suspended within the secretion-containing reservoir is a delicate cuticular lattice structure - the end apparatus (Fig. 9 - 12).

The End Apparatus

Scanning electron micrographs of glands with their cells removed by digestion provide a clear picture of the three-dimensional organization of the end apparatus and its association with the ductule system (Fig. 23 and 24). In partially digested preparations, where the basal lamina has been broken, one can also see that the secretory cells encapsulate the end apparatus within their central reservoir (Fig. 7 and 8).

The delicate lattice seen in the SEM is clearly visible as a strand network in the live preparation with Nomarski interference (Fig. 6 inset and 9 - 12), in thick sections (Fig. 21 and 25) and the TEM (Fig. 15 and 27). The integration of these various techniques permits us to provide the following overall interpretation of the organization and function of this unique structure.

The end apparatus is roughly spherical in configuration, being 6 µm in diameter, consisting of thin inner epicuticle that is attached to the end of the ductule. Figures 23 and 24 show that it is composed of slender cuticular strands, forming a complex spherical geometric lattice that attaches on one side to the collar of the ductule. In order for secretion to reach the ductule and central duct, it must first pass from the reservoir, through the lattice into the end apparatus. Thus the end apparatus functionally and structurally compartmentalizes the reservoir. The staining properties of the secretion change upon passing through the lattice (Fig. 21 and 25). Secretion within the end apparatus stains more intensely and is more condensed as the electron micrographs show (Fig. 27 and 28). This perhaps reflects an alteration in the physical or chemical properties of the secretion mediated by the presence of the end apparatus. This secretion modification results in a rod-like condensation beginning in a flame-like structure (Fig. 25) and continuing as a slender rod into the collar and the ductules draining each unit.

The secretory cell apex is closely attached, like a purse string, to the cuticle of the collar and to the cylindrical ductule cell, thereby enclosing the cuticular channel and preventing secretion from leaking into the extracellular space. The apical plasma membrane of the secretory cell is specialized to form a dense cytoplasmic filament meshwork at the region of cuticle contact (Fig. 27). Prominent regular septate junctions also ensure a seal and adherence to the ductule cell in this region. Consequently, secretion can only pass from the collar into the conduit created by the tubular ductule cell and its cuticular lining.

Ampulla and Ductule

The cuticular ductule consists of inner and outer epicuticle and an enveloping cell that attaches to itself by an extensive septate junction (Fig. 33, 34, and 36) as well as gap junctions and desmosomes (Fig. 36). The region close to the gland cell is enlarged creating the ampullary part; however most of the ductule is a slender tube (Fig. 25 and 26).

The ductule cell cytoplasm contains sparse mitochondria, little RER, some longitudinally arranged microtubules, Golgi and numerous free ribosomes. The plasma membrane adjacent to the cuticular duct has some short microvilli (Fig. 33). Cells of adjacent ductules are in contact with each other by cytoplasmic projections traversing large intercellular spaces (Fig. 31 and 32). Closely opposed ductule cells are sometimes joined together by septate junctions (Fig. 30 and 33).

A squamous layer of cells surrounds the cuticle of the central duct (Fig. 38). The entire length of membrane-membrane associations in this region is characterized by extensive septate junctions. Ductule cells penetrating this cell layer are also joined to the epithelium by septate junctions (Fig. 38). The cytoplasm of the epithelial cells is similar to that of the ductule cell, containing numerous free ribosomes but sparse RER, Golgi and mitochondria.

Extracellular Compartment

Much extracellular space is present between the various cellular components from the smooth basal lamina through to the central cuticular duct (Fig. 39). After gland discharge at oviposition, this space becomes more extensive. The light flocculent material in the intercellular space (Fig. 30, 32) is morphologically different from the flocculent secretion in the reservoirs (Fig. 35).

Secretory Route

Although the precise mechanism of secretion is unknown, the secretion, which accumulates in the reservoirs, passes down the cuticular ductule and eventually pools in the large central lumen of the gland. In section (Fig. 39 inset), it appears as a condensed core with staining properties similar to the secretion passing through the ampullae of the ductules. The secretion is sometimes lost when the gland is broken into pieces during the embedding procedure (Fig. 6). In the SEM (Fig. 39, 40, 41), the continuity of the thin strands of secretion, emerging from the ductules opening, with the large

secretion core in the central duct, is clearly evident. In the preparation procedure, the physical displacement and slight shrinkage of the central secretion has resulted in many of these strands breaking, leaving the central core with a prickly surface due to the severed contact. Microdissections of freeze-dried unfixed glands indicate that in the native state, the secretion entirely fills the lumen. The lumen diameter is about 41 μm, and with a length of 9 mm, the total volume is about 12 picoliters.

Thus, the secretory synthetic unit (Fig. 42) has a complex three-dimensional conformation comprised of a synthetic cell component, and a cuticular ductule surrounded by an enveloping cell. Secretion, produced in these units, pools in the central lumen for conveyance to the excretory region of the gland.

Excretory Region

There is an abrupt demarcation between the secretory distal and excretory proximal regions of the gland (Fig. 43, 44, 45). The proximal region differs dramatically in size, superficial appearance, cellular and cuticular constituents.

Superficially, the proximal area, although variable, is relatively short (2 mm), of overall smaller diameter (115 μm) and unlike the smooth surface of the distal gland, has a fibrous branching, irregular surface of prominent, roughly longitudinal striated muscles, tracheoles and connective tissue components. The abrupt nature of the transition and overall features are clearly seen in section (Fig. 44) and SEM (Fig. 4 and 45).

Although the cuticular lining is continuous with that of the central distal cuticular duct lining, it differs significantly in structure being highly corrugated in a spiral fashion (Fig. 45, 52, 54). The spiral cuticle corrugations run the full length of the proximal gland. The diameter of the duct is uniform (46 μm) along its length except near its insertion, where it narrows to 34 μm (Fig. 46). The metachromatic nature and abrupt change in staining properties with toluidine blue also suggests that significant chemical differences must exist between the cuticle of the two regions. The proximal cuticle stains metachromatically (purple) with toluidine blue, while the distal stains orthochromatically (blue).

Attached to the cuticular lining is the proximal epithelial lining responsible for secretion and maintenance of the cuticle as well as providing an anchoring interface for muscle attachment crucial to the overall gland secretion.

The epithelial layer is continuous along the full length of the proximal region (Fig. 44). The epithelium, superficially similar to that of the distal gland, consists of a layer of flattened cells with extensive lateral interdigitations connected by septate junctions along the full length of the membrane-membrane association (Fig. 51). The epithelial cytoplasm consists of a modest amount of mitochondria, little RER and numerous free ribosomes. The cells are strikingly rich in elaborate arrays of microtubules arranged in parallel bundles, occupying a large volume of the cytoplasm (Fig. 50), associated with large zonular desmosomes along the interface

between the epithelium and muscle layers. Such a vast amount of regularly arranged microtubules imparts a rigidness to the epithelial layer. This helps to anchor the muscle layer to the cuticle to give it a sturdy base upon which to act during contraction.

The muscle layer is approximately 36 μm thick and is invested with numerous tracheoles (Fig. 43, 47, 48). They penetrate between muscle bundles right up to the epithelial layer (Fig. 49). Ultrastructurally, the muscle is typical insect striated muscle, containing numerous mitochondria widely spaced between the numerous actin-myosin filament bundles (Fig. 49). The filaments arrange in a usual insect conformation with one myosin thick filament surrounded by 12 thin actin filaments (Fig. 49 inset).

The rich muscle supply, innervations, and tracheation coupled through the epithelium to the corrugated central cuticular duct, permit the shortening of the proximal area seen in KCl treated dissections and presumably the normal secretory expulsion triggered at oviposition.

Fifth Instar Differentiation

The highly unique, complex cytoarchitecture of the adult gland arises due to stage-specific differentiation from a pseudostratified epithelium. The following sequence of results outlines the stages and cellular changes that occur in the development from a simple, short, tubular pseudostratified gland

to the large complex structure described in the previous pages. These events occur in the fifth instar and are initiated by a blood meal. By preparing glands at various intervals outlined below, and detailed examination with dissections, live Nomarski preparations, light microscopy sections, and electron microscopy, the various major phases of differentiation were elucidated.

Roughly, the following results indicate major growth aspects, cellular elongations, specific differentiation processes, cuticulogenesis and end apparatus formation. For clarity and convenience, these are dealt with in a developmentally sequential fashion beginning with the unfed fifth instar gland.

Unfed Fifth Instar Cement Gland

The newly emerged fifth instar undifferentiated cement gland is a simple epithelial tube, 200 µm in length (Fig. 55 and 56). In thick section, it appears as a tubule with a central lumen, lined by a pseudostratified epithelium, surrounded by a thin basal lamina (Fig. 58 inset). A squamous layer of mesodermal cells surround the full length of the gland. No mitotic figures are present in the epithelium. In the TEM, the cells lining the tubule appear elongated, with their basal smooth plasmalemma on the basal lamina of the gland. Thrown into elaborate plasmalemmal folds, their apical membrane has an electron dense layer of material at the tips of the folds (Fig. 58 and 59). This material is perhaps a remnant of the larval cuticle all epidermal cells secrete. The lateral

membranes, in the apical third of the cells, are elaborately folded resulting in extensive interdigitation with adjacent cells (Fig. 58, 60, 61). The lateral membranes are joined at the lumen by regular zonular desmosomes (Fig. 59) and along the full length of the lateral interdigitating membranes by elaborate septate junctions (Fig. 60 and 61). Basally, from the nucleus to the basal lamina, no obvious junctions occur.

The cytoplasm of the day 0 epithelial cells contains numerous longitudinally arranged microtubules, free ribosomes, but sparse RER and few, if any, Golgi complexes. The nuclei are oval and contain a large single nucleolus with densely staining chromatin ringing the nuclear envelope.

Mitotic Stage

Feeding the fifth instar initiates differentiative events. Day 2 post-feed thick sections reveal numerous mitotic figures in various stages (Fig. 62). From feeding until approximately day 11, the spindles of the dividing cells orient parallel to the lumen of the gland (Fig. 63 and 71). Cell divisions during this phase result in an overall increase in the length and diameter of the gland and thus are proliferative divisions. Anchored at the lumen by desmosomes, cells retract from the basal lamina toward the lumen and take on a spherical shape adjacent to the lumen prior to cytokinesis (Fig. 67, 68 69). After nuclear division, the microtubular cytoskeleton reassembles and the cells begin to re-elongate (Fig. 71). Cytokinesis is not completed until the cells have almost fully elongated, towards the basal lamina.

These proliferative divisions occur throughout the initial growth phases resulting in the enlarged gland with primarily a thick pseudostratified epithelium, but little evidence of any differentiative events that foreshadow the adult gland morphology. However, by day 11 or 12, one begins to see evidence of tubular structures appearing. This heralds the beginning of the next developmental phase, namely ductule formation.

Ductule Formation

After day 11 or 12, the spindles of the dividing cells rotate 90^{o} and orient perpendicularly with the lumen (Fig. 74 and 75). This type of cell division is differentiative, because, in addition to an increase in cell number, the cells retract while undergoing complex three dimensional shape changes.

Since the spindle is perpendicular to the lumen in a differentiative division, the cell divides so that one of the daughter cells has its apical surface adjacent to the lumen while the other lies basal to it, thus differing significantly from the proliferative divisions (Fig. 75). The daughter cell adjacent to the lumen will be referred to as cell A and the other as cell B. TEM examination of various stages of cells, found enclosed within cells, over a developmental time course and their relationship to the differentiative mitosis indicate that ductule formation involves a sequence of cell shape change, elongation and cell associations as follows.

After cell division, the microtubular cytoskeleton of cell A reassembles, and starts to elongate toward the basal lamina. Unlike the proliferative division, cytokinesis is complete well before the cell has fully elongated. At this time, cell B also elongates. Cell A actually begins to invaginate into the apical part of cell B (Fig. 77 inset). Although initially anchored at the lumen by desmosomes (Fig. 75) as in proliferative divisions, cell A does not maintain this attachment here (Fig. 92 and 93). As cell A elongates, an adjacent cell (C), wraps itself around the apical end of A (Fig. 77, 84, 85). As cell A continues to elongate, it leaves behind a tubular space created by cell C (Fig. 77 and 92). Cell C continues to wrap around on itself, elongating the tubular space it creates (Fig. 85). Vesicles containing fibrous material form in cell C's cytoplasm and are probably released into the ductule. Cell A continues its elongation, invaginating into cell B, basal to it and is eventually completely enveloped by cell B except for long microvilli that extend apically into the forming ductule (Fig. 85). Cells A and B further elongate as a unit while cell C continues to envelop the space left by the retracting pair (Fig. 86). This results in an elongating ductule attached basally to a double cell unit with microvilli partially extending up the lumen.

When cell C wraps around, it initially adheres to itself by a desmosome (Fig. 89 and 95), but, in a later stage, at the start of cuticulegenesis, an extensive septate junction forms, adhering the cell to itself (Fig. 96). Thus, initially, the area of adherence is small, but, at the time that septate

junctions appear, the area of adherence increases.

Another cell (D) is less intimately associated with the forming ductules. Cell D is an elongated electron lucid pillar-like cell found parallel to the ductule cells either singly or in clusters of two or three (Fig. 88 and 90). Its cytoplasm contains numerous widely spaced, longitudinally arranged microtubules, mitochondria, and an electron light cytoplasm containing few ribosomes (Fig. 91). This contrasts with cell C which contains a greater number of longitudinal microtubules, numerous free ribosomes and polysomes, RER, Golgi and a darker staining cytoplasm. The position of the nucleus varies, but is often situated at the basal end of the cell (Fig. 88). The microtubules give rigid support to these cells and perhaps function in providing a geometric, cellular, girder-like support system from the lumen to the basal lamina as support for the elongating, differentiating glandular constituents.

Reservoir Formation

By day 14, the two cells (A and B) responsible for the formation of the ductule, cease their elongation. Cell C completes a tubular shape, while cells B and A round up, and attach at the end of cell C by a desmosome that rings the ductule and septate junctions over the rest of the area of contact between cells B and C (Fig. 191). Cell A is entirely enclosed by cell B so that it has lost contact with the ductule

(Fig. 101 and 102). The lumen of the ductule is continuous with a flask-shaped space created by the attachment of cells A and B to cell C (Fig. 101 and 102). Cell A connects to cell B by desmosomes adjacent to the lumen, and over the remaining contact area by septate junctions, except the basal region where no junctions exist.

The change in cell shape and cell association that has resulted in the ductule attached to the "cell within a cell" unit, resulting in a ductule lumen continuous with the small cavity (reservoir) within the presumptive secretory unit, is clearly seen in both live (Fig. 98) and fixed preparations. This phenomenon indicates the start of the next complex developmental phase involving cuticulogenesis, gland cell reservoir differentiation and end apparatus development.

Cuticulogenesis - Ductule, Ampulla and Gland Cell-End Apparatus Development

When cells A, B and C have finished their morphologic movements, the microtubules of cells A and B arrange circumferentially around the central reservoir, presumably maintaining the spherical shape (Fig. 104). Microvilli extend from the lumenal surface of both cells A and C, and vesicles in their cytoplasms release fibrous material into the ductule. While end apparatus and related differentiation, as outlined before, proceed, ductule differentiation continues with both ductule differentiation and end apparatus formation intimately

associated with cuticulogenesis. The ductule calibre fluctuates before reaching their final diameter. Initially, during their formation near the lumen, ductules are 555 nm in diameter (Fig. 95). When the ductule cell has completely formed the ductule (day 14, Fig. 96), it is 570 nm in diameter.

Between day 15 and 16, the ductule cells secrete a thin outer epicuticular lining comprised of cuticulin (Fig. 96 and 125). As it is laid down, the final ductule diameter is variable but averages at 730 nm. Some regional variation is present. At cuticulogenesis, the ductule nearest the reservoir dilates in volume, and will be referred to as the ampulla (Fig. 97 and 102). In cross section, the shape of the ampulla varies from semi-circular (Fig. 97) to irregular (Fig. 128). The mouth of the ampulla narrows abruptly to 200 nm, giving it a flame-like appearance (Fig. 103 and 109). This narrow region that is bordered by cell B (Fig. 102) shall be referred to as the collar.

When the cuticulin layer is complete it lines the ductules, the apical reservoir and the gland lumen (Fig. 108, 109, 133, 134). The region of epicuticle that extends into the reservoir (Fig. 108) shall be referred to as the reservoir funnel. Thus, the ductule cell (C) lays down outer epicuticle in the ductule, cell B lays it down in the collar, and cell A lays it down in the reservoir (Fig. 107). Once cell A has completed outer epicuticular deposition, it draws away from the reservoir ductule in an apical direction (Fig. 108).

Once a thin layer of cuticulin is complete in the ductule and central gland duct, a layer of inner epicuticle is deposited in these regions. Simultaneously, cell A, which lines the developing reservoir, continuous with the ampulla, accumulates localized patches of epicuticle on the surface of membrane areas that are forming microvilli (Fig. 108). The cuticle is eventually intimately associated with the tips of the microvilli that characteristically have fibrous condensations (Fig. 109, 110, 111). The distribution of microvilli is not random, but rather in a polygonal fashion, thus forming a template for cuticle deposition in selected areas on the inner lumenal cell surface (Fig. 112). This results in the accumulation of struts of inner epicuticle that join together forming a delicate lattice suspended in the central lumen and attached to the collar. This lattice-like end apparatus is completed by day 18 or 19. The geometry of the structure is a mirror image of the cell surface microvillar pattern of cell A (Fig. 112).

Inner epicuticle deposition continues during this time in the ductules and ultimately reaches a thickness of 12 nm (Fig. 129 - 132). Cells (E) surrounding the lumen of the central duct stop secreting inner epicuticle once it reaches a thickness of 88 nm, and start to deposit a thick layer of endocuticle (Fig. 136 and 137). Thus cell E deposits endocuticle while ductules and A cells synthesize only inner epicuticle. Prior to endocuticle deposition, cells E and C were indistinguishable from each other by cytoplasmic constituents alone.

Cell E deposits a total of three layers of endocuticle around the lumen (Fig. 137 and 138). The first layer is a little less dense than the inner epicuticle and attains a thickness of 500 nm. The second layer is fibrous and reaches 150 nm. The laminated thick layer is less dense than the second, and is 350 nm thick.

The complex cell differentiation and various aspects of cuticulogenesis described above, has resulted in the central duct and epithelium, ductule ampulla cuticle and its enveloping cell, and the presumptive secretory complex with cell B surrounding cell A, that has synthesized the end apparatus. The adult morphology described earlier revealed only one cell, the secretory cell, surrounding the reservoir and end apparatus, thus leading to the question of the fate of cell A, once the end apparatus is formed.

Fate of cell A

Prior to inner epicuticle deposition, a basal extension of cell A penetrates through cell B and partially extrudes into the extracellular space beyond B (Fig. 112 - 115). Serial thin sections show that cell A passes through a hole in the dome of cell B while simultaneously drawing away from its contact with the collar. Presumably, cell A does this to increase its effective volume so that it can produce sufficient synthetic cyto-machinery and at the same time, can retain its thin profile within the developing reservoir. Thus cell A's cytoplasm becomes compartmentalized into the reservoir

cytoplasm, which remains enclosed within cell B, and the extra-reservoir cytoplasm, which extends into the extra-cellular space outside of cell B. When cell A begins to lay down the end apparatus (Fig. 113), its extra-reservoir cytoplasm is well endowed with organelles such as RER and Golgi. When microvilli become associated with epicuticle deposition of the end apparatus, the reservoir cytoplasm retains a comparatively low profile (Fig. 119). Thus, a functional compartmentalization occurs in cell A, with the majority of protein synthesis occurring in the extra-reservoir cytoplasm, while the reservoir part of the cell deposits the cuticle and mobilizes it to the tips of the microvilli (Fig. 115). The two regions of this cell are interconnected by the thin channel passing through the hole in cell B. Microtubules extend through this cytoplasmic channel, perhaps serving a cyto-skeletal role or function to direct the flow of materials between the two compartments (Fig. 114 and 115).

When cell A has completed the cuticular end apparatus, it is still seen in section. One hour after adult ecdysis, cell A appears as fragmented dark staining bodies within the reservoir (Fig. 116). The reservory cytoplasm breaks down, presumably due to lysosomal action, during the final day of larval life (Fig. 117). It is not known whether the extra-reservory cytoplasm is pinched off by cell B and breaks down or retracts back within the reservoir. This stage specific cell death thus results in the cellular reorganization characteristic of the adult gland unit, namely a single

synthetic cell surrounding the reservoir. By the time the adult gland is functional (after the first blood meal), no evidence of cell A remains. Cell B becomes the functional gland cell which elaborates its RER for the adult proteinaceous secretion.

The Fate of cells C and D

Cell D, the long columnar cell found among ductule cells (C cells) at the time of ductule formation, continue to associate with ductule cells throughout the fifth instar to the adult ecdysis (Fig. 124, 125, 127, 132). Cross and longitudinal sections show that they maintain a parallel array of microtubules with interspersed elongate mitochondria in their cytoplasm, but a paucity of other organelles.

During the course of inner epicuticulogenesis, large intercellular spaces develop between the ductule cells and columnar D cells (Fig. 132). These large spaces appear around the developing gland cells as well, and persist into the adult stage. Within the extracellular space occupied by C and D cells, occasionally some tracheoles invert, having penetrated the smooth basal lamina of the gland (Fig. 121 and 122). The ductule cells change shape from the fairly cylindrical shape they have around the time of cuticulin deposition, to an irregular form with long processes that extend across the intercellular space (Fig. 132). They maintain contact with neighboring ductules via these processes, while D cells maintain their columnar shape. No evidence for the column

shaped D cell is found in the adult cement gland. If they are present, they have taken on an irregular shape similar to ductule cells and are indistinguishable from cytoplasmic processes of ductule cells.

Secretory Activity of the Fifth Instar Gland

Throughout gland development, the central lumen contained a light flocculent material released in vesicles at the lumen cell surface (Fig. 94). Throughout ductule and reservoir formation this same material is released into these new structures (Fig. 109). At the outset of inner epicuticular deposition, a denser material appears in the ductules, the source of which appears to be the reservoir (Fig. 129). In thick sections, the material stains blue with toludine blue, unlike the adult secretion, which stains metachromatically violet (Fig. 118 and 119). It persists throughout the remainder of inner epicuticulogenesis,and main duct endocuticle deposition (Figs. 123, 136, 137), abruptly ceasing when these structures are complete (Fig. 132). Just prior to and immediately after adult ecdysis, no secretion is found in any of these structures (Fig. 135).

Development of the Proximal Region

Prior to the blood meal, the entire fifth instar cement gland is surrounded by a thin mesothelial cell layer. During the first four days after feeding, the gland segregates into two distinct regions, a distal region that is only sparsely

surrounded by mesothelium and a proximal region which retains the thick mesodermal sheath (Fig. 140).

The epithelial cell during the early stages in the proximal gland, is ultrastructurally similar to its counterpart in the distal gland. The cells are pseudostratified, with the position of the ovate nuclei varying from mid-cell to the basal cytoplasm (Fig. 140 and 142). The cytoplasm is rich in longitudinally arranged microvilli, elongate mitochondria, ribosomes and polysomes, but little RER (Fig. 142). The apical plasma membrane has microvilli with a cuticulin layer at their tips, and the apical-lateral plasma membranes interdigitate, connecting by band desmosomes at the luminal border (Fig. 142 and 143). The basal plasma membrane has a smooth outline and is in contact with a thin basal lamina that totally encompasses the epithelial layer (Fig. 142).

Proliferative divisions occur in the proximal epithelial layer throughout the entire mitotic stage, and cease prior to cuticulogenesis. During this time, the cells retain the basic ultrastructure outlined above. Cells divide in the same manner as those in the distal gland, i.e. draw away from the basal lamina and become luminal. The mitotic spindles always align to a tangent or parallel to the long axis of the gland, and re-extend towards the basal lamina, while retaining a band desmosome at the luminal border (Fig. 144). No unusual morphogenic movements occur analogous to those occurring during ductule formation in the distal gland.

Cell divisions cease at the onset of cuticulogenesis. Prior to cuticle deposition, the luminal epithelial border assumes a wavy appearance, and the epithelial cells deposit the duct cuticle such that a continuous spiral ridge runs the full length of the proximal gland (Fig. 141 and 143). This spiral duct is continuous with the central duct cuticle of the distal gland, but in thick sections, it stains metachromatically with toluidine blue, whereas the distal gland's duct cuticle stains orthochromatically, implying a chemical difference between the two cuticles (Fig. 139).

While cuticle is deposited, the epithelial layer flattens, with the basal ends of the cells orienting distally (Fig. 141). This flattening continues so that at the adult ecdysis, the epithelial layer is reduced from its larval maximum of 7 µm to a thickness of 5 µm prior to cuticulogenesis.

During the mitotic stage, the proximal gland sheath consists of a single layer of mesodermal cells that surround the inner epidermal layer and is surrounded also by a thin basal lamina (Fig. 84, 140, 147). The cells in this layer orient longitudinally, parallel with the long axis of the duct. They retain only spot contact to each other (Fig. 149), leaving large intercellular spaces between them. These spaces contain a fibrous material ultrastructurally identical to the basal lamina surrounding the inner epithelium (Fig 149). The cell cytoplasm contains many longitudinally arranged microtubules, many elongate mitochondria, irregular shaped basally located nuclei (with prominent chromatin) and some

RER (Fig. 150 and 151). The rich bundles of microtubules develop in concert with the muscle cell-epithelial cell interaction creating the structural framework on which the muscle will act. The apical membrane connects by spot desmosomes with the inner epithelial layer across the basal lamina surrounding it (Fig. 149 - 151).

When cuticulogenesis begins, the mesodermal sheath cells differentiate, forming well developed striated muscle in longitudinal fibers with the clear striation banding pattern evident in longitudinal section (Fig. 141). The filament and organelle components indicative of striated muscle are clearly seen in TEM at this point also. Prior to the appearance of the contractile framework, the cells contain a well developed complement of longitudinally arranged microtubules (Fig. 151). By day 17, it is functionally contractile, as observed during spontaneous contraction or the addition of KCl to the dissecting Ringers. Thus, the sheath differentiates to a functional muscle layer between day 14 and day 17 of the fifth instar. This muscle layer does not run the full length of the proximal gland. At approximately 74 µm from the gland terminus, the muscle layer stops (Fig. 141). At this same point, the regular corrugations of the cuticle diminish in size and regularity, and the calibre of the duct reduces from a maximum of 50 µm near the proximal-distal gland interface, to a minimum of 12 µm.

DISCUSSION

As described in the results, the Rhodnius cement gland is a complex organ, specialized for the synthesis, release and transport of a proteinaceous secretion. Cells that produce proteins for export contain RER and Golgi, to a degree that reflects the synthetic capacity of that cell (Mercer and Brunet, 1959). Throughout both the vertebrates and invertebrates, cells with an enhanced protein synthesis function, have RER and Golgi greatly accentuated (Jameson and Palade, 1967a and b; Selman and Kafatos, 1975; Anderson et al., 1970). Within secretory glands, the protein secreting function is usually carried out in specialized cells that are intimately associated with a cavity bounded by the cells or the lumen of an attached duct. As the results demonstrated, the Rhodnius cement gland secretory cell conforms to this general pattern. Unlike the multicellular units of the vertebrate pancreatic acinar cell (Jameson and Palade, 1967a and b) or the bicell units of the artemia shell gland (Anderson et al., 1970), the cement gland has single cell synthesis units as is characteristic of a variety of other insect glands (Mercer and Brunet, 1959; Eisner et al., 1964; Happ et al., 1966; Berry, 1968; Happ et al., 1971; Bonnanfant-Jais, 1974; Martin, 1977).

The Secretory Cell

Although the rim of the secretory cell cytoplasm appears very thin in any one area, the large cell size surrounding the central cavity, or secretion reservoir, insures a significant overall volume of cytoplasm, while also providing a large

surface area for secretion. Presumably this is important in ensuring the successive synthesis and release pattern that accompanies each 7 - 10 day egg laying cycle.

General basophilia of the secretory cell cytoplasm, coupled with the histochemistry and preliminary electrophoresis of gland extracts indicate that the glands are protein secreting. These results were verified by the presence of copious quantities of RER, seen with electron microscopy. Other insect glands are also rich in RER (Mercer and Brunet, 1959; Berry, 1968; Bonnanfant-Jais, 1974; Stay and Coop, 1974). Often, however, these other glands are also rich in Golgi complexes such as Hyalophora cecropia colleterial glands (Berry, 1968) and Glossina austeni milk glands (Bonnanfant-Jais, 1974). Golgi was not a prominent feature of the Rhodnius cement gland secretory cells. Since the histochemistry indicated neither a glycoprotein or lipoid secretion, the relative lack of Golgi is not surprising.

In Hyalophora cecropia adhesive-producing colleterial glands (Berry, 1968), Tenebria molitor spermathecal glands (Happ and Happ, 1970) and Diploptera punctata brood sac secretory cells (Stay and Coop, 1974), the route of the secretory product is assumed to be from the RER to the Golgi and then to the cell surface, fusing with the plasma membrane at the base of microvilli, rather than forming blebs that protrude into the reservoir as in the spermatheca of Periplaneta americana (Gupta and Smith, 1969). No vesicles were observed fusing to the reservoir plasmalemma surface in any of the sections.

Recently, Isenman and Rothman (1979) have raised doubts about the role of secretory vesicles in the export of amylase from rabbit pancreas. A stoppage in flow or an induced back pressure on the pancreatic duct causes a cessation of amylase synthesis, implying that synthesis is dependent on the concentration of secretion in the pancreatic duct. They argue that such results are inconsistent with the paradigm of vesicular transport but agree with a simple "diffusion" mechanism. Although these conclusions do not agree with accepted dogma of protein export, perhaps similar mechanisms exist in the Rhodnius cement gland. The ligaturing of the duct end of the gland for two or more ovulation cycles, and subsequent quantitative analysis of accumulated secretion would supply some insight into the mechanism of cellular secretion export.

The association of numerous mitochondria with the lumenal or reservoir plasmalemma suggests that the secretory mechanism is energy dependent. This intimate plasma membrane association has not been reported in any other insect secretory gland, but has been observed in systems actively transporting solutes such as insect Malpighian tubule (Berridge and Oschman, 1964; Sohol, 1974),cecropia midgut (Anderson and Harvey, 1966) and the anal papillae of mosquitoes (Copeland, 1964). In Musca domestica Malpighian tubules, mitochondria are intimately associated with the plasma membrane, actually occupying the microvilli that extend into the tubule lumen. Since active transport occurs across the tubule wall, Sohal (1975) assumed that the

mitochondria may play an energetic role. The mitochondria in the Rhodnius cement gland secretory cells merely associate with the reservoir plasma membrane but not within the microvilli, which have the classical internal filament structure. Although suggestive, proof of an energy dependent transport mechanism requires further experimentation with agents such as sodium azide, and their effect on the secretory process and accumulation.

In addition to the distinctive cytoplasmic constituents (RER and mitochondria), many free ribosomes are present suggesting significant endogenous synthesis of cytoplasmic substances must also occur. Since the reservoir undergoes an increase in volume during the ovulation cycle, presumably its enveloping gland cell increases in size and surface area to accommodate it. Concomitant with an increased volume is an increase in membrane surface. Probably, the general cytoplasm and few Golgi complexes present contribute membrane constituents at both the reservoir and external plasmalemmal surfaces.

Dark staining bodies, present in the cytoplasm associated with RER, are assumed to be autophagic vacuoles, similar to those observed in brood sac secretory cells of the viviparous cockroach Diploptera punctata (Stay and Coop, 1974). In these cells, mitochondria and RER undergo a cyclic degeneration concurrent with the cessation of milk release to the embryos, and subsequent parturition. These organelles are resynthesized and proliferate during the next pregnancy cycle. The Rhodnius cement gland does not undergo a major complete cyclic breakdown

of its organelles, although some regression and resynthesis apparently does occur. A detailed ultrastructural and enzyme histochemical study of the gland cell, on each day after the first blood meal, throughout the ovulation cycle, would further elucidate the degree to which autophagy occurs.

Secretory Unit

The synthetic cells and associated reservoir together with the attached ductule, and cuticular components, is referred to as the cement gland synthetic-transport unit. Examination of a variety of insect glands has led various investigators (Noirot and Quennedey, 1974) to establish a general classification scheme. This scheme involves a Class 1, 2 and 3 type of gland cells, Class 1 being a simple cuboid unicellular gland, while Class 2 and 3 have a more specialized cytoarchitecture. The Rhodnius cement gland in some respects is typical of Class 3 epithelial glands (Noirot and Quennedey, 1974). The secretory cell is directly attached to the ductule cell whose lumen is continuous with the reservoir space enclosed by the gland cell. The cuticle lining of Class 3 gland ductule cells terminates in a cuticular end apparatus, that is suspended in the reservoir. Although generally similar, the cement gland secretory unit has unique specializations not observed in other glands.

End Apparatus

In general, the end apparatus consists of two layers of epicuticle, similar to the ductule with which it is continuous (Noirot and Quennedey, 1974). The cement gland end apparatus is composed only of inner epicuticle, the outer layer being absent. This is also true in the scent gland of Nezara (Filshie and Waterhouse, 1969) and the pheromone-secreting gland of Harbobittacus (Crossley and Waterhouse, 1969), but in these cases, the innerfibrillar layer is in continuity with the inner epicuticle of the ductule. In Rhodnius, the end apparatus and the inner epicuticle of the ductule are both composed of the same material, but they are not in physical continuity, although the lattice struts of the end apparatus make contact with the inner epicuticle of the ductule.

In other glands, the inner layer of end apparatus epicuticle is absent, with only outer epicuticle present, as in the prothoracic nycangium of Dendroctonus (Happ et al., 1971) and spermathecae of Tenebrio (Happ and Happ, 1970). In this case, the outer epicuticle is in continuity with the outer epicuticle of the ductule. In addition to these variations in cuticular layers, the associated end apparati vary in shape ranging from vesicle-like to tube-like shapes. The tube type of end apparatus is little more than a blind end to the ductule that resides in the reservoir (Berry, 1968; Johnson and Berry, 1977). The end apparatus of this type is perforated with many small holes through which the secretion passes into the ductule (Beams et al., 1959; Evans, 1967; Gupta and Smith, 1969;

Forsyth, 1970; Happ and Happ, 1970; Happ and Happ, 1977; Plattner et al., 1972; Suzzoni, 1972; Barbier, 1974; Barbier, 1975; Selman and Kafatos, 1975; Sreng and Quennedey, 1976; Foldi, 1978).

The Rhodnius cement gland end apparatus is of the more complex vesicle type. The vesicle-shaped end apparatus has also been observed in the accessory gland of tsetse flies, (Tobe et al., 1973; Bonnanfant-Jais, 1974; Ma et al., 1975), as well as in the defense gland in tenebrionid beetles (Eisner et al., 1964), the scent glands of Nezara (Filshie and Waterhouse, 1968), the spermathecal gland cells of the mosquito Aedes aegypti (Clements and Potter, 1967), as well as in Myriapod (millipede) tegumentary glands (Jubethie-Jupeau, 1975).

Although generally conforming to the vesicle-type category, the cement gland end apparatus is unique in its geometry and its elaborateness when compared with the above examples. Its structure is reminiscent of the pheromone-producing brush-organ in the males of Phlogophora (Birch, 1970). Although cylindrical, the apical section of the hairs has a strikingly similar lattice-like structure with struts bonded together at intervals, enclosing diamond-shaped spaces. Such a mesh-like structure increases surface area to facilitate evaporation of the pheromone when the structure is everted. Perhaps the cement gland end apparatus lattice-like structure also increases its surface area so that the secretion can come into intimate contact with the cuticle as it passes through the lattice.

The end apparatus's unique geometry may play a role in the change in secretion staining density once it passes through to the ampulla.

Some apparent shrinkage evidently is due in part, to dehydration and tissue preparation, but this explanation is not sufficient to account for the difference since the secretion within the reservoir does not "shrink" during preparation. This suggests that the staining difference reflects either physical or chemical differences in the secretion. Its staining density only changes upon passing through the end apparatus reservoir ductule complex. Perhaps an enzymatic change occurs in the secretory proteins as they pass through the end apparatus. Enzymes have been observed in the epicuticle of insects such as Calpodes and Sarcophaga (Lai-Fook, 1966). In Eleodes and Tribolium defensive glands, which release benzoquinones and hydrocarbons, the end apparatus shows a positive reaction for a phenolase while the ductule cuticle, with which it is continuous, is positive for a peroxidase. Thus each step in quinone production in this gland is associated with an extracellular compartment, and the cytoplasm of the cell is never exposed to a toxic product (Happ, 1968). Perhaps the end apparatus and the reservory ductule cuticle in Rhodnius contain a hydrolytic enzyme that cleaves off a peptide from the protein, altering its conformation and thus its physical properties. The large surface area provided by the lattice would ensure intimate contact with the secretion as it passes through. As suggested by Happ (1968), such an

enzyme would progressively denature with age, thus it must be repeatedly renewed. Another possibility could be that a proenzyme is produced by the gland itself and is released into the reservoir with the secretion. The proenzyme may then be altered by an activating factor in the end apparatus, and then the enzyme would act on the secretion. In order to precisely determine the changes and mechanism, detailed biochemical and histochemical experimentation is required. It is very difficult to get an experimental handle on this problem, but a possible way to isolate the end apparatus is to place an isolated cement gland in a solution of EDTA and then into distilled water, to wash away the cells, leaving the cuticle intact. The use of trypsin to remove the cells is tempting, but unwise, since the hypothetical enzyme may not survive the digest. Then the appropriate biochemical enzymatic tests could be run.

The possibility of an enzyme modification and/or secretion heterogeneity is supported by the isoelectric focussing results. The three band difference between actively synthesizing and inactive glands, as opposed to the 34 in common, indicates that the secretion has more than one protein component. Since the isoelectric points of these three proteins are close (9.1, 8.8, 8.6), possibly one or two of them may be the products of enzyme digestion of the original secreted protein, or three similar proteins are produced. Molecular weight and

amino acid analysis of these three components would solve this question.

The high isoelectric points of the secretory proteins indicate that they contain basic amino acid residues such as lysine and arginine. The secretion's metachromatic staining with toluidine blue also suggests that sulfur containing amino acids like cysteine and methionine may be part of the proteins' primary structure.

The presence of the polar amino acid residues lysine and arginine in the secretion is consistent with the physical properties of the secretion. The large degree of polar amino acids accounts for the protein's readily solubility in water. Upon drying when the eggs are laid, perhaps a three dimensional conformation change occurs in the protein, due to the polar residues seeking charge neutrality. Presumably the new conformation resulting would have a different tertiary structure with all the polar groups oriented internally and all the non-polar groups on the periphery. This arrangement would explain the insolubility of the secretion after drying. Amino acid sequencing of the proteins and comparisons of the X-ray diffraction patterns of the soluble versus insoluble forms of the secretion must be performed in order to verify these speculations.

Secretory Cell - Secretory Cell Interaction

The intact gland consists of numerous secretory units arranged in a random, tangled fashion between the basal lamina and central duct cuticle. Over three hundred units can be

observed in any one section (Fig. 6). Thus there are clearly several layers of secretory cells with much variation from area to area in terms of the arrangement. This complex arrangement is unlike the general picture presented in the literature for most other insect glands. Most accessory gland cell units in other insects are arranged in a single cell layer. This is observed in the accessory glands of Glossina (Tobe et al., 1973; Bonnanfant-Jais, 1974; Ma et al., 1975), in Periplaneta (Mercer and Brunet, 1959), Galleria (Barbier, 1975) and Hyalophora (Berry, 1968). In addition, these Class 3 gland cells are either cuboidal or columnar in shape, having distinct basal, apical and lateral plasma membranes, the same being true also for the pygidial defence glands of Pterostichus (Forsyth, 1970), the spermathecal gland of Phosphuga (Suzzoni, 1972) and others. Thus, the cement gland cells differ in cell shape (spherical) as well as their arrangement. Similar spherically shaped gland cells occur in the spermathecal duct of Aedes aegypti (Clements and Potter, 1967), and the defense glands of tenebrionid beetles (Eisner et al., 1964; Happ, 1968).

Junctions are lacking between adjacent cement gland cells. This is consistent with Class 3 epidermal gland cells in general (Noirot and Quennedey, 1974), but there are some exceptions. Glossina milk gland cells are joined laterally by spot desmosomes (Bonnanfant-Jais, 1974), while septate junctions laterally join pheromone secreting gland cells in the scorpion fly (Crossley and Waterhouse, 1969), the scent

gland cells of the green vegetable bug (Filshie and Waterhouse, 1968), and the colleterial glands of Galleria (Barbier, 1975).

Ductules and Junctional Coupling

As in all other Class 3 glands, the ductule cell connects to the gland cell via septate junctions (Noirot and Quennedey, 1974). A similar enveloping cell surrounds the campaniform sensilla in the sternal gland of primitive termites (Stuart and Satir, 1968). Since it is generally accepted that the septate junction acts as an occluding junction in arthropods, it is tempting to suggest that the septate junction joining these two cells effectively retains the secretion within the reservoir and ductule. Secretion enclosure is further ensured since the cuticular ductule within the ductule cell continues past this junction into the reservoir space, and thus secretion passing by this junction is enclosed within cuticle, and is not directly in contact with the plasma membranes of the two cells. Similarly, the septate junction that adheres the ductule cell to itself, surrounding the cuticular ductule, does not directly contact the secretion since the secretion is enclosed within the cuticle.

The septate junctions would prevent extracellular substances from passing between the cells, through the cuticular lining to the secretion. Thus the junctions and cuticular lining effectively isolate the secretion-containing compartment from the extracellular one. The septate junctions presumably also perform an important structural adhering role.

Along with septate junctions, the ductule cell also adheres to itself via desmosomes (macula adherens) and gap junctions. It is unusual for a cell to make a gap junction with itself, although it has been observed in human ovarian decidual cells and was termed "reflexive" gap junction by Herr (1976). The function of gap junctions is to metabolically and ionically couple cells, therefore it seems odd that a cell should be ionically connected with itself. If the mechanism that governs gap junction formation is mediated through cell surface recognition sites between cells, then it seems possible that the two adjoining surfaces of the ductule cell membrane recognise the other as if forming a gap junction with another ductule cell. This hypothesis would seem more possible, if different ductule cells formed gap junctions between each other, which they do not, although some are joined by septate junctions. Thus the ductule cell must be able to recognize itself and distinguish itself from other ductule cells before forming gap junctions.

The function of a reflexive gap junction in a ductule cell could be to short circuit two areas of cytoplasm that are relatively remote from each other, although part of the same cell. The functional significance of such a reflexive junction is not known. Perhaps it permits informational and metabolic coordination in regions within the cell.

The presence of the macula adherens may seem redundant in view of the presence of the lengthy septate junction. However, the desmosome's complex anchoring to the cytoplasmic filament framework may provide certain regions of cell contact with

firmer support. Desmosomes are found in ductules in the 5th instar (Fig. 96) and also between gland and ductules in Diploptera brood sac glands only at the membranes adjacent to the lumen of the ductule, with septates making the rest of the connection. In both of these cases, the desmosomes are zonular desmosomes. In some ductules, the desmosome is found in the midst of a long septate, and not at the lumen border. The ductule cell of Bledius pygidial glands adheres itself exclusively by desmosomes, and serves the same function as the septate junction and desmosome in Rhodnius (Happ and Happ, 1973).

As stated above, very little junctional coupling exists between neighbouring ductule cells, that lie within the vast extracellular space. Ductule cell processes extend across the space forming cell—to—cell associations with similar processes from other cells but usually form no junctions. However, ductules penetrating the lumenal epithelial layer do form septates with each other and the epithelium. A similar arrangement occurs in the pygidial glands of Pterostichus (Forsyth, 1970), Galleria accessory glands (Barbier, 1975), the terpene glands of Anismorpha (Happ et al., 1966), Nezara scent glands (Filshie and Waterhouse, 1968), Diploptera brood sac glands (Stay and Coop, 1974) and Glossina milk gland (Bonnanfant-Jais, 1974).

The lack of junctions between neighbouring ductules and adjacent gland cells is consistent with the vast intercellular space in the Rhodnius cement gland. Such intercellular space

is unparalleled in scope in any tubular insect gland studied to date. The functional significance of the extracellular space may relate to the mechanism of secretion expulsion from the reservoir into the ductules and ultimately the central lumen. Negative pressure alone, produced by contractions of the collecting duct muscle, may be enough to draw the lumenal secretion out of the gland, but the amount of negative pressure needed to draw the secretion down thousands of ductules 730 ηm in diameter, would be enormous (on the order of several atmospheres). Perhaps the extracellular space is a pool of solutes, or even proteins, that is isosmotic with the hemolymph, until the time of oviposition. At oviposition the osmotic pressure of the extracellular space may be increased by a change of material or ions in it. Such an hyperosmotic extracellular space would create an osmotic gradient across the basal lamina of the gland, causing water to flow in, thus increasing the size of the extracellular space. Presuming that the basal lamina stretches only minimally, any increase in the extracellular space would force the gland cells to decrease in size, resulting in the expulsion of secretion down the ductules towards the lumen. Since the extracellular space appears to increase in size after ovulation, the presence of such a mechanism is possible. Since the material within the extracellular space is preserved during preparation for electron microscopy, a portion of it is likely proteinaceous. Isolation of the extracellular fluid for analysis, prior to and during oviposition necessary to test this hypothesis, is enormously difficult.

One drawback of this speculation is that some secretion is always present in the gland lumen, even as early as one day after the first adult blood meal. Perhaps the gland reaches a critical volume and releases the secretion for storage in the gland lumen. The lumen hardly seems suitable as a vast storage area, since the total lumen volume is a mere 12 picoliters, which seems insufficient to coat the 30-40 eggs with enough adhesive to fasten them securely. Since the total gland volume is about 1.7 µl, it is more probable that the secretion is stored in the gland cell reservoirs and mobilized by some mechanism at the time of ovulation.

Proximal Gland

The proximal muscular gland duct plays an important role in the release of the secretion at ovulation. Its structure is well suited to a pumping function. The spirally corrugated lumen cuticle assists its spring-like action during contraction. A similar morphology is seen in the Glossina milk gland common collecting duct (Tobe et al., 1973). The corrugated structure provides flexibility as well as strength, while maintaining its tubular integrity, even during contraction.

The large compliment of cytoplasm microtubules in the epithelium to which the muscle layer connects is reminiscent of a similar epithelium in spider web-silk glands (Smith, 1972). Such an array of parallel microtubules imparts rigidness to the epithelial layer for the muscles to act upon, giving the epithelial layer a connective tissue function. The squamous

nature of the cells in conjunction with the microtubules would also contribute to this rigidness, since a cuboidal or columnar cell would be much more susceptible to lateral distortion during contraction, effectively reducing the muscle's contractile force.

The muscle arrangement is only roughly longitudinal, as separate bundles in cross-section are not in the same plane of section, but oblique. Contraction of the muscle effectively reduces the proximal gland length. The muscle of the Glossina milk gland collecting duct is spirally arranged with the long axis, so that in addition to a reduction in the length of the duct, there is also a lateral twisting of the duct cuticle. Such a distortion in the Rhodnius collecting duct does not occur, although it seems probable that the cuticle is under considerable elastic stretch during contraction. Its metachromatic staining characteristics precludes the possibility of the presence of resilin (a rubber-like elastic cuticle) in the collecting duct cuticle, as resilin stains orthochromatically with toluidine blue (Weis-Fogh, 1960). Perhaps the corrugations in the duct itself provides enough structural flexibility so that molecular bending, responsible for elasticity, is at a minimum but sufficient to return the duct and the enveloping muscle to its resting length.

The duct cuticle's reduction in diameter at its connection with the ovipositor may function as a valve. After secretion is forced out during duct muscle contraction, the elastic action of cuticle would provide sufficient force necessary to

draw secretion back into the gland. More of the force would pull secretion down through the larger opening at the transition between the proximal and distal gland.

This study of the adult cement gland in Rhodnius reveals an intricate structure, the understanding of which is only partially correlated with its function. Several questions requiring further investigation arise. A detailed biochemical analysis of the secretion could determine how the secretion changes its water solubility after it hardens. Little is known of the hormonal control of synthesis and secretion or the timely release at oviposition. A variety of endocrine experiments should be performed. Experiments on the mechanism of secretion are also needed.

The most interesting question raised by this first part of the study, is how such a complex cellular system developed from the simple, barely dissectable tubule present at the beginning of the penultimate stage, the 5th instar. Analysis of the ontogeny of the units should provide further insight into the intercellular relationships that exist in the adult gland.

Fifth Instar Differentiation

Microscopic evidence presented clearly shows that the complex structure of the adult cement gland in Rhodnius arises from a simple pseudostratified epithelial tube. During the course of the twenty day fifth instar, complex cell movements triggered by specific mitotic arrangements occur. These can be timed precisely in relation to the blood meal. Larval Rhodnius will not moult if starved, and will live indefinitely in that larval stadium if fed small blood meals (Wigglesworth, 1933). Differentiation is only triggered if sufficient blood is imbibed to activate the stretch receptors located in each abdominal segment. These receptors, when stretched, set up impulses in the nerves leading to the corpus cardiacum, which releases neurosecretion turning on the prothoracic glands to release moulting hormone (Van der Kloot, 1954). Such physiological control allows for easy timing of experiments, as many animals can be accumulated, all arrested at the same stage of development.

Female accessory glands in the insects undergo their major growth and differentiation in their last immature, pre-adult stadium. This is true in holometabolous insects, that is, insects that pass through a pupal stage prior to adult eclosion, such as in the Lepidoptera and Coleoptera. Examples of accessory gland differentiation studies in the Lepidoptera include the moths Galleria mellonella (Barbier,1974) and Actias luna (Johnson and Berry, 1977), and the spermathecal accessory gland in the Coleopteran Tenebrio molitor (Happ and

Happ, 1977). This is the first ultrastructural study of the differentiation of an accessory gland in a hemimetabolous insect. Differences between the two types are subtle, yet fundamental.

Cell Division

The blood meal initiates cell division in the cement gland, which proceeds similarly to that seen in the Lepidopteran studies. As in Actias luna (Johnson and Berry, 1977), the column-shaped epithelial cell breaks down its microtubular cytoskeleton, and retracts from the basal lamina to lie adjacent to the lumen. Such an arrangement is reminiscent of cell division in the primary mesenchymal cells in the sea urchin Arbacia punctulata. In Arbacia blastulae, individual blastomeres are thin conical cells, but when they divide, they shorten up near the surface of the embryo, only re-extending to their conical form after division (Gibbons et al., 1969). By such proliferative cell divisions, the cement gland increases its diameter and length. Interestingly, the proximal region of the gland does not increase appreciably in diameter beyond about day 4 post feed, until ductule and end apparatus formation. This cessation in diameter growth is explained by the spindle orientation. In the proliferative divisions, the spindle is oriented either at a tangent to the lumen or parallel to it. When at a tangent to the lumen, dividing cells will re-extend towards the basal lamina, but at the same time increase the cross-sectional diameter of the gland, whereas when it is parallel to the long axis of the lumen, the cells will divide in a longitudinal direction, thus increasing the

length of the gland. When the gland reaches the day 4 diameter, the spindles probably orient in a parallel fashion, since the gland does not reach its maximal length until day 14. Detailed observations to substantiate this phenomenon were not made.

During cell division, no evidence of a microtubular cytoskeleton is observed, except the spindle apparatus. Loss of cytoskeletal microtubules is coincident with retraction and loss of the columnar shape, indicating their normal role in cell shape maintenance. Exposure of Arbacia blastulae to D_2O, an agent known to prevent microtubule breakdown, prevents cell shape change dependent development, with the inhibition of the assembly and change in mesenchyme cells (Tilney et al., 1969). Upon post-mitotic cement gland cell re-elongation, cytoplasmic microtubules reappear parallel to the longitudinal cell axis supporting their role (either direct or indirect) in both cell retraction and elongation.

The cell shape of Arbacia blastomeres was influenced by junctions, lateral interdigitations and basal lamina association (Tilney et al., 1964). During these early proliferative stages of the Rhodnius cement gland, lateral interdigitations, as well as a prominent circumferential apical zonular desmosome are important in anchoring cells within the gland during their shape changes and ensuring the physical interrelationships that develop.

Morphogenesis

The second phase of cell division not only increases the cell number, but also initiates a phase of morphological movements that lead to ductule and secretory cell differentiation. Characteristically, cells undergoing differentiation (Happ and Happ, 1977) mitosis have their spindles oriented perpendicular to the lumen in a manner similar to differentiative divisions in Actias luna colleterial glands (Johnson and Berry, 1977) and Tenebrio moliter spermathecal glands (Happ and Happ, 1977).

Luminal division results in two sister cells with one cell remaining luminal and the other basal to it. Subsequently, elongation occurs, but the cell to cell association is unlike the proliferative divisions, where cells elongate next to each other. In Tenebrio (Happ and Happ, 1977), Actias (Johnson and Berry, 1977) and Galleria (Barbier, 1975), the sister cell left adjacent to the lumen extend a pseudo-cilium at the apical lumenal border. The ensuing basal elongation proceeds with the pseudo-cilium extending into the ductule that is formed by the third cell lying adjacent to the dividing cells. In Actias and Galleria, the pseudo-cilium extend from the cell, up the ductule, right into the main lumen of the gland (Barbier, 1975; Johnson and Berry, 1977). A similar pseudo-cilium is observed in the cytodifferentiation of the tergal glands in the male of Blattela germanica (Sreng and Quennedey, 1976) and the cocoonase producing silkmoth galea (Selman and

Kafatos, 1975). In each of these cases, the pseudo-cilium has a non-motile 9 + 0 arrangement. Johnson and Berry (1977) suggest that it serves as a passive core around which the duct is organized, while Selman and Kafatos (1975) go further to suggest that they may act as structural elements maintaining the integrity of the tube until the cuticulin finalizes the duct's tubular shape. Barbier (1975) suggests the cilia acts as a full cylindrical mould, determining the accurate shape and location of the ductule.

In Rhodnius, the overall geometric association of the morphogenetic cells is similar, but important differences are evident. The most significant is the luminal sister cell (cell A) does not extend a pseudo-cilium, but rather has a number of long microfilament rich microvilli, that extend into the forming ductule, as the two sister cells elongate, with cell C forming the ductule as they re-elongate toward the basal lamina. The speculations on the role of the pseudo-cilium cited above are unlikely since the Rhodnius ductule forms and is maintained without the need of a pseudo-cilium, although it has basically similar cellular constituents and arrangements. The intracellular filaments are more likely candidates for the formation and maintenance of ductule integrity.

Furthermore, in the examples cited above, the pseudo-cilium does not occupy the full ductule diameter nor contact the ductule cell plasmalemma. It is difficult to envisage a cellular mechanism for the ascribed roles of the pseudo-cilium. Similar morphogenetic events in Rhodnius indicate the role of the pseudo-cilium requires re-examination.

A similar comment can be made about the role of the apical microvilli in Rhodnius. Given the ultrastructural data, the most plausible present interpretation is that ductule formation is dependent on changes in intercellular association and cell shape.

Ductule Formation

The ductule elongates as the two sister cells A and B elongate basally. The unusual relationship between the cell A - cell B retracting unit and cell C has not been fully described in the literature. The fact that cell C wraps around the other two implies cell A and B act as a slip mold during their basal movement, while cell C has the active role of ductule formation. The enveloping of cell A and B by cell C is analogous to glial cell myelination in nerves, but at a much simpler level. Contractile and enveloping processes in cell C must act in a very precise manner in response to the position of cell A and B, implying that an intimate communication exists between them. If this communication is at the gap junction level, constant assembly and re-assembly must occur as cell A - B moves basally along the side of C. This communication may also involve cell surface recognition sites, i.e. cell C recognizes cell A - B surface components and responds by envelopment. In this case, cell A - B could be changing its surface components to signal a change in its position and thus elicit a change in the contractile behaviour of cell C.

The mechanics of cell C's enveloping cell A - B may roughly be analagous to ameoboid phagocytosis. The recognition of the proposed cell surface signal, mentioned above, may alter the microfilament cytoskeleton at the interacting surface. If contraction occurs only at the interacting surface, it would be accompanied by a longitudinal flattening of cell C to form a cylindrical shape around cell A - B as they elongate. Cell C would continue to flatten until it totally envelops cell A - B. Cell C must then be able to recognise itself, as the two processes of cell C make contact and form reflexive desmosomal attachments. As the elusive cell A - B unit passes, one can imagine a zipper-like action of desmosome formation as cell C wraps around a moving "target". One can assume that the rate of desmosome disassembly and re-assembly along cell C's length would determine not only the rate of cell A - B's movement, but also the degree of elongation the unit achieves. Although a good deal of the above is mere speculation on a complex developmental process, a major junctional role in the mechanism of ductule formation in the cement gland is probable. Elucidation of the changing cell interactions and the role of junctional assembly awaits further work and the development of new techniques that permit the study of junction assembly and disassembly during morphogenesis in complex tissues.

Reservoir Formation

When cell A and B come to rest at the basal end of cell C, they become rounded in shape. The forming globular reservoir shape is maintained by the circumferential arrangement of microtubules in both cells A and B. Thus cell A and B again act as a mold, creating a vesicle-like space until the end apparatus has been completely constructed. Cell A is also responsible for the synthesis and release of the cuticle that makes up the end apparatus. The apparent fate of cell A is autolysis, while cell B becomes the adult gland cell. In Blattela germanica tergal glands (Sreng and Quennedey, 1976) and Actias luna accessory glands (Johnson and Berry, 1977), the cell A in these systems also break down, leaving cell B as the gland cell, while in Galleria mellonella accessory glands (Barbier, 1974, 1975), vesicle formation, end apparatus deposition as well as adult gland function are all carried out by the same cell. Thus the contention by Noirot and Quennedey (1974) that the end apparatus in Class 3 epidermal gland cell units is probably laid down by the gland cell, does not hold for certain accessory and epidermal glands.

Cell A Autolysis

The ultimate fate of cell A in Rhodnius is unique amongst those studied. In Actias accessory glands (Johnson and Berry, 1977), and Blattela tergal glands (Sreng and Quennedey, 1976), cell A breaks down and is actively phagocytosed by cell B. The Rhodnius cement gland cell A undergoes autolysis and

fragmentation in the reservoir with the breakdown products presumably passing down the ductule, or phagocytosed by cell B, or the molecular products of breakdown are absorbed by cell B. The daily time frame of this study was not sufficient to determine the precise fate of cell A after fragmentation. A detailed time sequence,at short intervals at eclosion and shortly thereafter,may yield further information on this aspect of stage specific cell death.

An unusual characteristic of cell A in Rhodnius is that much of its cytoplasm retracts through a hole created in the dome of cell B. This phenomenon has not been reported in the differentiation of any other Class 3 gland. Since cell A is confined within cell B during end apparatus formation, perhaps this retraction through cell B allows cell A to increase its cytoplasmic volume greatly while permitting it and cell B to maintain the precise spherical shape needed for end apparatus construction. Since most of cell A's RER is in the extra-reservoir cytoplasm, it is likely that enhanced protein synthesis is possible, due to this increase in cytoplasmic volume. Transport of materials from one region to the other would occur through the interconnecting cytoplasmic channel. The numerous parallel microtubules are reminiscent of the trophic cords in the telotrophic ovary of Rhodnius (Huebner and Anderson, 1972) and the stalks connecting Ascaris oocytes to the central rachis (Foor, 1967), where cytoplasmic transport is well known.

Upon completion of end apparatus cuticle deposition, cell A is no longer required, as the surrounding cell B becomes the

adult secretory cell. Whether the extra reservoir cytoplasm breaks down outside of cell B or whether it retracts back inside the reservoir and breaks down, is not known. Once cell A has disintegrated and been absorbed, cell B closes up, forming an intact spherical cell surrounding the reservoir.

In discussing the formation of the ductule reservoir and secretory cell, cuticle formation was essentially ignored in order to focus on the cellular interaction and shape changes noted above. However, in concert with the secretory unit morphogenesis, there has been the elaboration of the cuticular lining from the duct lumen through the ductules and ampulla to the elaborate end apparatus seen in the adult. The following section now focuses on cuticulogenesis.

Cuticle Deposition

Cells lining the lumen in unfed fifth instar cement gland have an incomplete layer of cuticulin present at the tips of long microvilli. This observation is consistent with the deposition of cuticulin generally in insects (Locke,1966). It is doubtful that cuticle is deposited at this time, since the cell's cytoplasm is poor in RER, hence not involved in major protein synthesis. Presumably this cuticle was deposited in late 4th instar. Two days after the 5th instar blood meal, little evidence of cuticulin at the microvillar tips remains.

The disappearance of cuticulin is correlated with the appearance of apical pinocytotic activity, presumably incorporating the previous cuticulin components. Pinocytotic activity continues throughout the mitotic stage, ceasing at adult

cuticulin deposition at day 15 - 16. Cuticulin is first noted in the ductules as dark staining condensations at the tips of ductule microvilli (Fig. 96), which is consistent with the pattern of initial cuticulin deposition reported by Locke (1966). It is completed and appears as a continuous flat layer by day 16. Cuticulin is deposited by cells A and B as a short funnel extending into the reservoir, and by cell C extending the full length of the ductule lumen. A cuticulin layer also surrounds the full length of the central duct. No cuticulin is deposited by the reservoir plasma membrane area that will form the end apparatus. The sole component of the end apparatus is inner epicuticle, which is deposited when epicuticle is deposited in the ducts and lumen. A similar sequence of events occurs in Tenebrio molitor spermathecal accessory glands, with the ductule (Happ and Happ, 1977). The significance of the end apparatus' inner epicuticle composition is unknown. If cuticular enzymes are present in the cement gland end apparatus, it seems likely they would be in the inner epicuticle rather than the cuticulin layer (Lai-Fook, 1966).

End Apparatus Formation

Clearly, the end apparatus constitutes a distinct, highly specialized cuticular area that is likely endowed with special enzymatic and structural properties that will be important to adult pro-secretion modification. As the early part of the discussion noted, in the adult, the three-dimensional morphology is perhaps the most elaborate yet described for any insect gland.

Analysis of the development revealed that the epicuticular lattice network is produced by a pattern of surface microvilli on the luminal plasmalemma of cell A. The epicuticle initially was clearly recognizable at the tips of single and branching microvilli, with subsequent accumulation resulting in epicuticular struts mirroring the polygonal microvillar pattern as revealed in tangential sections. Presumably, there is a mosaic molecular pattern already established in the plasma membrane that is crucial to the condensation and/or release of epicuticular precursors in a precise pattern. Since this is one of the rare instances within the insects, in which one can precisely correlate a cell surface geometry with the morphogenesis of a surface cuticular pattern, this may prove to be a valuable cell for elucidating cuticle formation mechanisms.

Regional Epicuticle - Endocuticle Deposition

Although, like the end apparatus, the ductule cells deposited inner epicuticle, they do not deposit endocuticle. Thus, the central duct lining cells are distinguished from the ductule cells with which they are continuous, since they do produce an endocuticle. Central lumen endocuticle deposition occurs concurrently with epicuticle deposition in the ductules, illustrating the differing developmental time course as well as differentiative events between these superficially similar cell types.

Careful analysis of the regional nature and pattern of cuticle deposition within the secretory units indicated that, although all cells are presumably derived from the same epithelial stem cell, their respective morphogenetic changes location and differing cell interactions have had precise effects on the timing and nature of their extracellular secretion properties. Although the differences are simple, we are a long way, in any cell system, from linking gene mediated synthetic control mechanisms with developmental fates, altered by changes in cell shape, location and interaction.

Proximal Gland Differentiation

The differentiating proximal cement gland arises from the same stem cell population as the distal gland despite the pronounced ultrastructural contrast with the distal gland. Early in the 5th instar, the two regions become distinct from each other by the presence of a thin mesodermal cell layer surrounding the proximal gland, while the distal gland is enveloped only by a thin basal lamina. Throughout the mitotic stage, both the proximal and distal gland epithelia retained a similar morphology. By the outset of ductule formation in the distal gland, the proximal epithelial layer has still retained a relatively "undifferentiated" morphology. The presence of the mesodermal cell layer, ultimately becoming the longitudinal muscle layer, is the major apparent ultrastructural difference between the two regions. Perhaps a classical mesodermal-epidermal interaction, as proposed in

many vertebrate systems, occurs where the presence of the mesodermal sheath induces the development, of lack of development, as in this case, in the epithelial layer.

The mesodermal cell cytoplasm, throughout development, has abundant longitudinally arranged microtubules. These microtubules may be responsible for the geometric arrangement of the pro-muscle cells in a longitudinal fashion along the epithelial layer. This, coupled with the formation of macular desmosomal attachments between the two cell layers, ultimately resulting in the extensive zonular desmosomes of the adult, support this contention. Ultimately, the microtubular cytoskeleton gives way to actin-myosis filament elaboration, resulting in a functional muscle a few days before adult eclosion. Along with the muscle, nerves necessary for subsequent muscle control are also clearly seen.

This study has presented the cytoarchitectural inter-relationships existing in the adult female Rhodnius accessory gland, and by time-sequence analysis during 5th instar growth and gland morphogenesis, determined the ontogeny of the complex cellular interactions present. The highly synthetic machinery, conduit conveying system and muscular expulsion system of the gland are well designed to produce the proteinaceous secretion that must be released at ovulation to ensure attachment of the eggs at sites that, in nature, presumably enhance the chances of survival.

Hopefully, these findings provide the necessary foundation for further work on gland control as well as the basic developmental questions raised in the text.

REFERENCES

Adiyodi, K.G. and R.G. Adiyodi. 1975. Morphology and cytology of the accessory sex glands in invertebrates. Int. Rev. Cytol. 43: 353-398.

Altmann, R. 1890. Die Elementarorganismen und ihre Beziehungen zu den Zellen. Viet Co., Leipzig.

Anderson, E. 1964. Oocyte differentiation and vitellogenesis in the roach Periplaneta americana. J. Cell Biol. 20: 131-155.

Anderson, E. and H.W. Beams. 1956. Evidence from electron micrographs for the passage of material through pores of the nuclear membrane. J. Biophys. Biochem. Cytol. 2: suppl., 439-444.

Anderson, E. and W.R. Harvey. 1966. Active transport by the Cecropia midgut. II. Fine structure of the midgut epithelium. J. Cell Biol. 31: 107-134.

Anderson, E., J.H. Lockhead, M.S. Lockhead and E. Huebner. 1970. The origin and structure of the tertiary envelope in thick-shelled eggs of the brine shrimp Artemia. J. Ultrastruc. Res. 32: 497-525.

Anderson, W.A. and R.A. Ellis. 1965. Ultrastructure of Trypanosoma lewisi: flagellum, microtubules and the kinetoplast. J. Protozool. 12: 483-499.

Barbier, R. 1974. Presence de structures ciliares ou cours de l'organogenèse des glandes colletérique de Galleria mellonella L. (Lepidoptère pyralide). Colloque annuel de la société francaise de microscopie électronique. J. Microscopie. 20: 18-19.

Barbier, R. 1975. Differenciation de structures ciliares et mise en plance des canaux au cours de l'organogenèse des glands collétériques de Galleria mellonella L. (Lepidoptère, Pyralide). J. Microscopie 24: 315-326.

Berridge, M.J. and J.L. Oschman. 1969. A structural basis for fluid secretion by Malpighian tubules. Tissue and Cell 1: 247-272.

Berry, S.J. 1968. The fine structure of the colleterial glands of Hyalophora cecropia (Lepidoptera). J. Morph. 125: 259-280.

Birch, M.C. 1970. Structure and function of the pheromone-producing brush-organs in males of Phlogophora meticulosa (L.) (Lepidoptera: Noctuidae). Trans. R. end. Soc. Lond. 122: 277-292.

Bonnanfant-Jais, M-L. 1974. Morphologie de la glande lactée d'une Glossine, Glossina austeni Newst, au cours du cycle de gestation. J. Microscopie 19: 265-284.

Buxton, P.A. 1955. The Natural History of Testse Flies. London School of Hygiene and Tropical Medicine. Memoir No. 10.

Clements, A.N. and S.A. Potter, 1967. The fine structure of the spermathecae and their ducts in the mosquito Aedes aegypti. J. Insect Physiol. 13: 1825-1836.

Copeland, D.E. 1964. A mitochondrial pump in cells of the anal papillae of mosquito larvae. J. Cell Biol. 23: 253-263.

Crossley, A.C. and D.F. Waterhouse. 1969. The ultrastructure of a pheromone-secreting gland in the male scorpion-fly Harbobittacus australis (Bittacidae, Mecoptera). Tissue and Cell 1: 273-294.

Eisner, T., F. McHenry and M.M. Salpeter. 1964. Defense mechanisms of arthropods XV Morphology of the quinone-producing glands of a tenebrionid beetle. (Elodes longicoltis Lec). J. Morph. 115: 355-368.

Filshie, B.K. and B.F. Waterhouse. 1968. The fine structure of the lateral scent glands of the green vegetable bug, Nezara viridula (Hemiptera, Pentatomidae). J. Microscopie. 7: 231-244.

Fisher, D.B. 1968. Protein staining of ribboned epon sections for light microscopy. Histochem. 16: 92-96.

Foldi, I. 1978. Ultrastructure des glandes tegumentaires dorsales, secretrices de la "Laque" chez la femelle de Coccus hesperidum L. (Homoptera: Coccidae). Int. J. Insect Morphol. & Embryol. 7: 155-163.

Foor, W.E. 1967. Ultrastructural aspects of oocyte development and shell formation in Ascaris lumbricoides. J. Parasitol. 53: 1245-1261.

Forsyth, D.J. 1970. The ultrastructure of the pygidial defense glands of the carabid Pterostichus madidus F. J. Morph. 131: 397.

Galliard, H. 1935. Recherches morphologiques et biologiques, sur la reproduction des réduvides hématophages (Rhodnius et Triatoma). Thèses Présentées a la faculté des sciences de l'université de Paris. Masson et Cie, Paris.

Gibbons, J.R., L.G. Tilney, and K.R. Porter. 1969. Microtubules in the formation and development of the primary mesenchyme in Arbacia punctulata. I. The distribution of microtubules. J. Cell Biol. 41: 201-226.

Gupta, B.J. and D.S. Smith. 1969. Fine structural organization of the spermatheca in the cockroach Periplaneta americana. Tissue and Cell 1: 295-324.

Happ, G.M. 1968. Quinone and hydrocarbon protection in the defensive glands of Eleodes longicollis and Tribolium castaneum (Coleoptera, Tenebrionidae). J. Insect Physiol. 14: 1821-1837.

Happ, G.M. and C.M. Happ. 1970. Fine structure and histochemistry of the spermathecal gland in the mealworm beetle, Tenebrio molitor. Tissue and Cell. 2: 443-466.

Happ, G.M. and C.M. Happ. 1973. Fine structure of the pygidial glands of Bledius mandibularis (Coleoptera: Staphylinidae). Tissue and Cell. 5: 215-231.

Happ, G.M. and C.M. Happ. 1977. Cytodifferentiation in the accessory glands of Tenebrio molitor. III Fine structure of the spermathecal accessory gland in the pupa. Tissue and Cell. 9: 711-732.

Happ, G.M., C.M. Happ and S.J. Barras. 1971. Fine structure of the prothoracic nycangium, a chamber for the culture of symbiotic fungi in the southern pine beetle, Dendroctonus frontalis. Tissue and Cell. 3: 295-308.

Happ, G.M., J.D. Strandberg and C.M. Happ. 1966. The terpene-producing glands of a phasmid insect. Cell morphology and histochemistry. J. Morph. 119: 144-159.

Hefetz, A., H.M. Fales and S.W.T. Butra. 1979. Natural polyesters: Dufor's gland macracyclic lactones form brood cell laminesters in Colletes bees. Science 204: 415-417.

Herr, J.C. 1966. Reflexive gap junctions. Gap junctions between processes arising from the same ovarian decidual cell. J. Cell Biol. 69: 495-501.

Huebner, E. and E. Anderson. 1972. A cytological study of the ovary, of Rhodnius prolixus. III. Cytoarchitecture and development of the trophic chamber. J. Morph. 138: 1-40.

Humason, G.L. 1972. Animal Tissue Techniques. W.H. Freeman & Co., San Francisco.

Isenman, L.D. and S.S. Rothman. 1979. Diffusion-like processes can account for protein secretion by the pancreas. Science 204: 1212-1215.

Jamieson, J.D. and G.E. Palade. 1967a. Intracellular transport of secretory proteins in the pancreatic exocrine cell. I. The role of the peripheral elements of the Golgi complex. J. Cell Biol. 34: 577-596.

Jamieson, J.D. and G.E. Palade. 1967b. Intracellular transport of secretory proteins in the pancreatic exocrine cell. II. Transport to condensing vacuoles and zymogen granules. J. Cell Biol. 34: 597-615.

Johnson, E. and S.J. Berry. 1977. Cellular differentiation in a highly specialized insect secretory organ. Differentiation 8: 39-52.

Juberthie-Jupeau, L. 1975. Les glandes tegumentaires de la fossette supra-anale des Scutigerellidae (Symphala, Myriapoda). Tissue and Cell 7: 347-356.

Karnovsky, M. 1965. A formaldehyde-gluteraldehyde fixative of high osmolarity for use in electron microscopy. J. Cell Biol. 27: 137a (Abstract).

Lai-Fook, J. 1966. The repair of wounds in the integument of insects. J. Insect Physiol. 12: 195-226.

Lane, B.P. and D.L. Europa. 1965. Differential staining of ultrathin sections of epon-embedded tissues for light microscopy. J. Histochem. Cytochem. 13: 579-582.

Locke, M. 1966. The structure and function of the cuticulin layer in the epicuticle of an insect, Calpodes ethlius (Lepidoptera, Hesperiidae). J. Morph. 118: 461-494.

Luftig, R.B., P.N. McMillan, J.A. Weatherbee and R.R. Weihing. 1977. Increased visualization of microtubules by an improved fixation procedure. J. Histochem. Cytochem. 25: 175-187.

Ma W-C, D.L. Denlinger, U. Jarlfors and D.S. Smith. 1975. Structural modulation in the testse fly milk gland during a pregnancy cycle. Tissue and Cell 7: 319-330.

Martin, N. 1977. Glandes dermiques chez deux Coleopteres cavernicoles (Catopidae). Int. J. Insect Morphol. and Embryol. 6: 179-189.

Maupin-Szamier, T. and T.D. Pollard. 1978. Actin filament destruction by osmium tetroxide. J. Cell Biol. 77: 837-852.

Mercer, E.H. and P.C.J. Brunet. 1959. The electron microscopy of the left colleterial gland of the cockroach. J. biophys. biochem. Cytol. 5: 257-262.

Noirot, C. and A. Quennedey. 1974. Fine structure of insect epidermal glands. Ann. Rev. Entomol. 19: 61-80.

Overton, J. 1977. Formation of junctions and cell sorting in aggregates of chick and mouse cells. Dev. Biol. 55: 103-116.

Pratt, G.E. and K.G. Davey. 1972. The corpus allatum and oogenesis in Rhodnius prolixus (Stal). I. The effects of allatectomy. J. Exp. Biol. 56: 201-214.

Roth, T.F. and K.R. Porter. 1964. Yolk protein intake in the oocyte of the mosquito Aedes aegypti L. J. Cell Biol. 20: 313-332.

Selman, K. and C. Kafatos. 1975. Differentiation in the cocoonase producing silkmoth galea: ultra-structural studies. Develop. Biol. 46: 132-150.

Smith, D.S. 1972. Muscle. Academic Press, Inc. New York.

Sohal, R.S. 1974. Fine structure of the Malpighian tubules in the housefly, Musca domestica. Tissue and Cell. 6: 719-728.

Sreng, L. and A. Quennedey. 1976. Role of a temporary ciliary structure in the morphogenesis of insect glands. An electron microscope study of the tergal glands of male Blattella germanica L. (Dictyoptera, Blattellidae). J. Ultrastruc. Res. 56: 78-95.

Stay, B. and A.C. Coop. 1974. "Milk" secretion for embryogenesis in a viviparous cockroach. Tissue and Cell 6: 669-693.

Stay, B. and L. Roth. 1962. The colleterial glands of cockroaches. Ann. Ent. Soc. Amer. 55: 124-130.

Stein, G. 1967. Uber den Feinbau der Duftdrüsen von Feuerwanzen (Pyrrhocoris apterus L., Geocorisae). Die 2 larvale Abdominaldrüse. Z. Zellforsch. mikrosk. Anat. 79: 49-63.

Stuart, A.M. and P. Satir. 1968. Morphological and functional aspects of an insect epidermal gland. J. Cell Biol. 36: 527-549.

Suzzoni, J-P. 1972. Ultrastructure de la glande de la spermathèque chez Phosphuga atrata L. (Coleoptera Silphidae). Z. Zellforsch. 128: 426-437.

Tobe, S.S., K.G. Davey and E. Huebner. 1973. Nutrient transfer during the reproductive cycle in Glossina austeni Newst: Histology and histochemistry of the milk Gland, fat body and oenocytes. Tissue and Cell 5: 643-650.

Venable, J.H. and R. Coggeshall. 1965. A simplified lead citrate stain for use in electron microscopy. J. Cell Biol. 25: 407-408.

Veratti, E. 1902. Richerche sulle fine struttura de la fibra muscolare striata. Mem. Ist. lomb. Sci. Lett. Classe Sc. Mat. Nat. 19: 87-133. (English transl.: J. Biophys. Biochem. Cytol. 1961, suppl. 10: 3-59.

Weis-Fogh, T. 1960. A rubber-like protein in insect cuticle. J. exp. Biol. 37: 889-907.

Wigglesworth, V.B. 1972. The Principles of Insect Physiology. Chapman and Hall Ltd., London.

Wilson, E.B. 1928. The Cell in Development and Heredity. MacMillan Comp., New York.

Plate 1

Gross Anatomy

Figure 1. Live dissection of posterior female adult abdomen. DCG - distal cement gland, PCG - proximal cement gland, CO - common oviduct, LO - lateral oviduct. 23 X.

Figure 2. Scanning electron micrograph of posterior female adult abdomen. Main abdominal trunk nerves (NR) appear to send branches to the cement gland 31 X.

Figure 3. Distal cement gland. The central lumen is visible in this Karnovsky fixed gland. 42 X.

Figure 4. Scanning electron micrograph of the junction between the distal cement gland, enveloped in a smooth basal lamina, and the proximal cement gland, with its longitudinal muscles. 154 X.

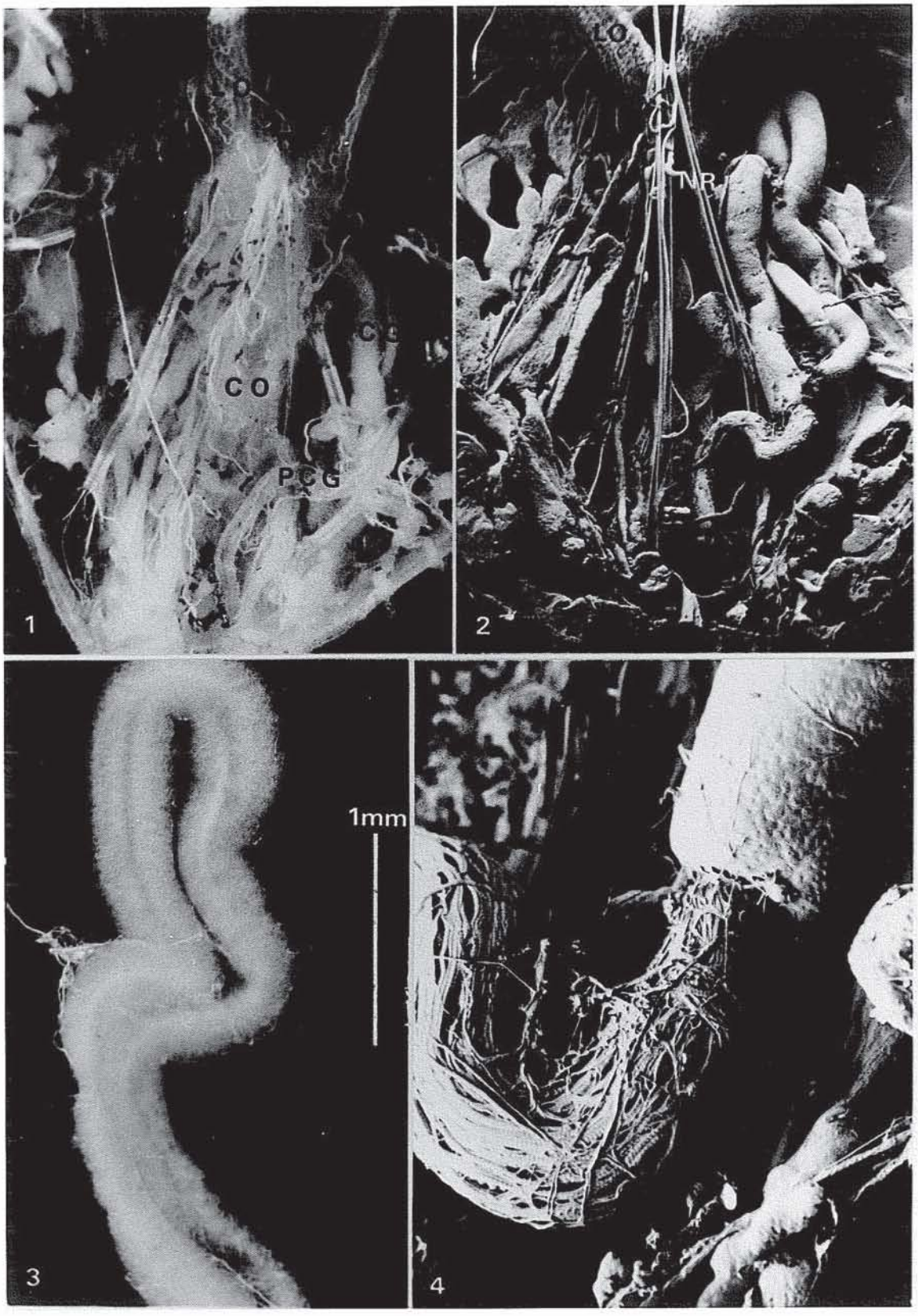
CO
PCG
1
2
NR
1mm
3
4

Plate 2

Distal (Secretory) Gland

Figure 5. The tip of the live distal cement gland, taken with Nomarski interference. The numerous gland cells (GC), are connected to the central duct (D) by long ductules 740 X.

Figure 6. Semi-thin section of posterior part of the distal gland. Note the numerous gland cells (over 300 in this section), surrounding a thin region with no gland cells, surrounding the central duct. Karnovsky's fixative. Toluidine blue 616 X.

Inset. Isolated gland cell unit with centrally located end apparatus and attached ductule. Rehydrated lyophilised material. Photographed by E. Huebner. Nomarski interference 1320 X.

Figure 7. Scanning electron micrograph of partially trypsinized distal gland. Note the gland cells through the peeled back basal lamina (BL). 1866 X.

Figure 8. Scanning electron micrograph of partially trypsinized distal gland, with some gland cells intact, some completely digested revealing the end apparatus, with ductules attached to the duct cuticle (DC). (BL) - basal lamina. 2342 X.

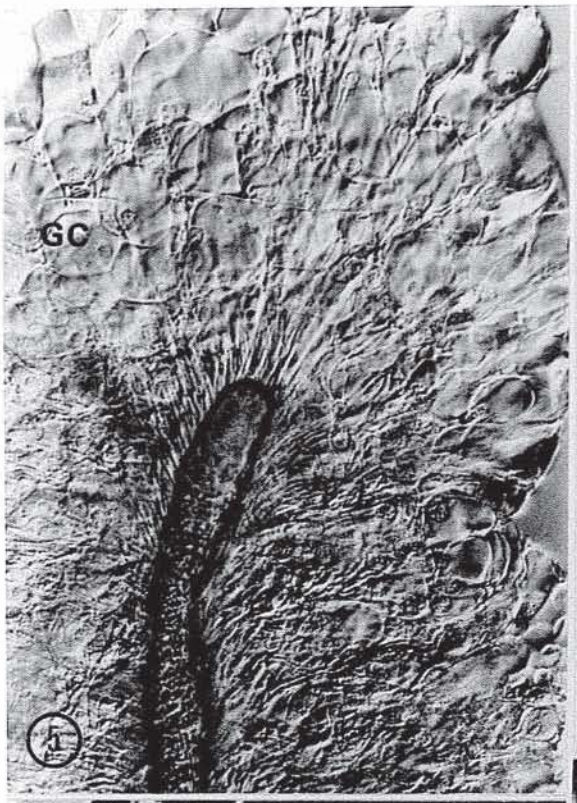

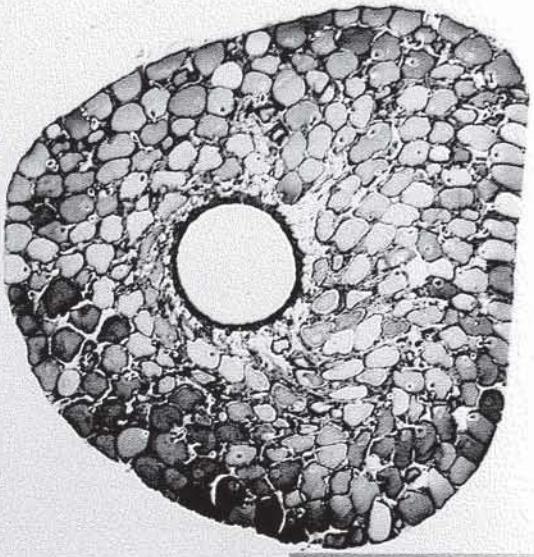

6

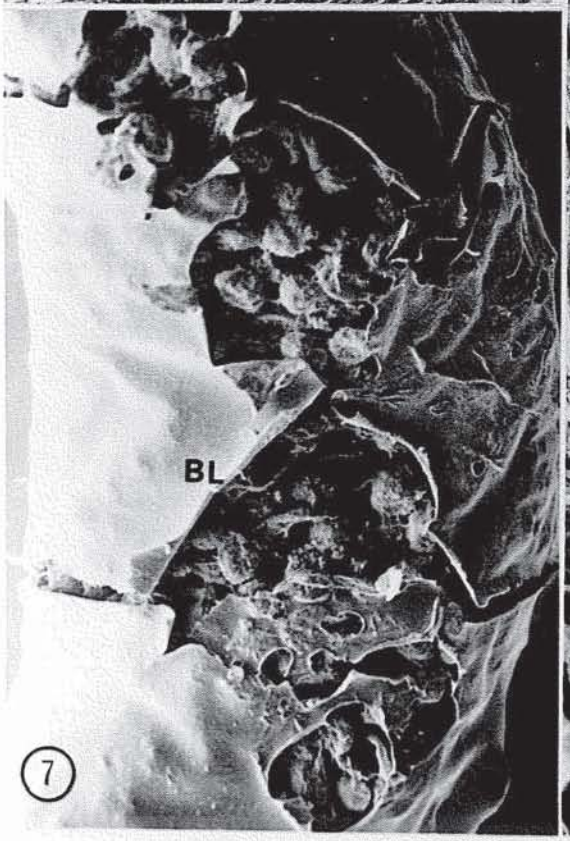

7

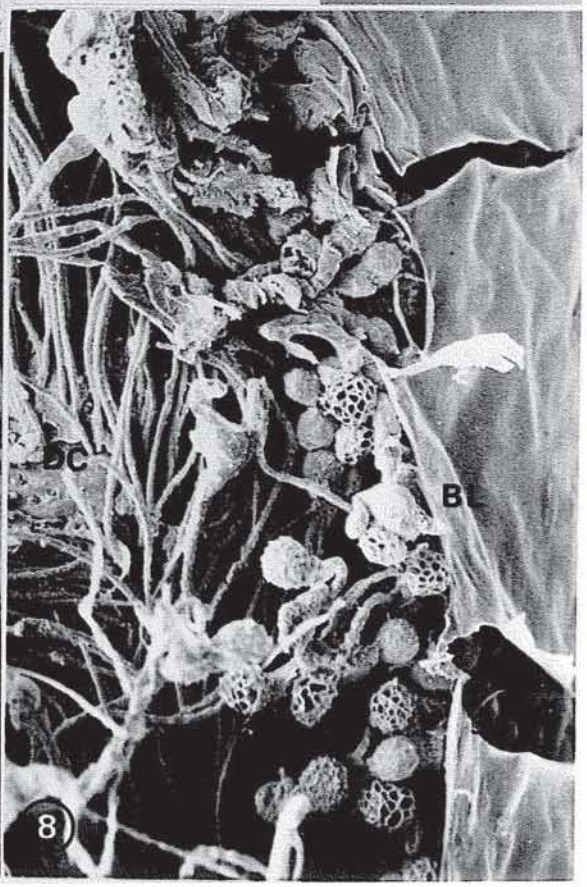

8

Plate 3

Secretory Unit

Figure 9 - 12. Live Nomarski micrographs of a cement gland cell, showing the central end apparatus, and ampulla, in 4 focal planes. 3076 X.

Figure 13. Electron micrograph of segments of three adjacent gland cells. Note the extensive rough endoplasmic reticulum (RER), flattened irregular nucleus (Nu) with large prominent nucleolus (N), mitochondria (m) adjacent to the reservoir (R) plasma membrane, which has occasional microvilli (M). Note the cell processes in the intercellular space between the cells (arrows). Karnovsky's fixative. 17,490 X.

Inset. Semi-thin section of gland cells. Karnovsky's fixative Toluidine blue. 2375 X.

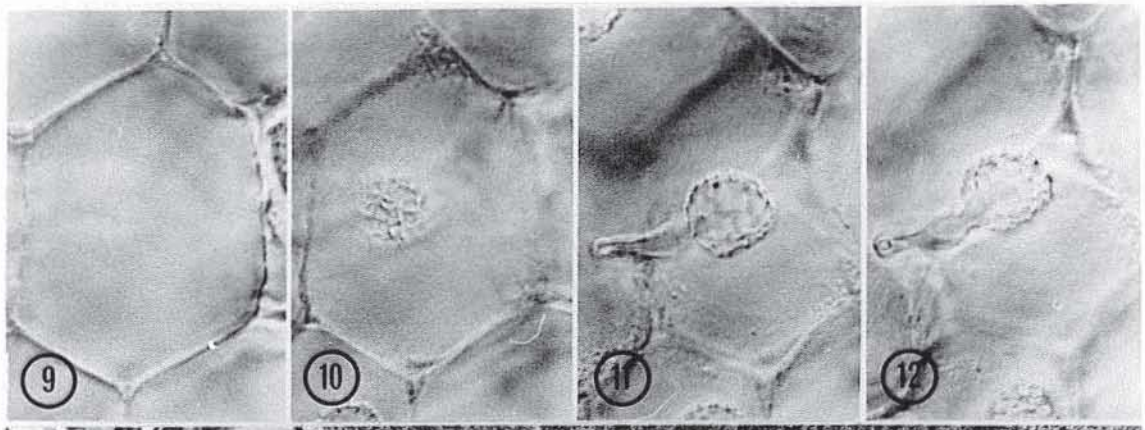
9
10
11
12

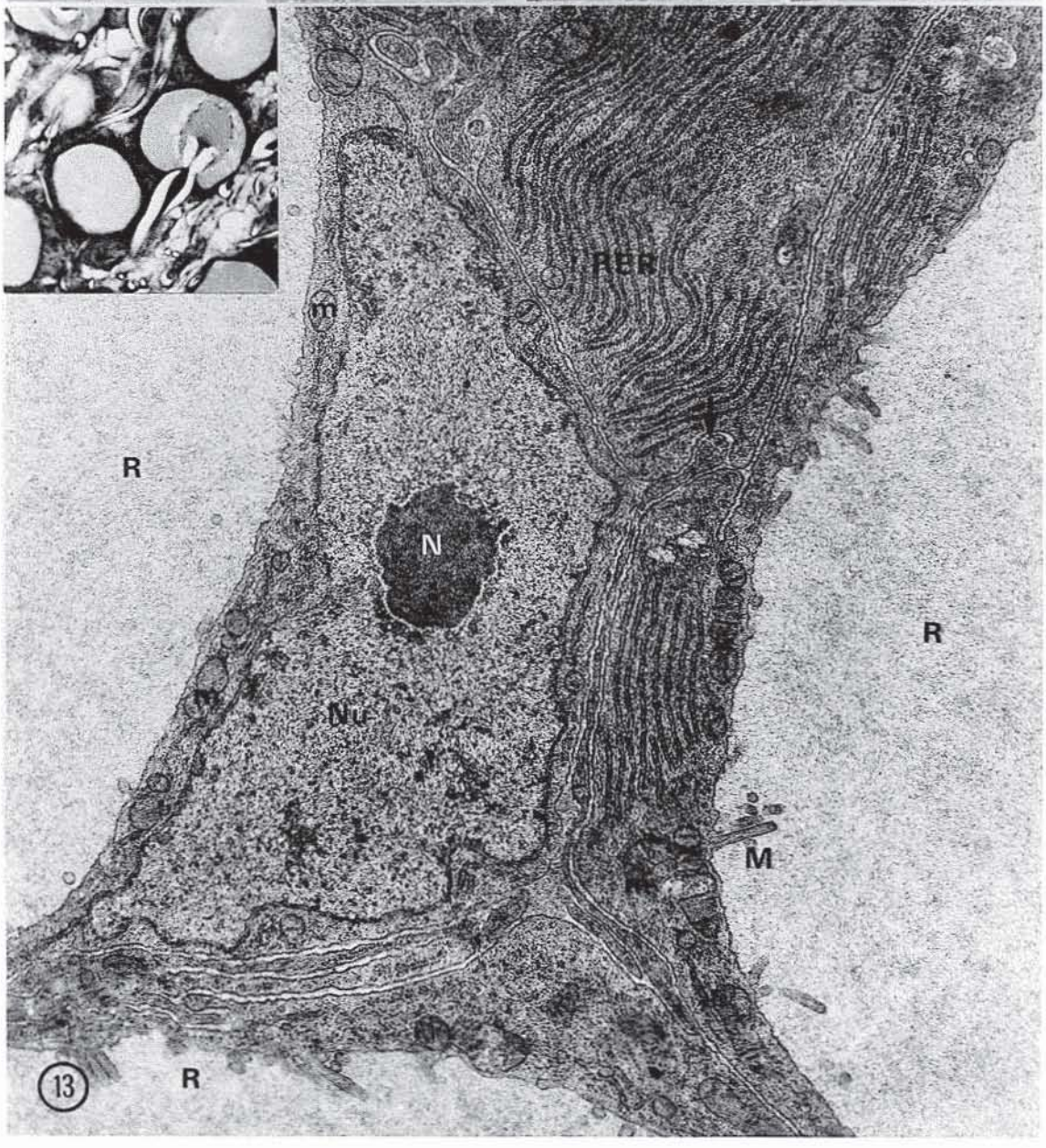
RER
m
R
N
Nu
M
R
R
13

Plate 4

Secretory Cell - Fine Structure

Figure 14. High magnification electron micrograph of nuclear region adjacent to the reservoir (R). Nu - nucleus, M - microvilli, arrows - microtubules. Karnovsky's fixative. 32,230 X.

Figure 15. High magnification of the prominent rough endoplasmic reticulum. Note the dense staining material within the RER tubules multi-vesicular body with contained ribosomes, and part of the end apparatus within the reservoir. Karnovsky's fixative. 22,580 X.

Figure 16. Electron micrographs of gland cell showing RER with associated multi-vesicular bodies (mvb) containing ribosomes, Golgi (G) near the plasma membrane lining the intercellular space (IS). Nu - nucleus, R - reservoir, d - ductule. Karnovsky's fixative. 23,075 X.

Figure 17. Grazing thin section of a gland cell showing cross-sections through microvilli (M) within the reservoir (R). Note how the cytoplasm projection of the adjacent cell invaginates (arrow) into the next cell. m - mitochondria. Karnovsky's fixative. 14,770 X.

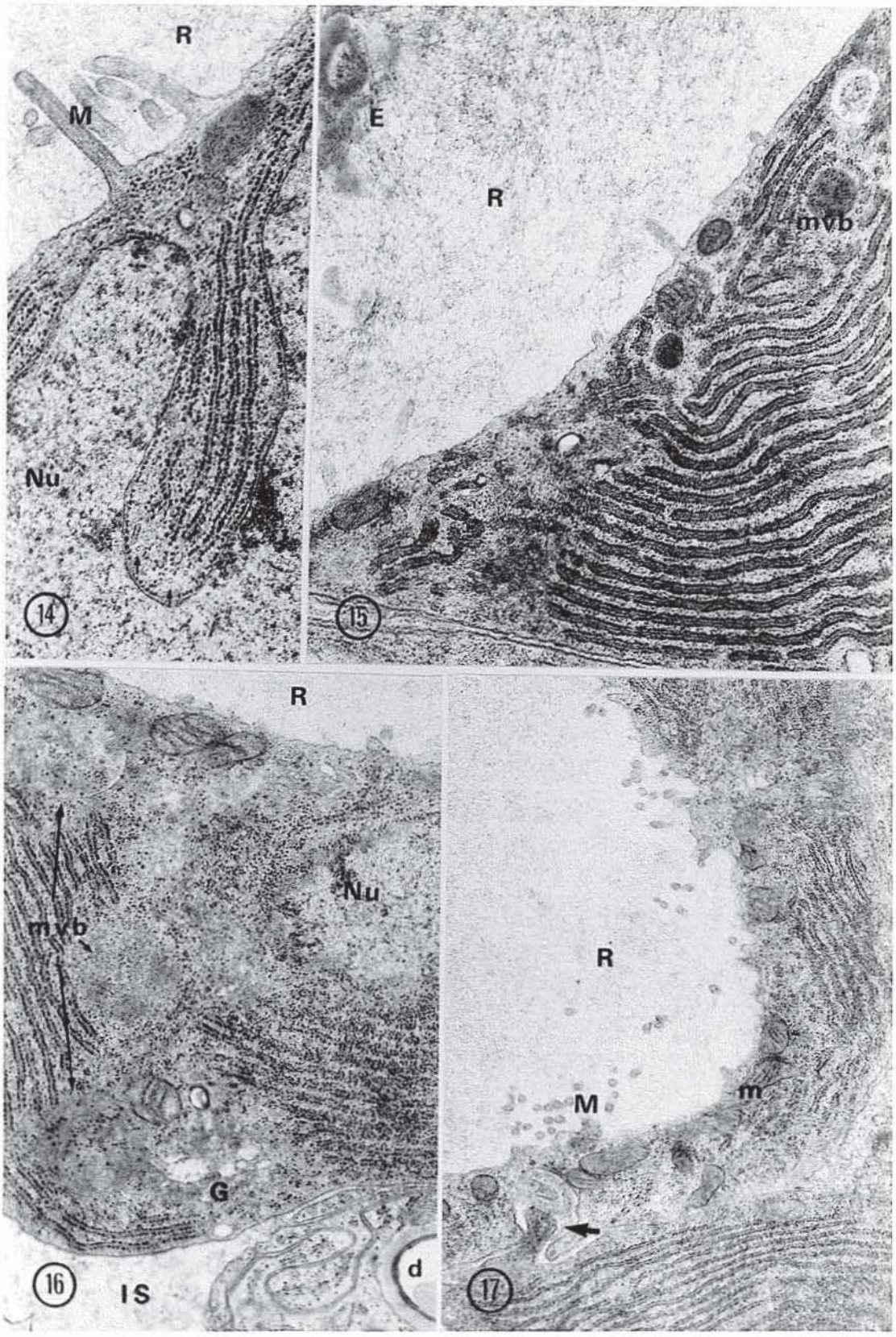
R
M
Nu
14
E
R
mvb
15
R
Nu
mvb
G
d
16
IS
R
M
m
17

Plate 5

Gland Cells and End Apparatus

Figure 18. Thin section of a gland cell adjacent to the intercellular space (IS), with nearby cytoplasmic projection. G - Golgi, mvb - multivesicular body. Karnovsky's fixative. 25,530 X.

Figure 19. Scanning electron micrograph of the distal cement gland with tracheoles (T) penetrating the enveloping basal lamina. Tr - trachea. Karnovsky's fixative. 185 X.

Figure 20. Nomarski micrograph of unfed adult gland. Note the size of the reservoir is not much larger than the end apparatus. 2,900 X.

Figure 21. Semi-thin section of fed cement gland with expanded reservoir. Karnovsky's fixative. Toluidine blue. 3960 X.

Figure 22. Scanning electron micrograph of trysin-treated distal cement gland. Note the numerous ductules with attached end apparati. Karnovsky's fixative. 1850 X.

Insert. Thin section of a tracheole. Karnovsky's. 25,860 X.

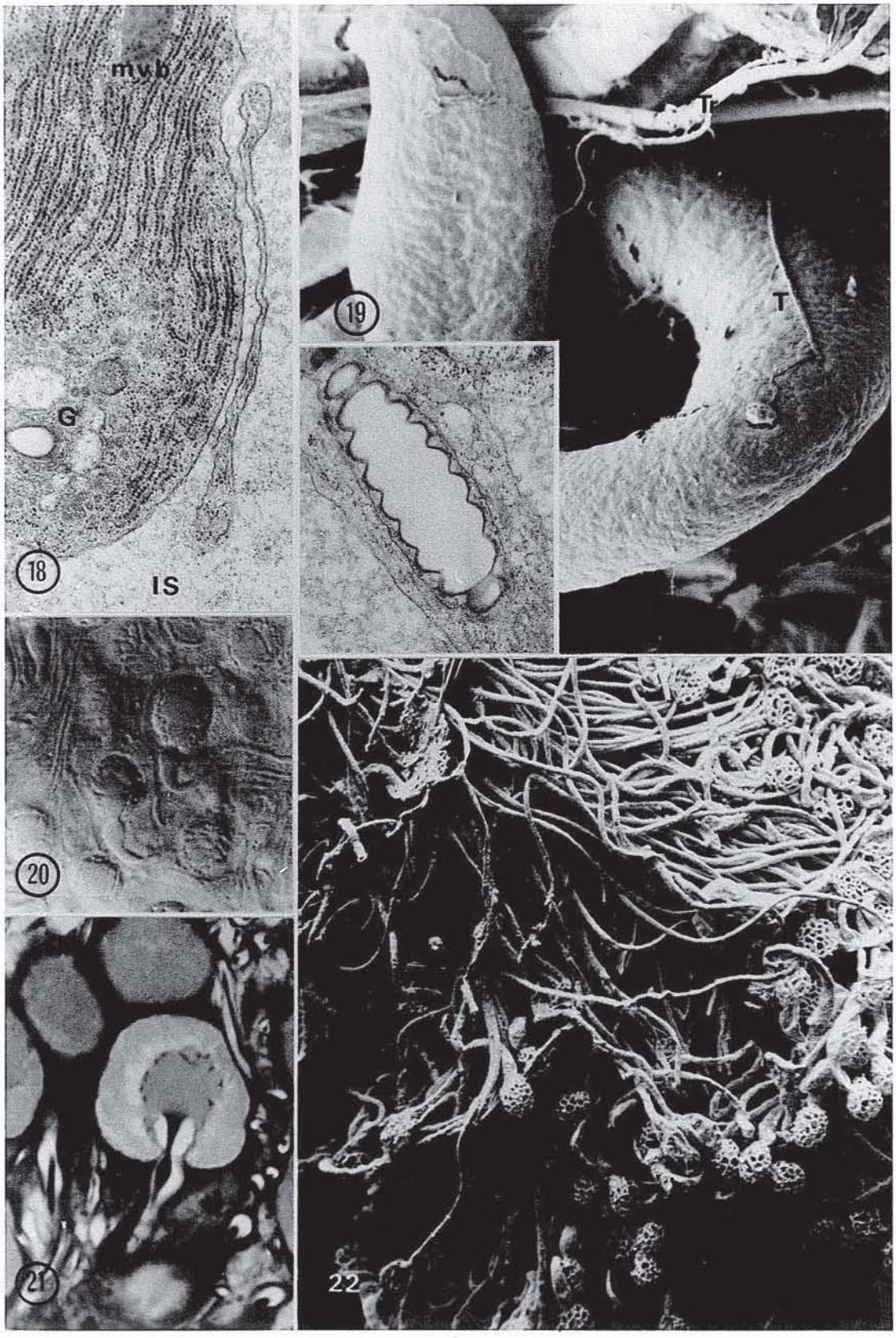
m.v.b
G
18
IS
19
Tr
T
20
21
22

Plate 6

End Apparatus and Funnel

Figure 23. Scanning electron micrograph of trypsinized end apparatus (E) with attached ampulla (A) and ductules (d). 7650 X.

Figure 24. High magnification scanning electron micrograph of the end apparatus (E) attached to the funnel (F). The collar (C) joins the funnel to the ampulla (A). d - ductule. The end apparatus is a highly elaborate interconnecting, polygonal cuticular lattice, with occasional cuticular projections. 21,100 X.

Figure 25. Semi-thin section of a gland cell unit. Note the difference in the staining densities of the secretion in the reservoir (R) as it passes through the end apparatus (arrows) and into the funnel and ampulla A. Karnovsky's fixative. Toluidine blue. 5100 X.

Figure 26. This cross-section through the ampulla region (A) shows the core of secretion (S) within the lumen (L) of the ampulla. R - reservoir. Karnovsky's fixative. 15,075 X.

Figure 27. Electron micrograph of section similar to Figure 25, with the end apparatus (E) within the reservoir. Note how the secretion (S) stains more electron dense as it enters the funnel (F) and ampulla (A). Karnovsky's fixative. 8870 X.

Figure 28. Note the dense secretion (S) within the funnel. Karnovsky's fixative. 9,230 X.

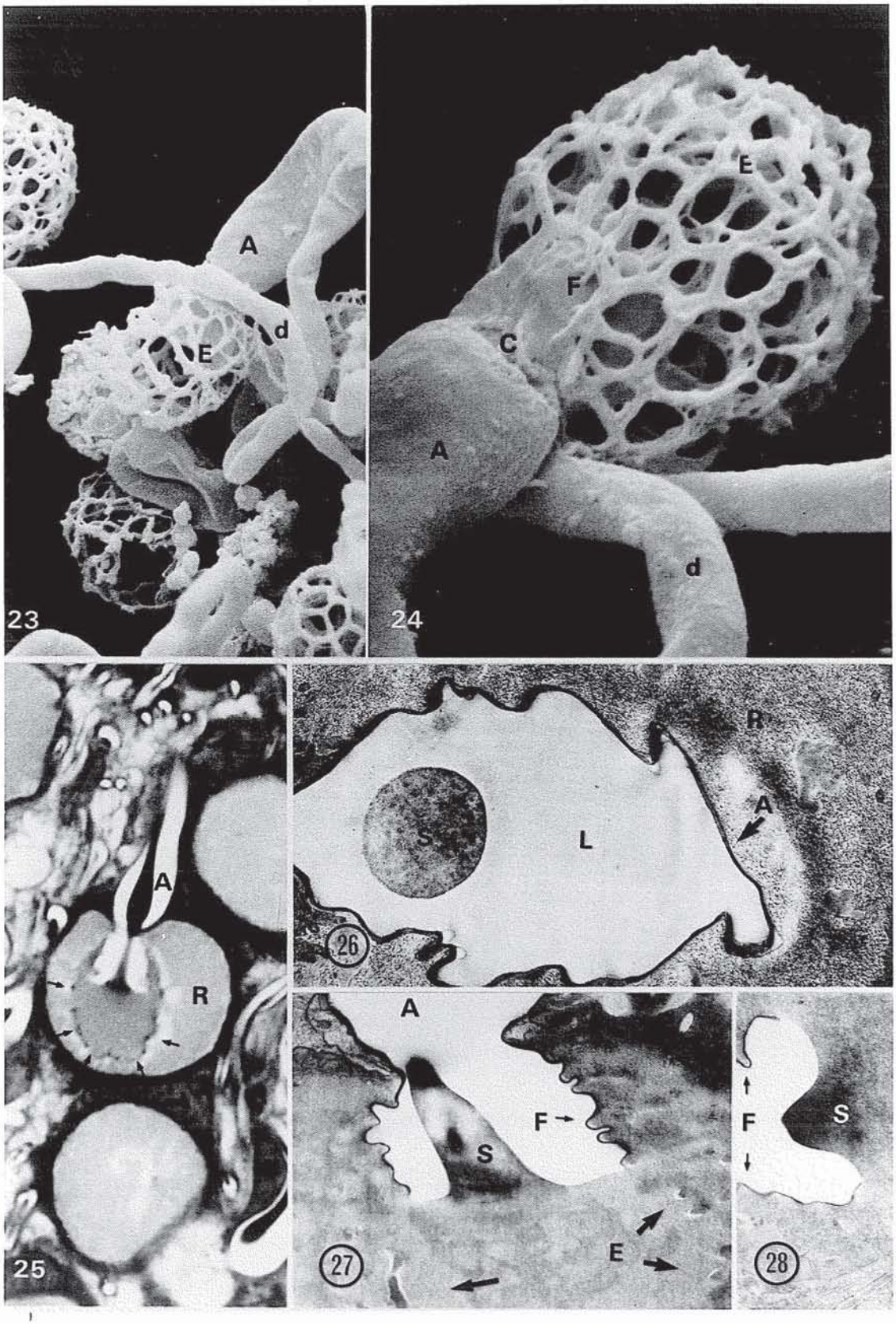
A
d
E
23
E
F
C
A
d
24
A
R
25
R
A
S
L
26
A
F
S
E
27
F
S
28

Plate 7

Ductules

Figure 29. Scanning electron micrograph of a completely trypsinized distal gland that had been broken, showing ductules (d) attached to the central duct cuticle (DC). 4120 X.

Inset. Live Nomarski micrograph of an end apparatus with ductules attached to the central duct cuticle (DC). 2900 X.

Figure 30. Thin cross-section of ductules (d) near the central duct. Some ductules are closely opposed and are joined by septate junctions (s) while others are separated by the large intercellular space (IS). Karnovsky's fixative. 13,850 X.

Figure 31. Semi-thin section of region near the main duct with ductules isolated in the vast intercellular space and some adjacent to the duct cuticle. Note the thin cellular projections traversing the intercellular space (arrows). Karnovsky's fixative. 2,640 X.

Figure 32. Thin section of an isolated ductule (d) with associated cytoplasmic projections from distant ductule cells. IS - intercellular space. Karnovsky's fixative. 10,820 X.

Figure 33. Thin section of two adjacent ductules. Note how the ductule cell wraps around the double layered cuticular ductule, with enclosed secretion (S), and adheres to itself by septate junctions. The two cells are joined together by a short septate junction (larger arrow). The cytoplasm contains sparse ribosomes and microtubules (small arrows). c - cuticulin, e - epicuticle. Karnovsky's. 39,670 X.

Figure 34. Thin section of single ductule through the nucleus (Nu). S - secretion, s - septate junction, IS - intercellular space, arrow - microtubule. Karnovsky's. 30,550 X.

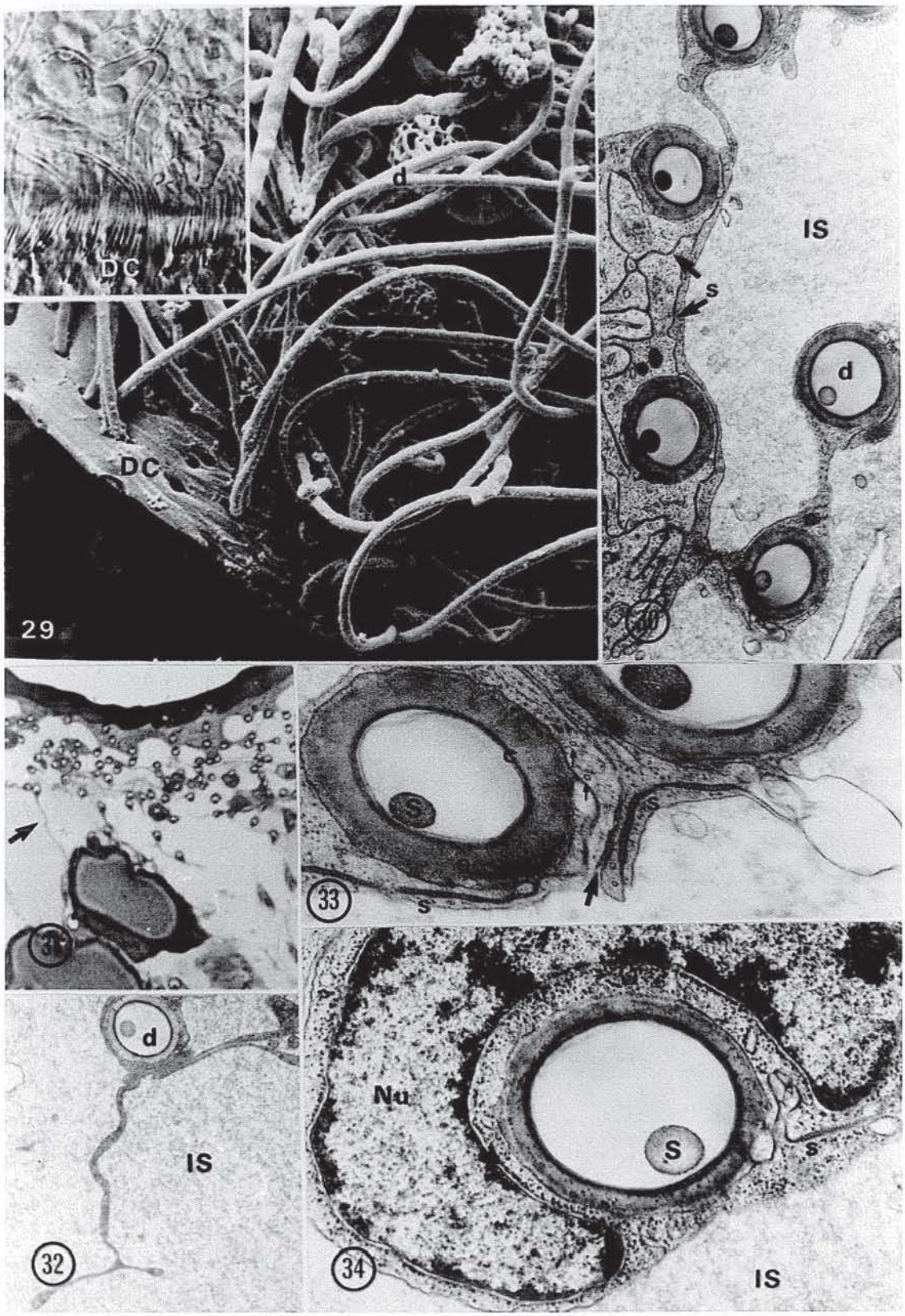
DC
d
DC
29
IS
s
d
31
33
S
s
d
IS
32
Nu
S
s
34
IS

Plate 8

Distal Gland - Cell Features

Figure 35. Thin section of a gland cell adjacent to the intercellular space (IS). Notice the Golgi (G) adjacent to the outer plasmalemmal surface, and the morphological difference between the flocculence in the intercellular space and the reservoir. Karnovsky's fixative. 26,250 X.

Figure 36. Slightly oblique thin section of a ductule (d). The ductule adheres to itself by an extensive septate junction (s), a macular desmosome (ds) and a gap junction (g). S - secretion, G - Golgi, IS - intercellular space, m - mitochondria. Karnovsky's fixative. 33,120 X.

Figure 37. Live Nomarsky micrograph of the central duct (DC) with attached ductules. 1820 X.

Figure 38. Thin section of epithelial layer adjacent to the central duct cuticle (DC). The thin cell layer is joined by extensive lateral septate junctions (s). IS - intercellular space, d - ductule. Karnovsky's fixative. 15,820 X.

Inset. Semi-thin section, low magnification, of a region similar to Figure 38. Karnovsky's fixative. 1320 X.

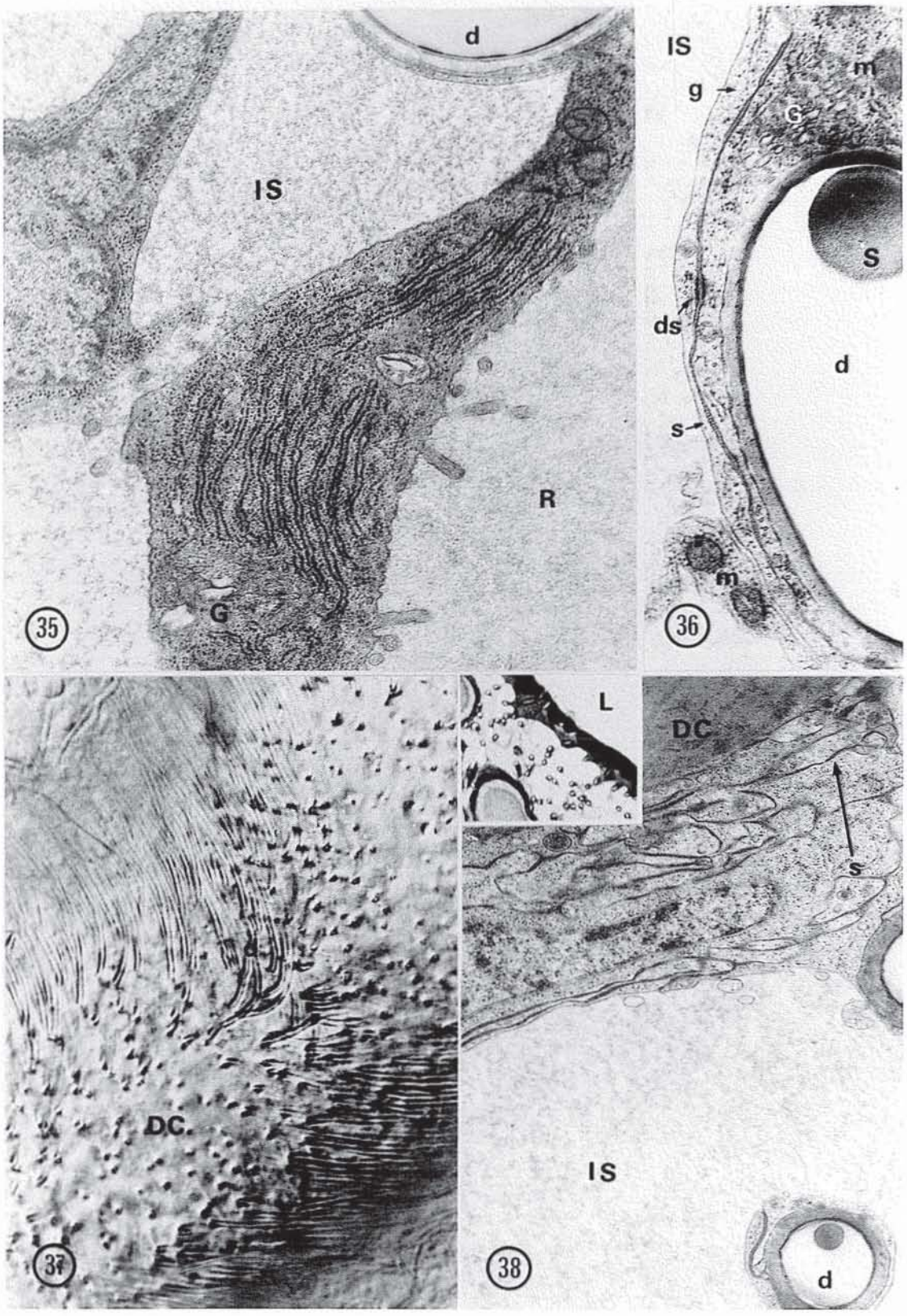
d
IS
R
G
35
IS
m
g
c
S
ds
d
s
m
36
L
DC
s
d
DC.
37
IS
38
d

Plate 9

The Central Duct - Secretion

Figure 39 - 41. Scanning electron micrographs of a broken distal cement gland with gland cells (GC) and ductules joined to the central duct. The secretion (S) appears as a spiny rod within the duct lumen. Strands of secretion pass through holes in the inner duct cuticle (arrows) and pool in the lumen. 410 X, 1025 X, and 4100 X, respectively.

Inset. Semi-thin longitudinal section of a distal gland. The ductules run from the gland cells, almost parallel to the lumen (L) before inserting. S - secretion. Karnovsky's fixative. Toluidine blue. 530 X. Photograph by E. Huebner.

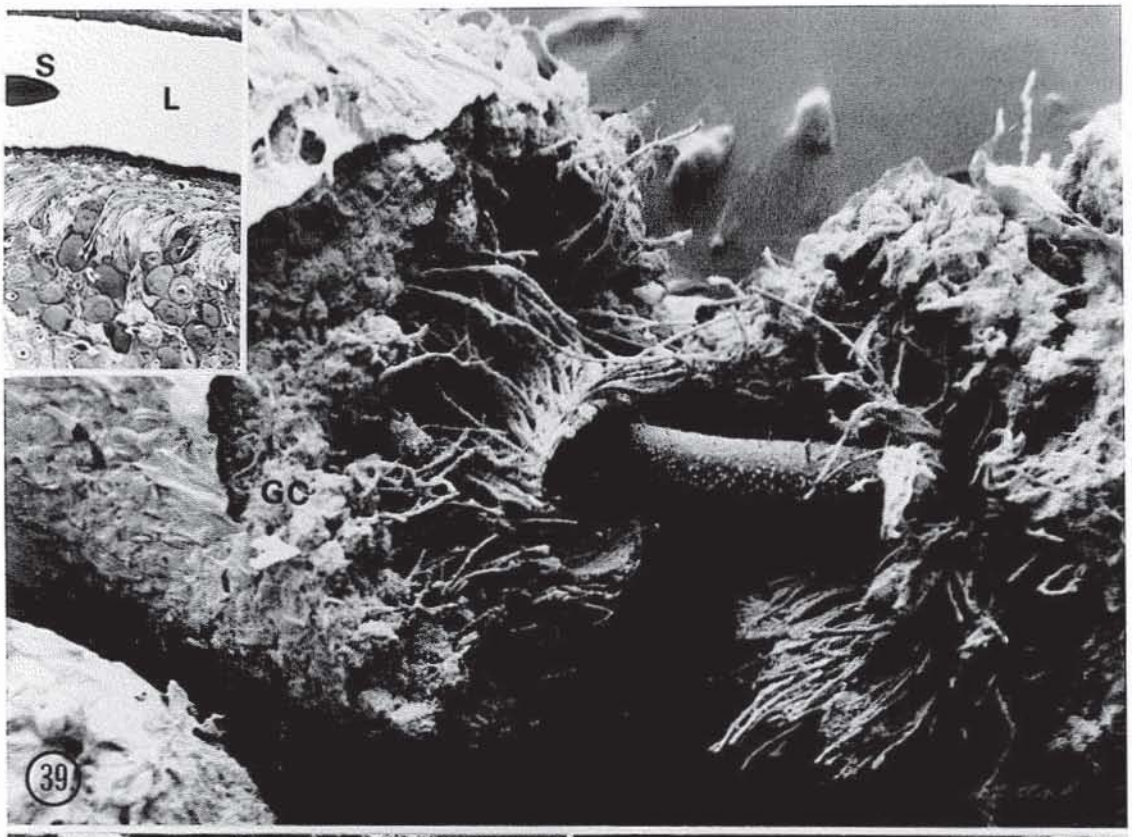
S
L
GC
39


S
d
40

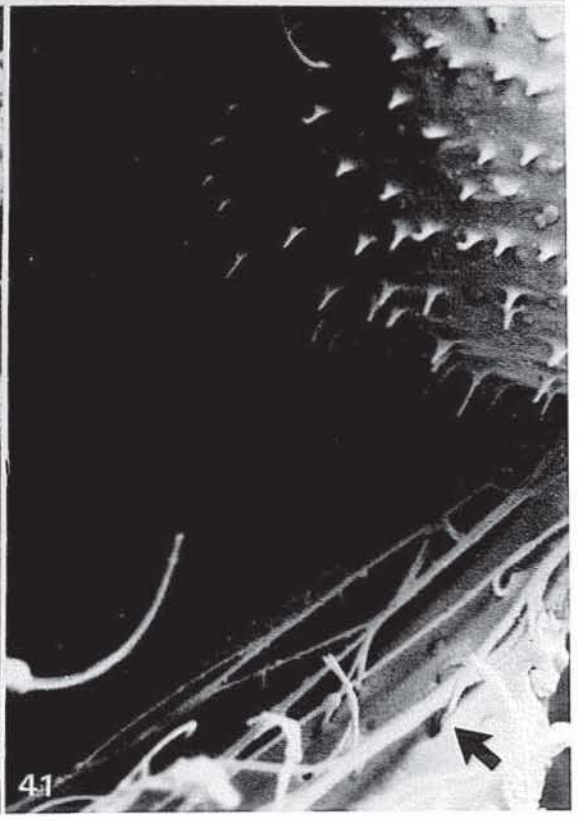
41

Plate 10

Gland Cell Secretory Unit

Figure 42. Line drawing of a distal cement gland cell unit, illustrating the thin spherical cell, wrapped around the reservoir, containing the end apparatus, attached to the ductule funnel, continuous with the ampulla. The gland cell attaches to the ductule cell by an extensive septate junction. The ductule cell wraps around the cuticle of the ductule and adheres to itself by a septate junction. The ductule penetrates the duct epithelial lining and joins to it by septates. The gland cell cyloplasm has abundant RER, and mitochondria. The reservoir plasmalemma is elaborated into widely spaced microvilli.

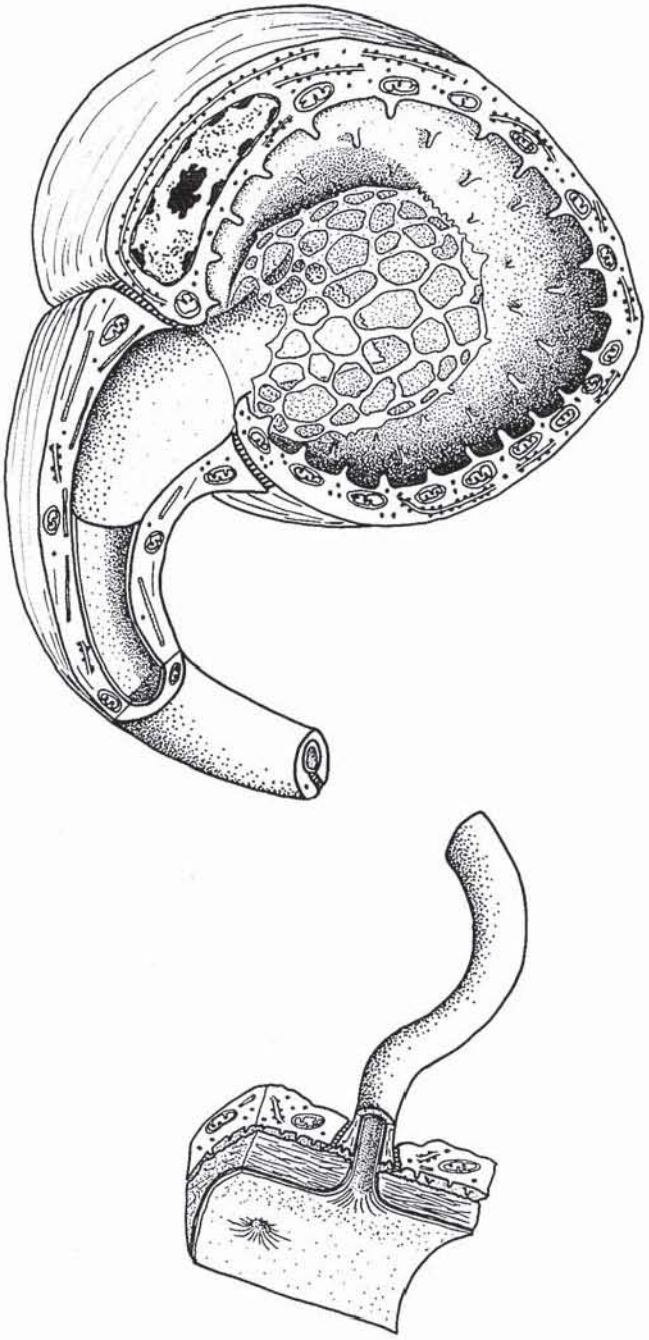

Plate 11

Proximal - Distal Gland Transition

Figure 43. Live Nomarski micrograph of the transition region between the proximal gland with its corrugated duct (CD), and the distal gland with its uncorrugated duct (D). 300 X.

Figure 44. Semi-thin section of the transition region between the distal and proximal glands. Note the abrupt change in cuticle and tissue morphology, with the distinct striations in the muscle of the proximal region. Karnovsky's fivative. Toluidine blue. 400 X.

Figure 45. Scanning electron micrograph of the proximal - distal transition region in a trypsin digested cement gland. Note the corrugated duct (CD). 760 X.

Figure 46. Polarizing micrograph of a live gland showing the intense birefringence of the muscle in the proximal gland compared to the slight birefringence of the ductules in the distal gland. Note how the muscle does not extend to the proximal duct terminus. 160 X.

Figure 47. Semi-thin cross-section of the proximal gland showing the muscle layer (ms) and the epidermal layer (e) adjacent to the thick cuticle. S - secretion, arrow - tracheole. Karnovsky's fixative. Toluidine blue. 840 X

Figure 48. Scanning electron micrograph of the muscle of the proximal gland, with striations evident in the longitudinally arranged muscle strands. T - trachea. Karnovsky's fixative. 315 X.

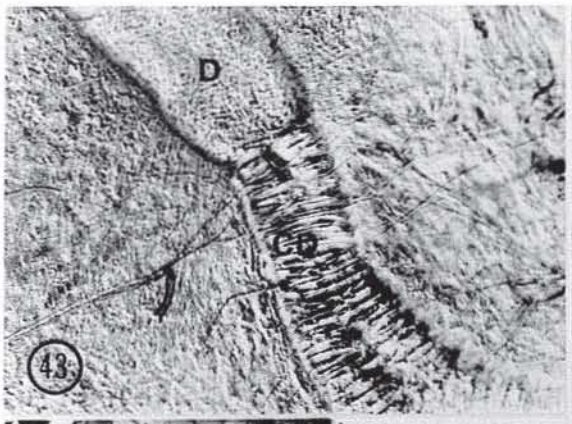
D
CD
43

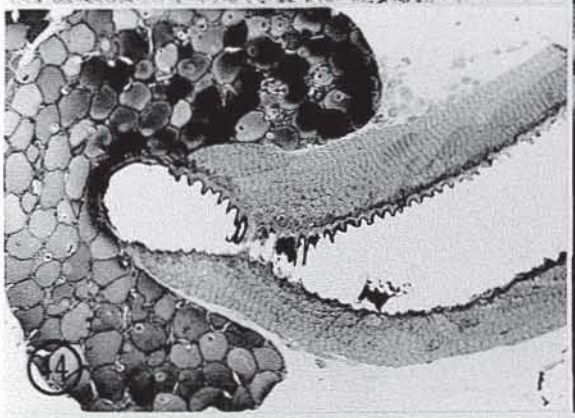
44

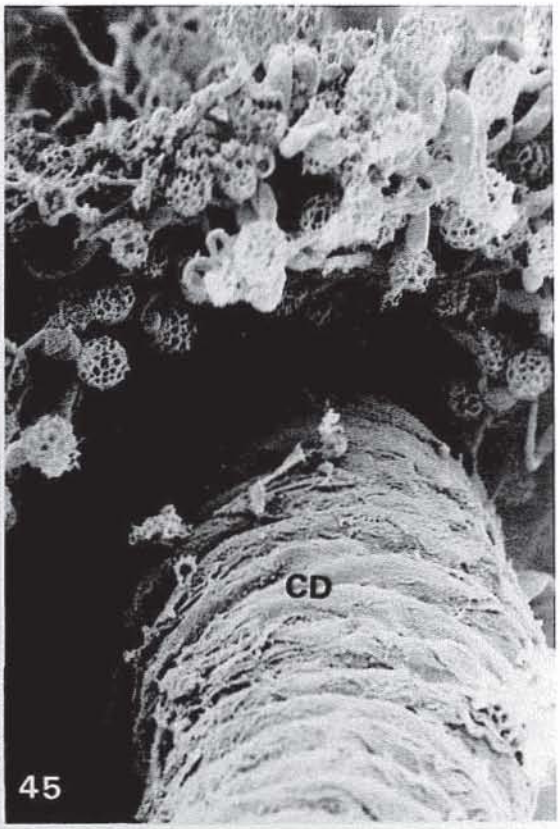
CD
45

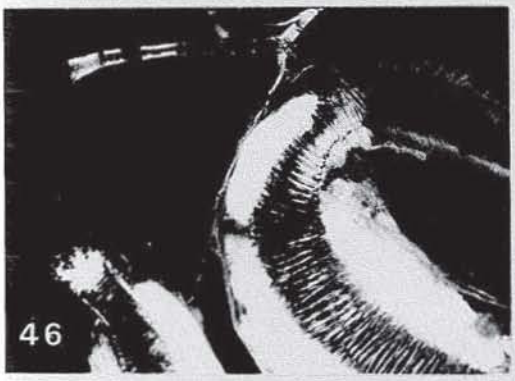
46

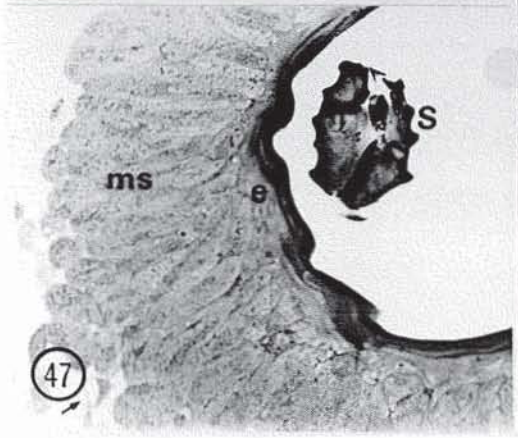
S
ms
e
47


T
48

Plate 12

Proximal Gland - Fine structure

Figure 49. Thin section of the muscle layer with a tracheole (T) lying between two muscle fibres. The filaments are arranged as one myosin filament surrounded by twelve actin filaments (inset). tt - t - tubule, Nu - nucleus, m - mitochondria. Karnovsky's fixative. 32,020 X.

Figure 50. High magnification of the proximal gland epithelium showing extensive cytoplasmic microtubules (t) associated with extensive zonular desmosomes (ds) joining the epithelial - muscle interphase. Karnovsky's fixative. 30,800 X.

Figure 51. Thin section of proximal gland squamous epithelium with lateral interdigitating membranes adjoined by extensive septate junctions (s). The luminal plasma membrane is in intimate contact with the duct cuticle (DC). The cytoplasm contains numerous microtubules (t). Nu - nucleus, ms - muscle layer. Karnovsky's fixative. 40,540 X.

Inset. Semi-thin section of the proximal region. 850 X.

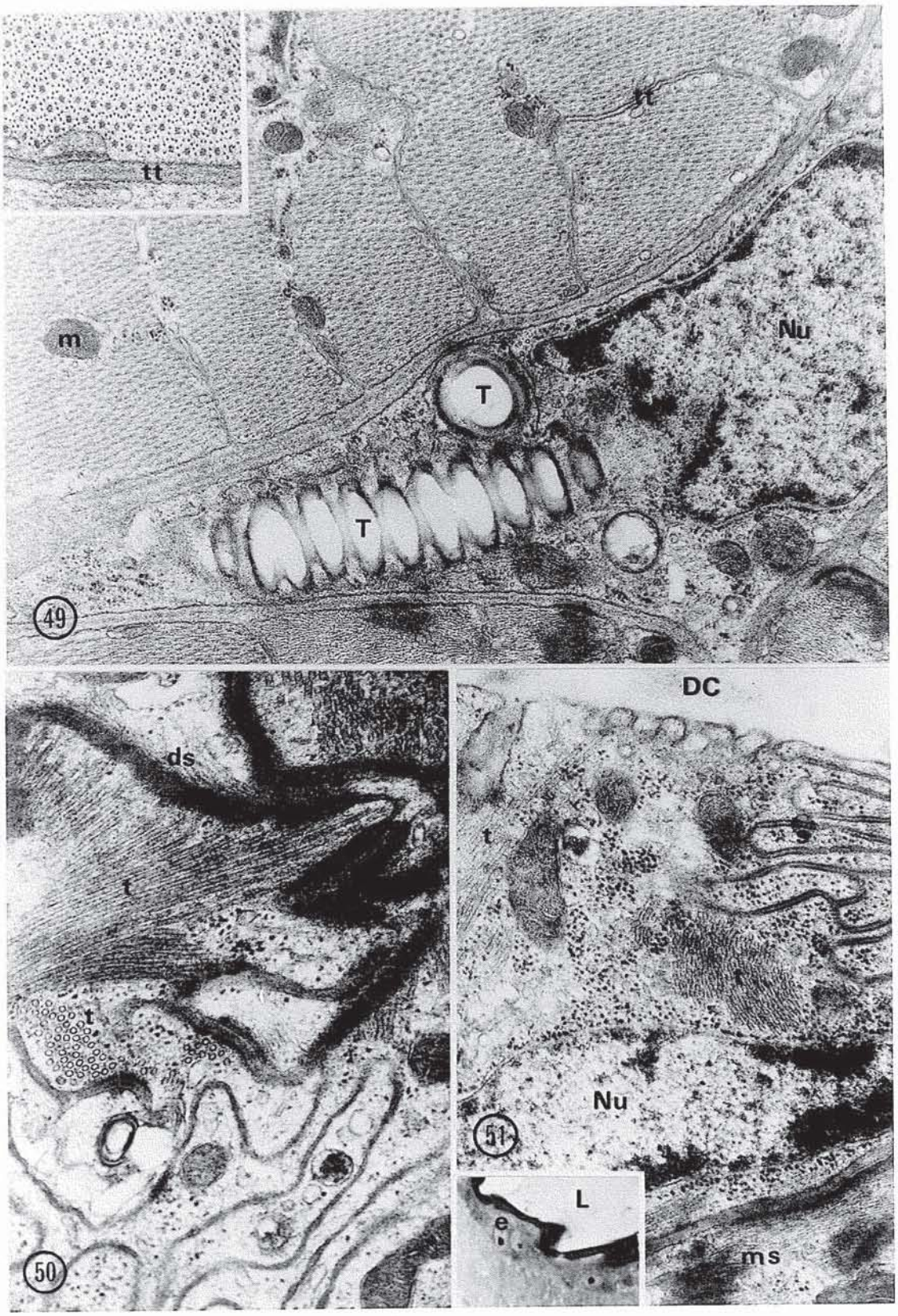
tt
m
T
T
Nu
49
ds
t
t
50
DC
t
Nu
51
L
e
ms

Plate 13

Duct Cuticle

Figure 52. Live Nomarski micrograph of the proximal gland showing the corrugated cuticle (CD) and muscle layers (ms).

Figure 53. Scanning electron micrograph of the proximal - distal gland transition, broken before viewing. Within the lumen (L) is the spiral shaped secretion (S), mirroring the shape of the duct. TR - trachea. Karnovsky's fixative. 720 X.

Figure 54. Scanning electron micrograph of a trypsinized proximal gland duct showing the corrugation, with some partially digested tissue attached. Karnovsky's fixative. 1530 X.

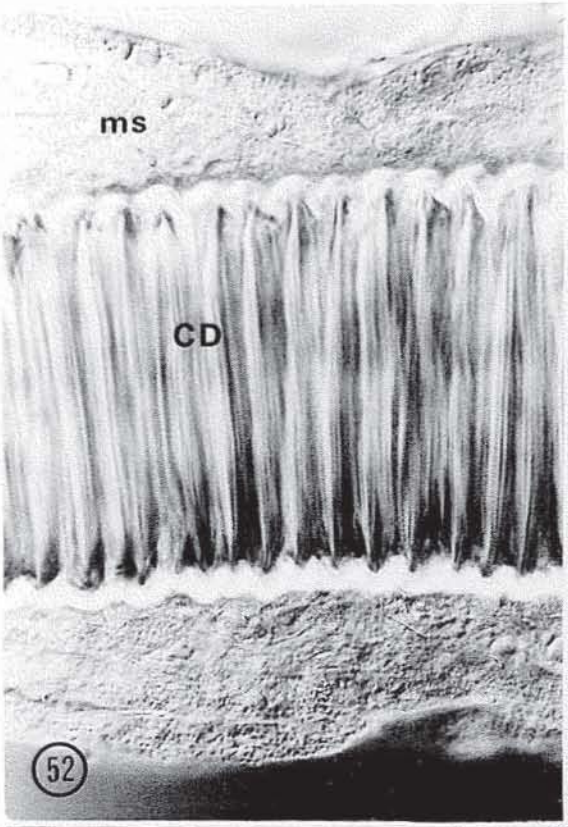
ms
CD
52


TR
L
S
53

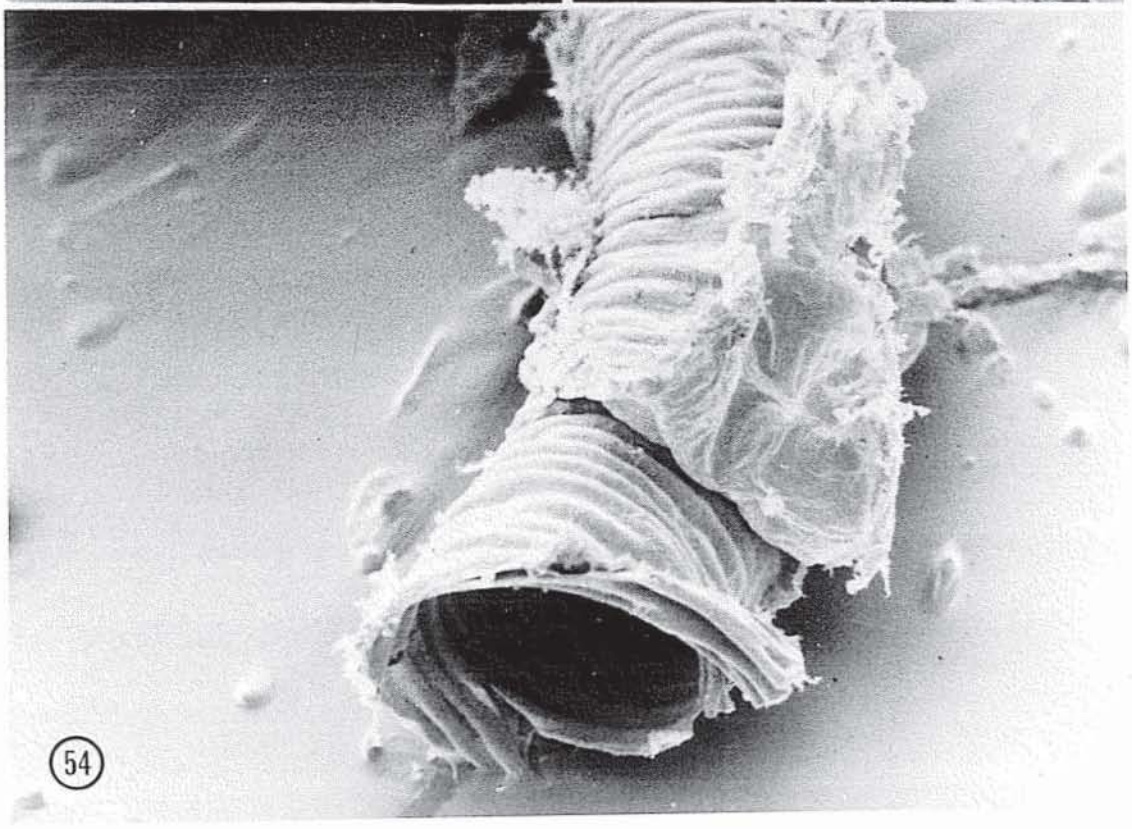
54

Plate 14

Unfed 5th Instar

Figure 55. Dissection of an unfed 5th instar abdomen with the gut removed. 7 X.

Figure 56. Scanning electron micrographs of a region similar to that circled in Figure 55, showing the undifferentiated 5th instar cement gland. Karnovsky's fixative. 370 X.

Figure 57. Cement gland differentiation series starting at day 0, day 2 and so on at two-day intervals to the adult, with the attached ovipositor, on the bottom right. Rapid overall growth proceeds from day 2 to day 14, when it reaches its adult length. Karnovsky's fixative.

Figure 58. Thin section of day 0 5th instar cement gland epithelium, near the central lumen. The luminal plasma membrane is in folds (f) with larval cuticle remnants at their tips. The cell cytoplasm is rich in free ribosomes and mitochondria. L - lumen. Karnovsky's fixative. 15,660 X.

Inset. Day 0 5th instar cement gland semi-thin cross-section, with inner epithelial layer (e) and outer mesothelial layer (ms). Karnovsky's fixative. Toluidine blue. 1480 X.

Figure 59. Higher magnification of Figure 58, showing larval cuticle (LC) at the tips of the membrane folds, and lateral membrane desmosomes (ds). Karnovsky's fixative 91,380 X.

Figure 60. The lateral membrane folds connect by extensive septat junctions (S).

Inset. Detail of septate junction. Karnovsky's fixative. 20,980 X.

Figure 61. Microtubules (t) extend longitudinally in the cytoplasi between the interdigitating lateral membranes. m - mitochondria, s - septate junctions. Karnovsky's fixative. 19,340 X.

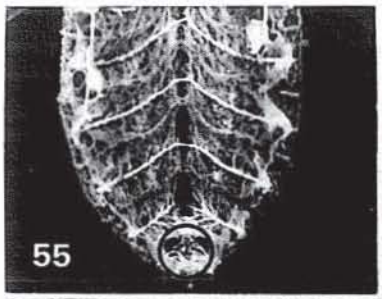
55


56

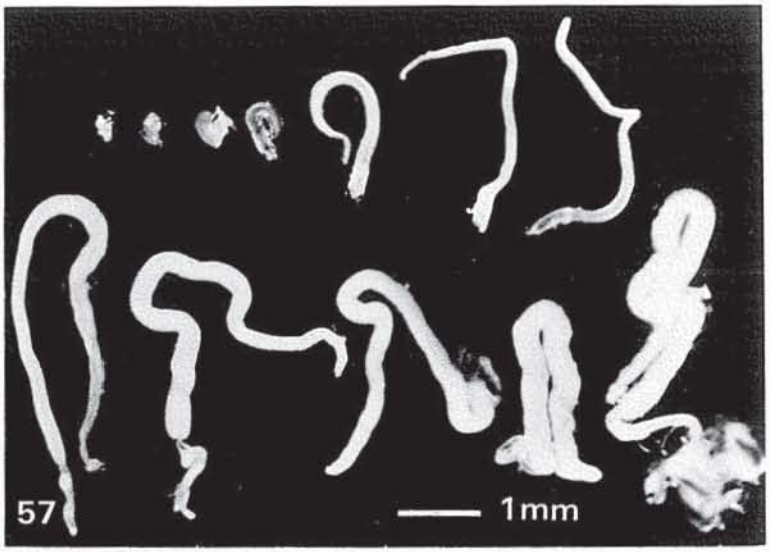
57
1mm

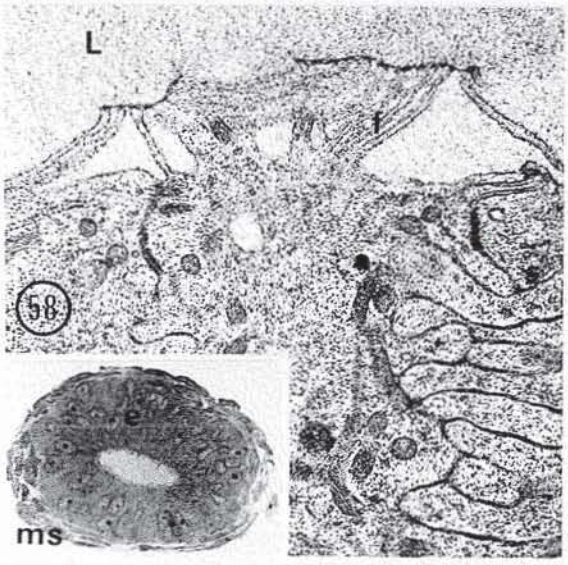
L
t
58

e
ms

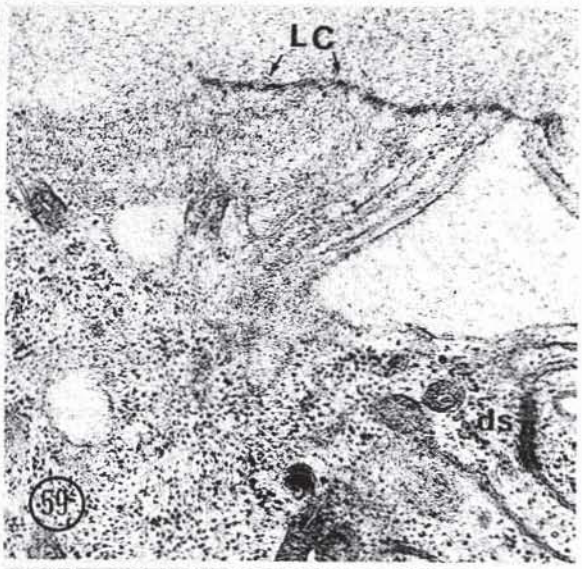
LC
ds
59

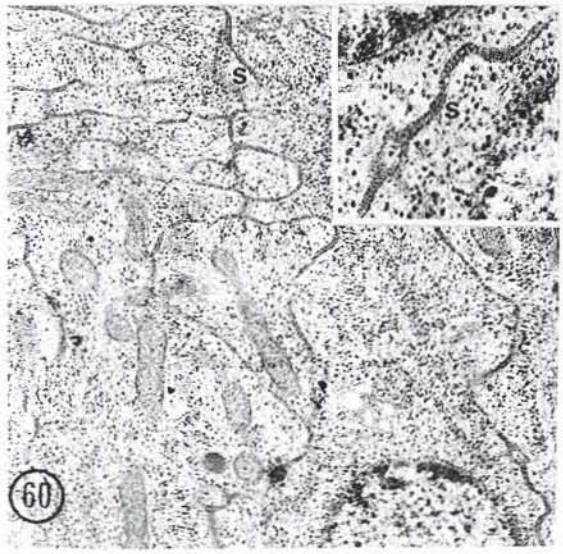
s
s
60

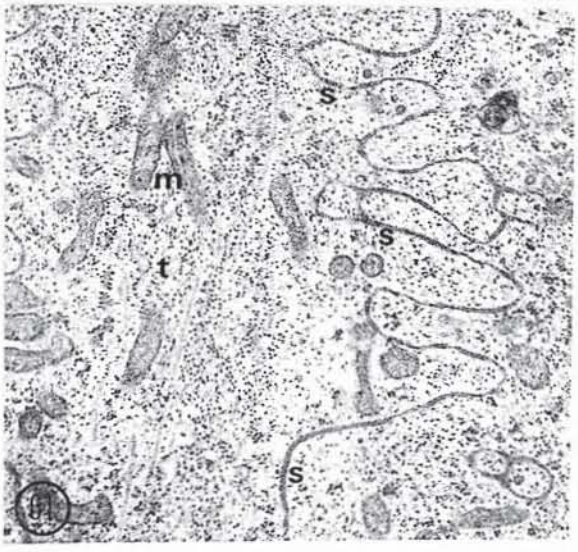
s
m
t
s
s
61

Plate 15

Early Growth and Mitosis

Figures 62 - 64. Semi-thin cross-sections of distal cement glands at day 2, 8 and 11 respectively. Mitotic figures are present adjacent to the central lumen. Figure 63 has an anaphase figure with the spindle parallel to the lumen. Non-dividing cells are elongate and pseudo-stratified. Hemocytes adhere to the basal lamina during fixation (arrow). Karnovsky's fixative. 1230 X.

Figure 65. Elongated epithelial cell extending from the lumen, part way to the basal lamina in a day 6 gland. Nu - nucleus, m - mitochondria. Karnovsky's fixative. 150 X.

Figure 66. High magnification of Figure 65, showing the numerous longitudinal microtubules. The lumenal microvilli (M) still have remnants of the larva cuticle present.

Inset. The lateral membranes connect by desmosomes (ds), and the centrioles are apically located. L - lume Karnovsky's fixative. 12,900 X and 14,400 X.

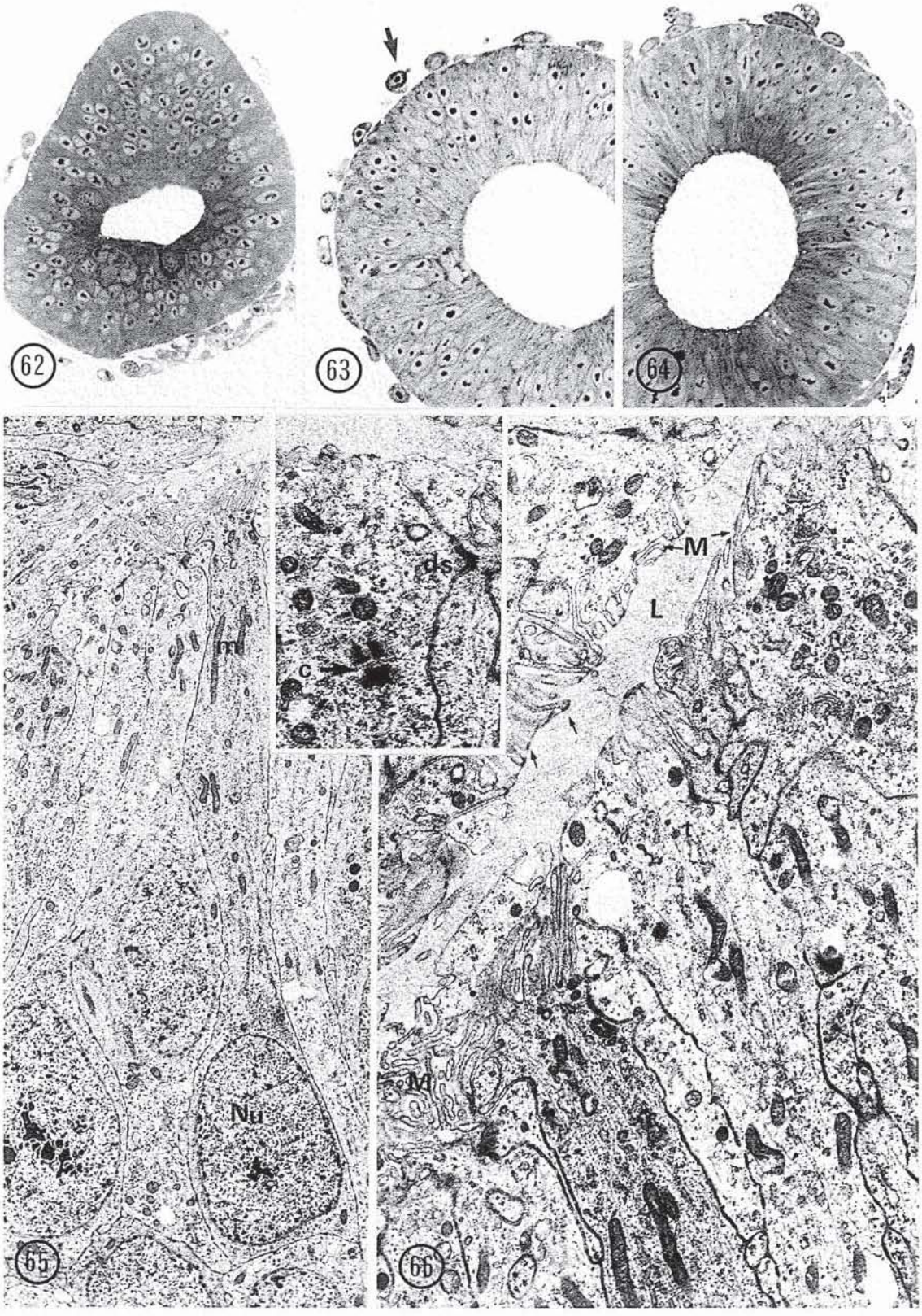
62
63
64
ml
ds
c
M
L
Nu
M
65
66

Plate 16

Proliferative Mitosis

Figure 67 and 68. Semi-thin sections of day 8 glands with lumenal cells in various mitotic stages. Karnovsky's.Toluidine blue. 2890 X and 1320 X.

Figure 69. A dividing cell, with only one set of chromosomes (Cr) in the plane of section. Karnovsky's fixative. 6,880 X.

Figure 70. Telophase cell with spindle still intact, with the nuclear envelope reforming. Nu - nucleus, t - microtubules, m - mitochondria. 26,660 X.

Figure 71. Divided cells, with the spindles (SP) still intact. The cells have begun to extend toward the basal lamina. Karnovsky's. 9,970 X.

Figure 72. High magnification of Figure 71 of the mid-body and spindle microtubules (t). Karnovsky's. 32,463 X.

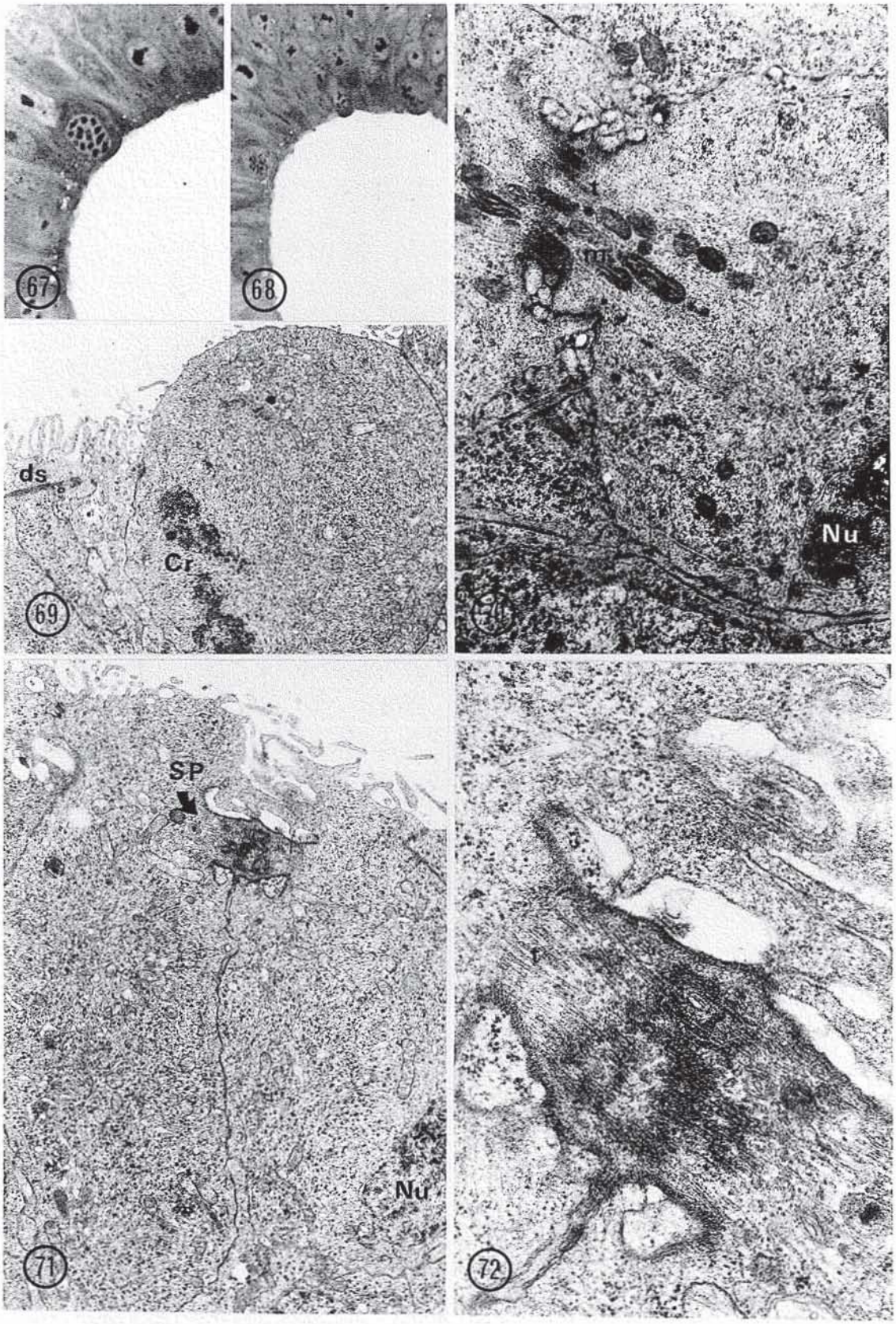
67
68
ds
Cr
69
m
Nu
70
SP
Nu
71
72

Plate 17

Differentiative Divisions

Figure 73. The epithelial cells' centrioles divide prior to rounding up and cell division. Single arrow - one set of centrioles. Curved arrows - double set. Karnovsky's. 12,080 X.

Figure 74. Two cells at metaphase, with spindles rotating perpendicularly to the lumen. Cr - chromosomes. Karnovsky's. 9,370 X.

Figure 75. Cell at anaphase. Karnovsky's. 6,210 X.

Figure 76. Telophase cell with spindle perpendicular to lumen. Nu - nucleus. Karnovsky's. 5,450 X.

Figure 77. Completely divided cell A (cA) beginning to extend towards the basal lamina (see inset). cC - cell C, d - ductule. Karnovsky's. 19,880 X.

Inset. 3,360 X.

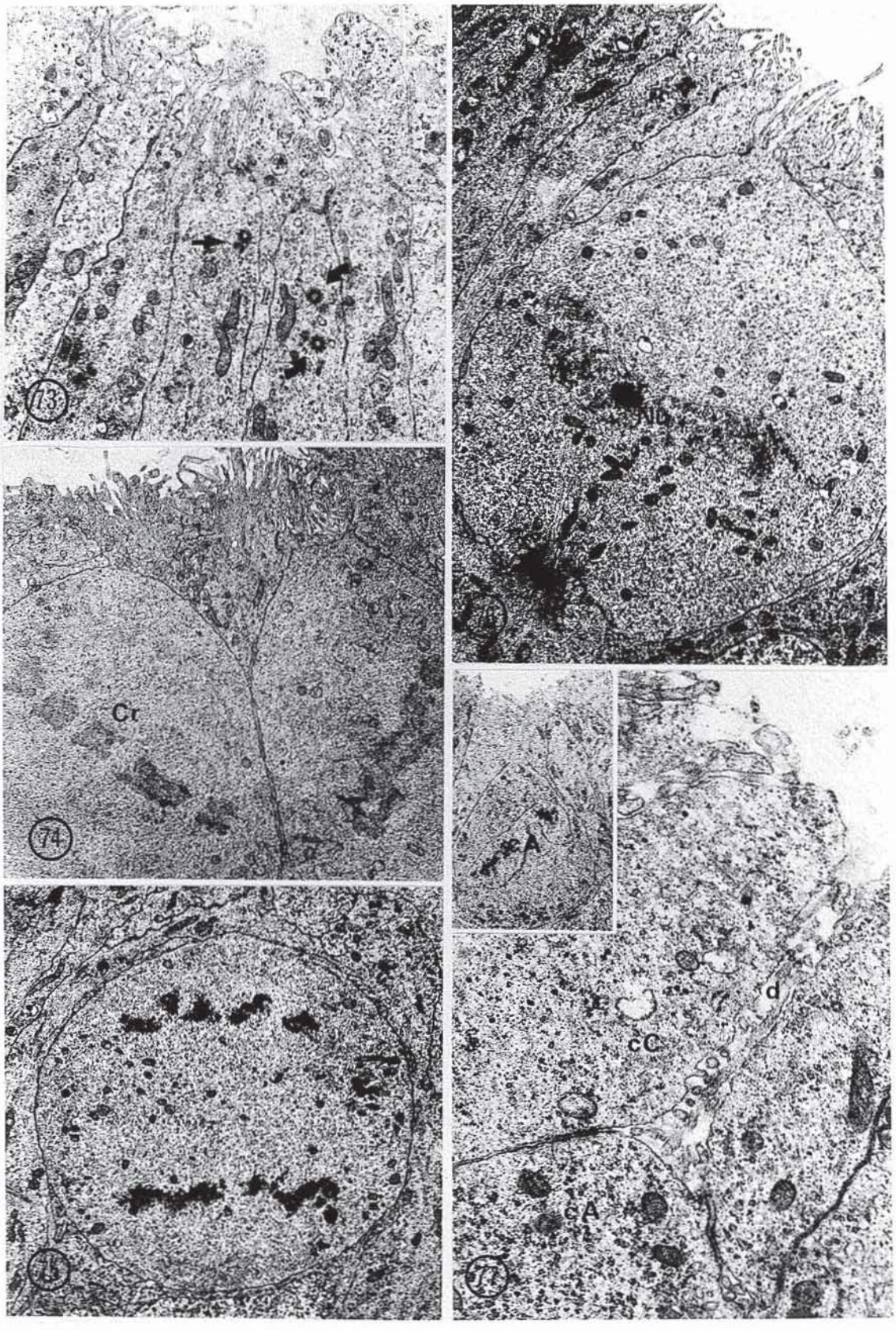
73
Cr
74
cA
d
cC
cA
77
75

Plate 18

Cell Features

Figure 78. Pinocytosis occurs at the lumenal plasma membrane (arrows). M - microvilli. Karnovsky's. 27,030 X.

Figure 79. Nuclei (Nu) and mitochondria are elongate. Microtubules arrange longitudinally. Microvilli (M) extend from the apical plasma membrane, while desmosomes (ds) connect the apico-lateral membranes. Karnovsky's. 11,670 X.

Figure 80. Re-extending cell with longitudinal microtubules (t). Karnovsky's. 23,320 X.

Figure 81. Detail of a desmosome (ds) with cross-sectional microtubules (t). Karnovsky's. 18,460 X.

Figure 82. Glycogen (GL) in a dividing cell. Karnovsky's. 26,600 X.

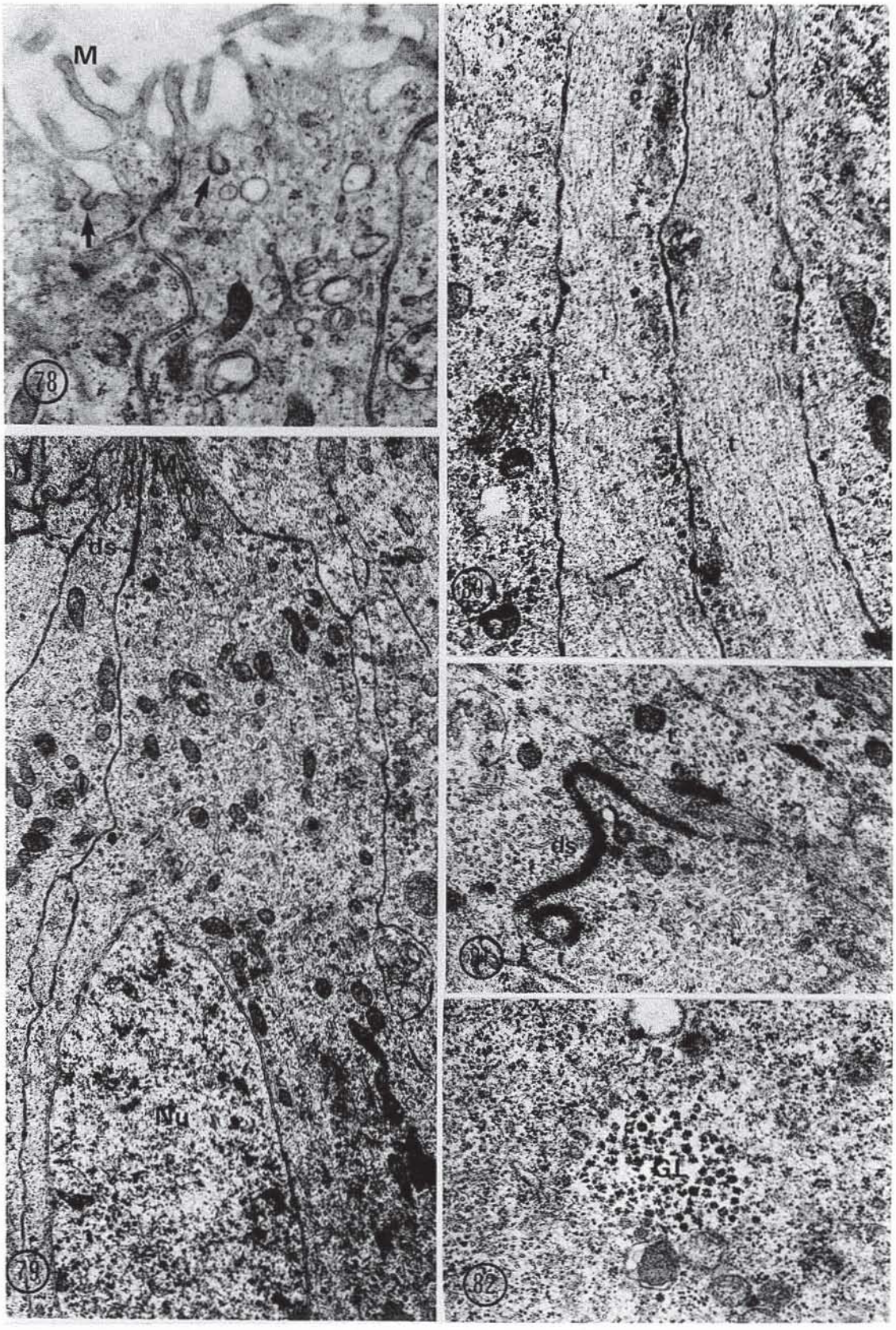
M
78
M
ds
Mu
79
t
t
80
t
ds
81
Gl
82

Plate 19

Ductule Formation

Figure 83. Semi-thin section of a gland during ductule formation showing luminal indentations (arrows) where ductules are forming. L - lumen. Microtubule fixative Toluidine blue. 2,860 X.

Figure 84. Thin cross-section of a forming ductule with microvilli (M) in the lumen and a desmosome (ds). Microtubule fixative. 20,380 X.

Figure 85. Thin section of forming ductules, showing cell A (cA) enclosed within cell B (cB) with cell C (cC) running to the luminal border, bordering the ductule (d). Long microvilli (M) of cell A extend into the ductule with only shorter microvilli lining cell C. There are numerous longitudinal microtubules and mitochondria. Desmosomes are on the apico-lateral membranes of cells A, B, and C. Pinocytotic vesicles are indicated with arrows. Microtubule fixative. 30,150 X.

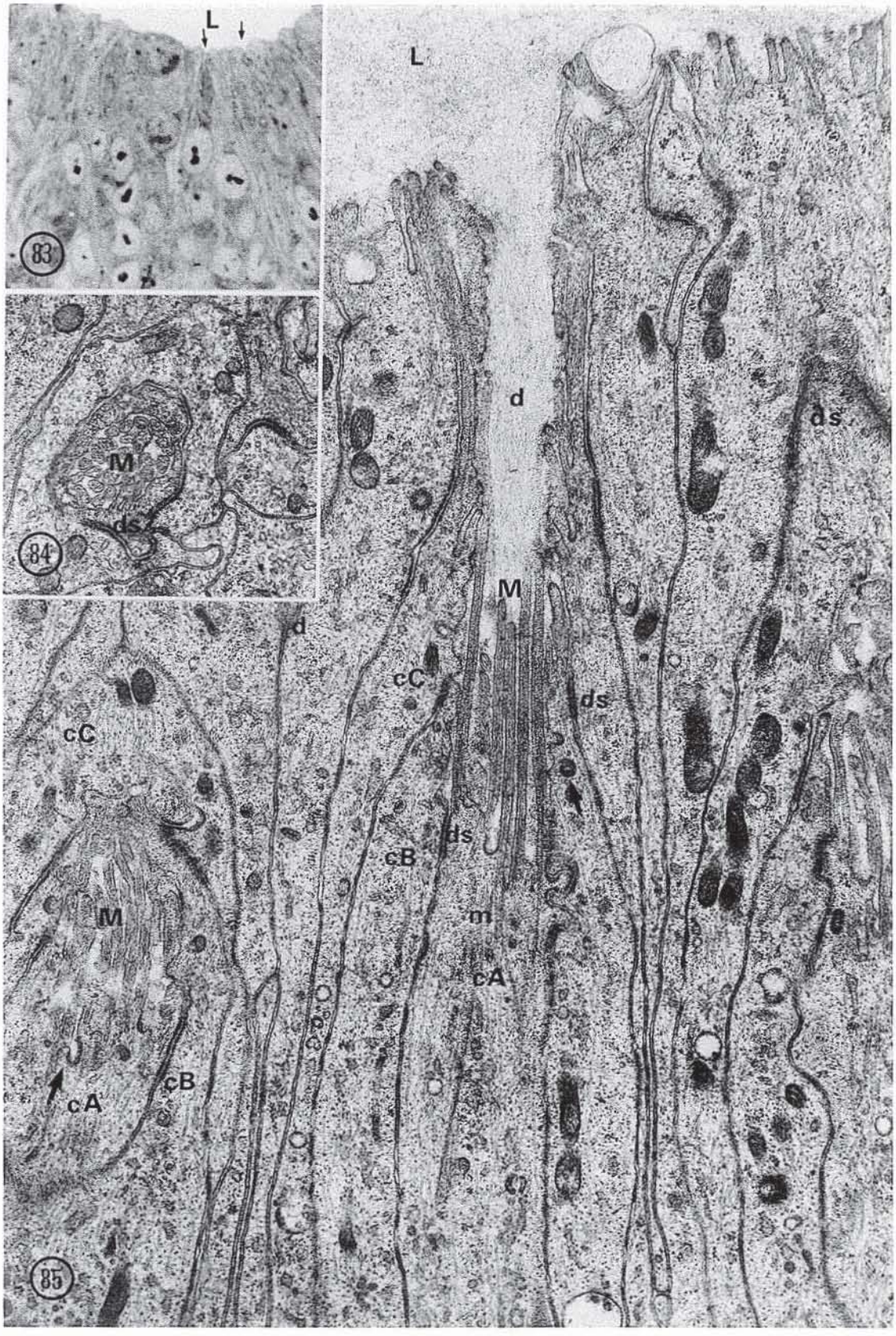
L
83
M
ds
84
d
cC
cB
cA
M
85
L
d
ds
M
cC
ds
ds
cB
m
cA

Plate 20

Early Ductules and Cell D

Figure 86. A lower magnification of a different sectional plane of Figure 85. Note how elongated cell A (cA) and cell B (cB) become as they extend towards the basal lamina. L - lumen. Microtubule fixative. 5,480 X.

Figure 87. Live Nomarski micrograph of a day 15 distal gland with evidence of ductules elongated from the lumen towards the basal lamina. 1,310 X.

Figure 88. Semi-thin section of a day 15 distal gland with arrows indicating light staining D cells. Karnovsky's Toluidine blue. 2,290 X.

Figure 89. Longitudinal section through a ductule (d) just initiating cuticulin deposition in the lumen. m - mitochondria. Microtubule fixative. 13,850 X.

Figure 90. Cross-section through ductule cells (d) with an adjacent cell D (cD). Karnovsky's. 12,940 X.

Figure 91. A cell C (cD) in longitudinal section showing electron lucid cytoplasm, containing longitudinal microtubules (t) and an adjacent cell C (cC) with the ductule in a partial plane of section. Karnovsky's. 8,510 X.

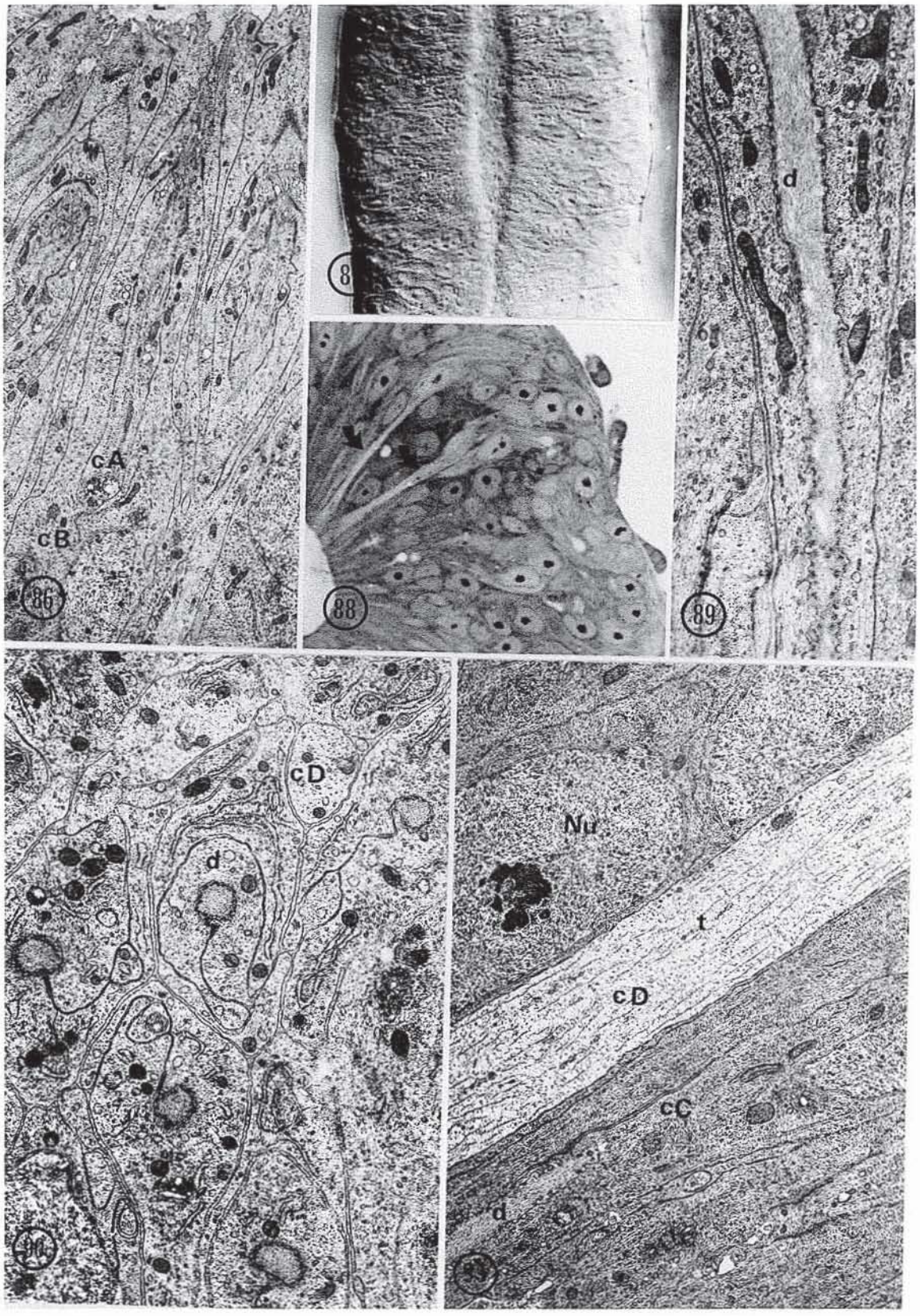
cA
cB
86
8
88
d
89
cD
d
96
Nu
t
cD
cC
d
93

Plate 21

Cell Features of Early Ductule

Figure 92. Cell A (cA) just beginning to extend away from the lumen. Right beside it, a ductule in a later stage, where cell A is within cell B (cB) surrounded by cell C (cC). ds - desmosome, t - microtubule, M - microvilli, c - centriole. Microtubule fixative. 21,400 X.

Inset. Forming ductule. Microtubule fixative. 12,860 X.

Figure 93. Slightly oblique section showing the filamentous details of the apical zonular desmosome (ds). Note how cell C (cC) engulfs cell B (cB) and cell A (cA). Note the lateral septate junctions. L - lumen, M - microvilli, m - mitochondria. Microtubule fixative. 28,270 X.

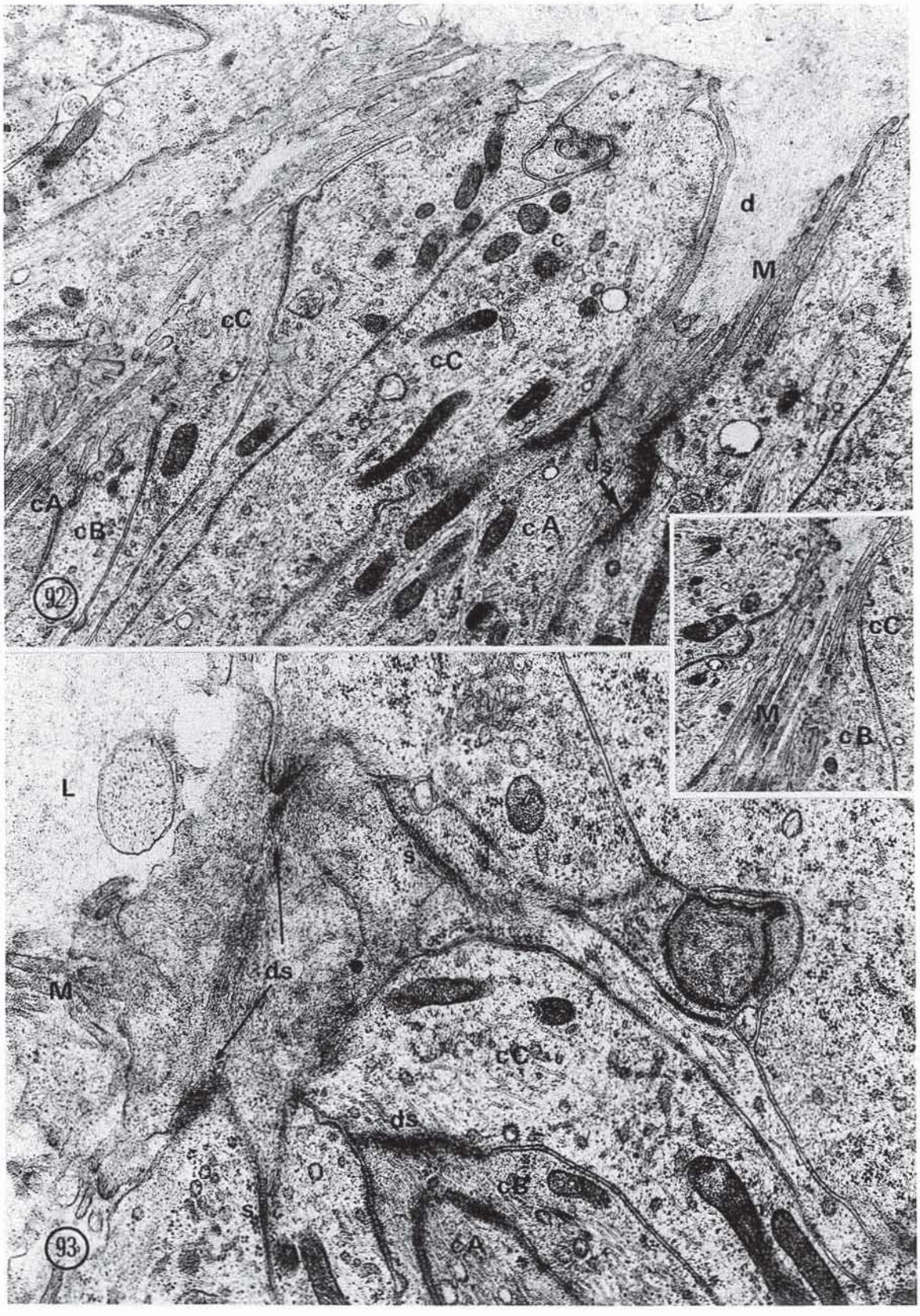
d
M
c
cC
cC
ds
cA
cB
cA
92
cC
M
cB
L
s
ds
M
cC
ds
cB
cA
93

Plate 22

Forming Ductules - Fine Structure

Figure 94. Ductule (d) just before cuticle deposition. The straight arrow indicates luminal pinocytosis in cell C (cC). Curved arrow shows branched endoplasmic reticulum. Microtubule fixative. 20,140 X.

Figure 95. High magnification cross-section of early ductule with the microvilli (M) of cell A in the lumen. Cell C (cC) surrounds the ductule adhering to itself by a desmosome (ds), with cytoplasmic microtubules (t) in cross-section. Karnovsky's. 43,840 X.

Figure 96. Ductule (d) with initial cuticular deposits (at tip of arrow). The cytoplasm contains rough endoplasmic reticulum (RER), Golgi (G), and mitochondria (m). Cell C adheres to itself, at the lumen, by a desmosome (ds) and a septate junction (s) over the rest of the area of contact. Karnovsky's. 31,580 X.

Figure 97. Ampullary part of a duct in active cuticulin deposition with a large Golgi complex (G) numerous free ribosomes and mitochondria. Curved arrow indicates a ductule in a non-ampullary plane of section. Karnovsky's. 14,550 X.

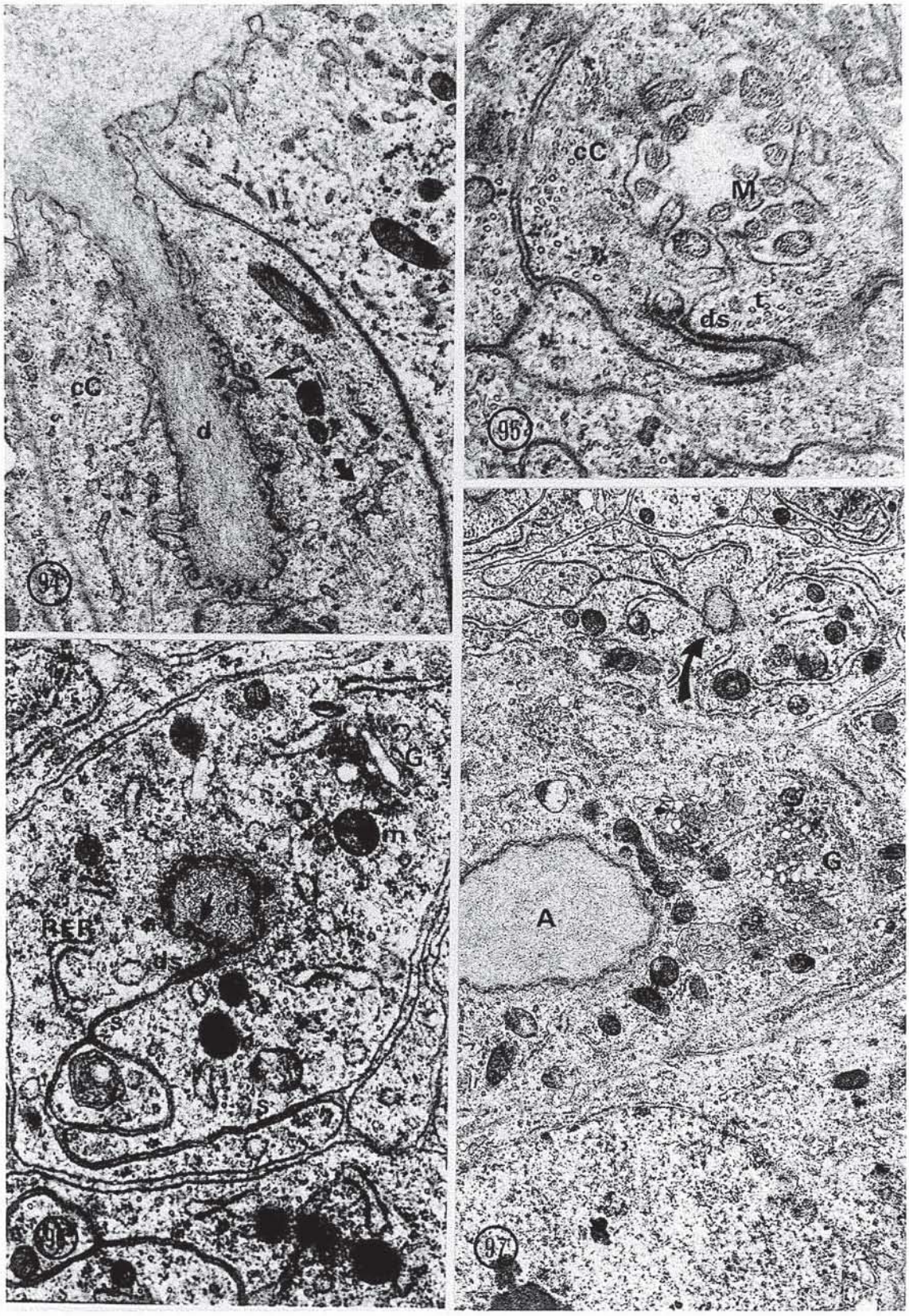
cC
d
94
cC
M
t
ds
95
G
m
REL
d
S
91
A
G
97

Plate 23

Reservoir Formation

Figure 98. Live Nomarski micrograph of a day 15 showing the developing reservoirs connected to ductules. 2,550 X.

Figure 99. Semi-thin section through a bend in the distal gland. Straight arrow - cross-section through a reservoir, curved arrow - longitudinal section through a reservoir and ampulla. Karnovsky's. Toluidine blue. 2,400 X.

Figure 100. Thin grazing section through cell A and B (cA, cB) with detail of Golgi (G). Karnovsky's. 11,750 X.

Figure 101. Longitudinal thin section through a reservoir and ampulla, showing the interrelationships between cells A, B, and C (cA, cB, cC). R - reservoir, A - ampulla, M - microvilli, Nu - nucleus. G - Golgi, BL - basal lamina. 14,930 X.

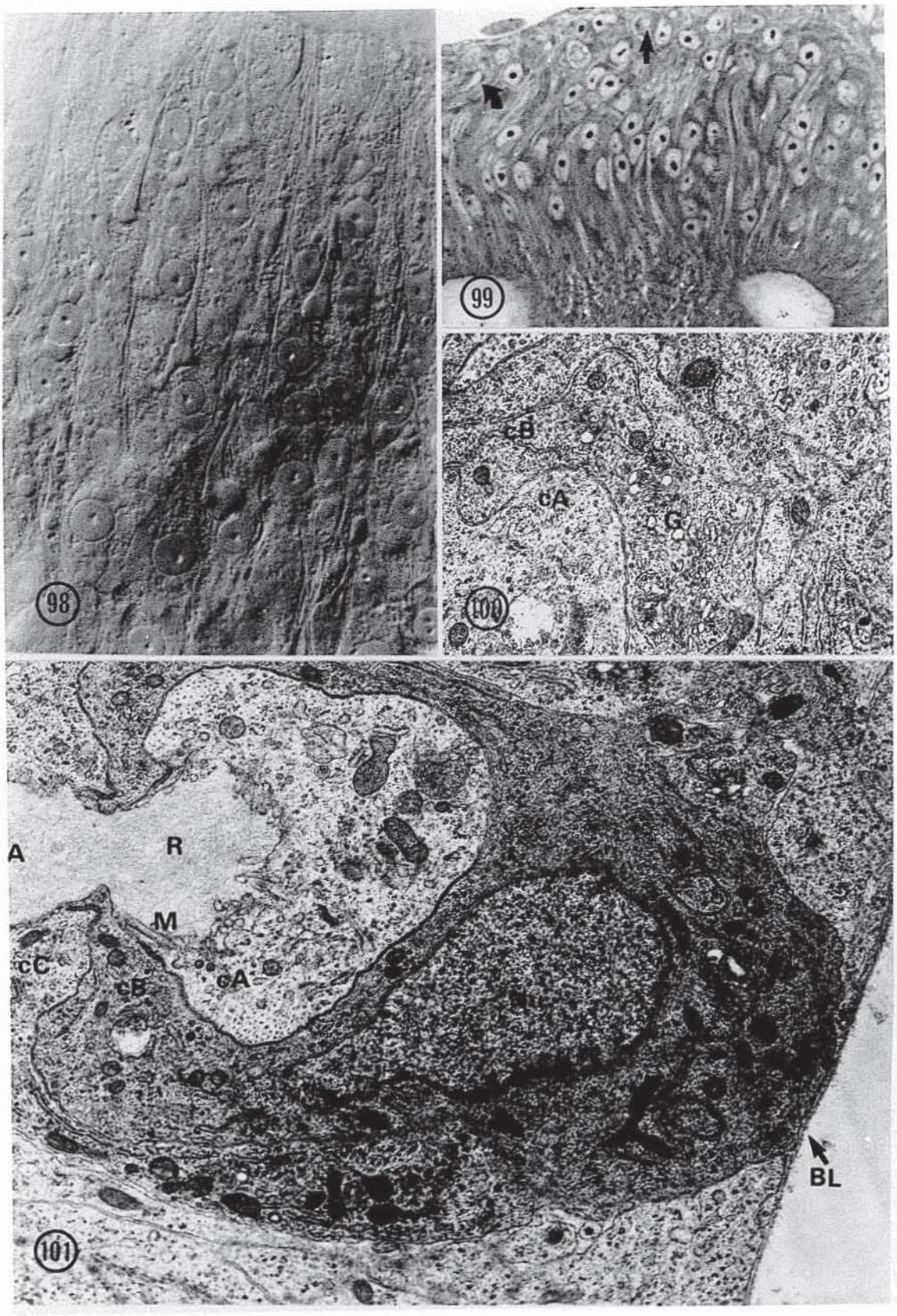
98
99
cB
cA
G
100
A
R
M
cC
cB
cA
BL
101

Plate 24

Reservoir Formation - Fine Structure

Figure 102. Cell A (cA) connects firmly within the enveloping cell B (cB) by septate junctions (s), and cell B connects to cell C (cC). Microtubules (t) in cell A and B maintain the reservoir's shape. Nu - nucleus, M - microvilli, R - reservoir, A - ampulla, ds - desmosome. Microtubule fixative. 16,400 X.

Figure 103. Basic cell features of cell C in a glancing section. Nu - nucleus, G - Golgi, RER - rough endoplasmic reticulum. Microtubule fixative. 8,250 X.

Figure 104. Cross-section through the reservoir. In this orientation, the microtubules arrange circumferentially in cell A (cA). Cell B's cytoplasm contains RER and Golgi - G. Microtubule fixative. 14,780 X.

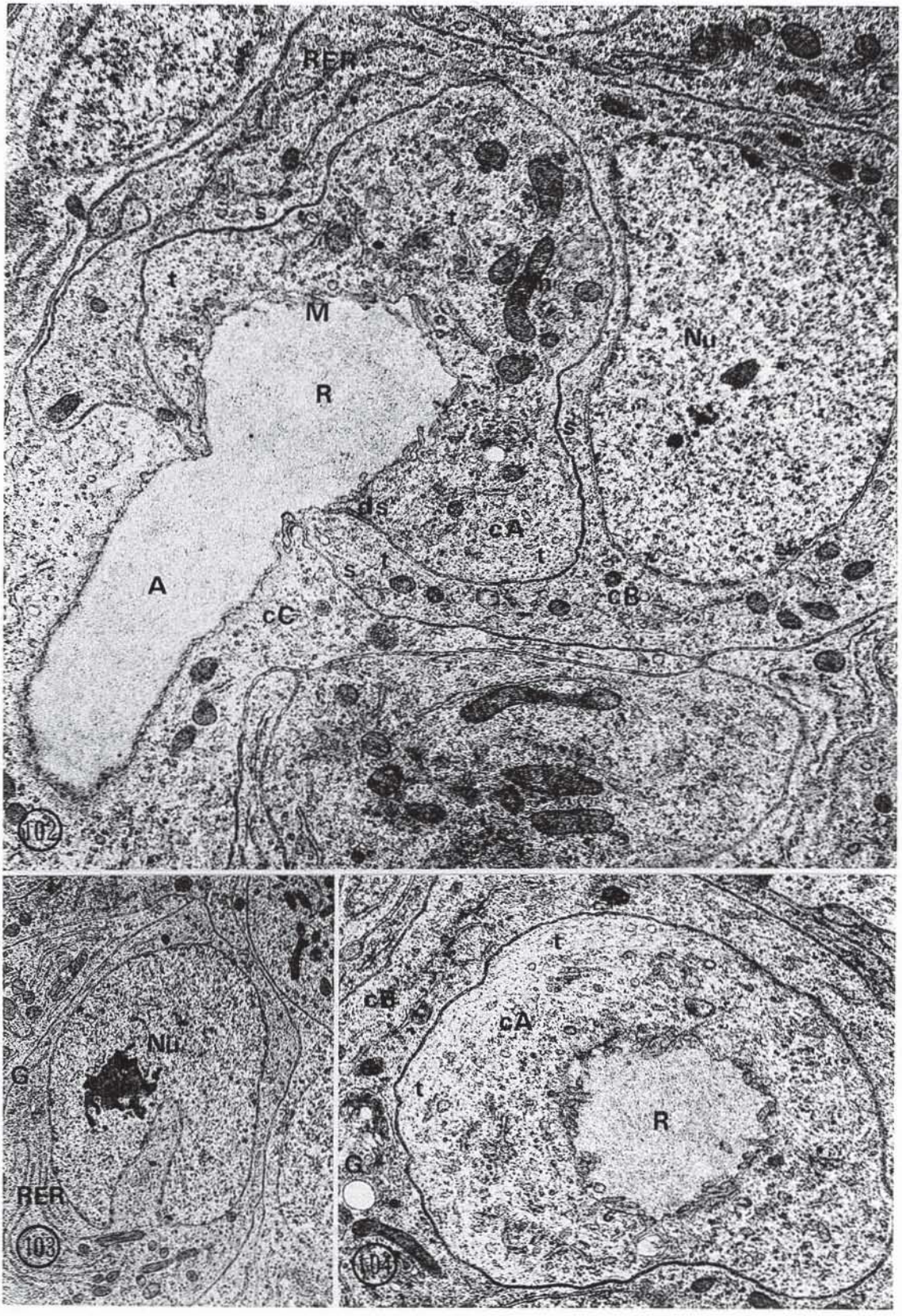
RER
s
t
t
M
R
Nu
s
ds
cA
t
s
t
A
cC
cB
102
Nu
G
RER
103
t
cB
cA
t
R
G
104

Plate 25

Reservoir Formation - Cuticle Deposition

Figure 105. Semi-thin section of a day 16 distal gland showing enlarged reservoirs and ampullae. Karnovsky's. Toluidine blue. 2,140 X.

Figure 106. Live Nomarski micrograph of day 17 reservoirs and ampullae. Arrow indicates a presumptive secretory unit, showing cell B's nucleus (on the lower left and cell A's on the upper right). 25,380 X.

Figure 107. High magnification of the junction between cells A, B and C on day 16, showing cuticulin (Ct) lining the ampulla (A), the collar adjacent to cell B (cB) and extending into the reservoir (R) past cell A (cA). s - septate junction.

Figure 108. Thin section of a day 16 reservoir, with epicuticle (arrows) being deposited as microvilli form at the plasma membrane. F - funnel, cD - cluster of four cell D's, Nu - nucleus. Karnovsky's. 7,640 X.

Figure 109. Thin section of a day 17 reservoir with well developed microvilli with epicuticle at the tips. R - reservoir, F - funnel, A - ampulla, Nu - nucleus. 6,420 X.

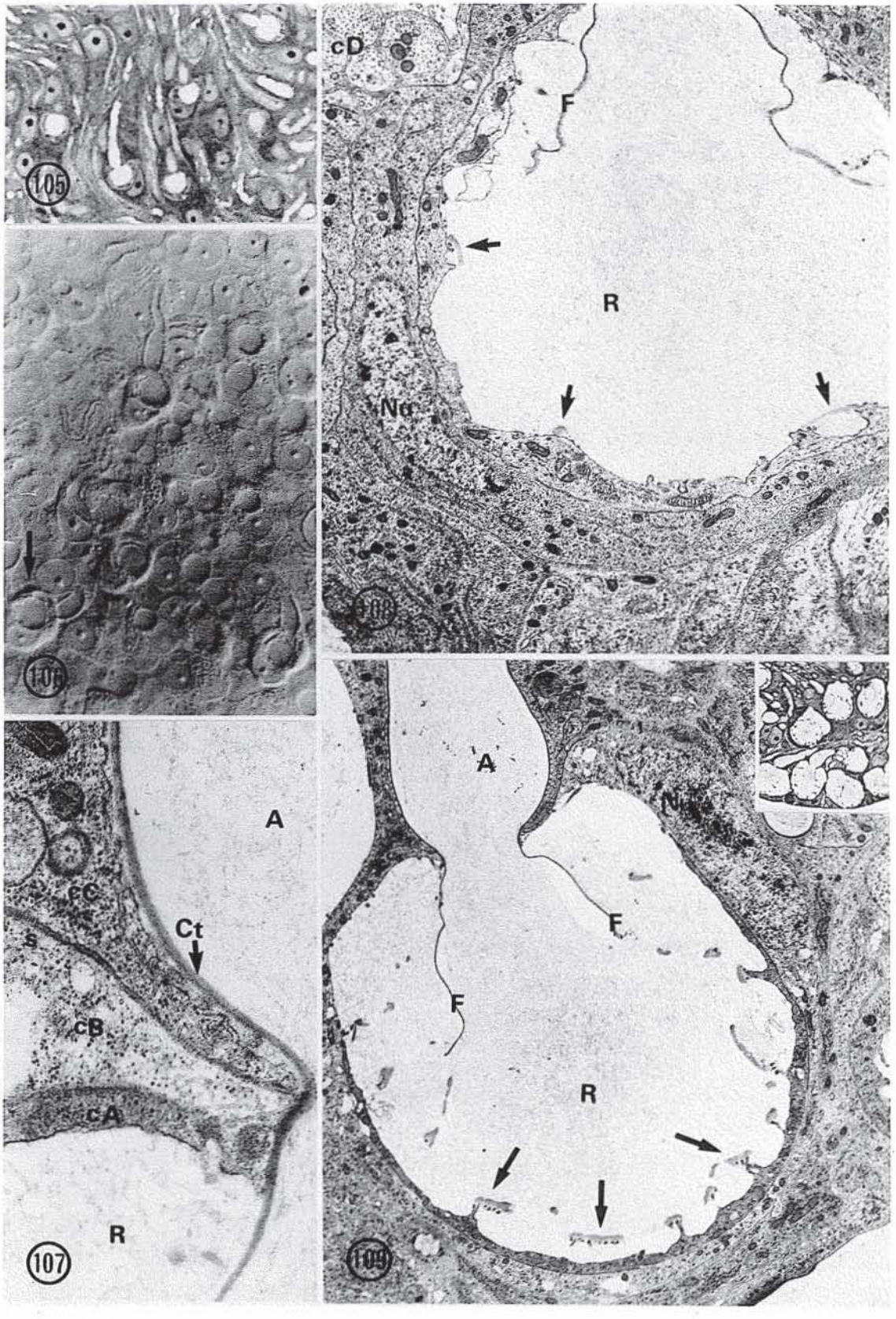
105
106
cD
F
R
Na
108
A
cC
Ct
S
cB
cA
R
107
A
N
F
F
R
109

Plate 26

End Apparatus Deposition

Figure 110. High magnification of a day 17 reservoir with epicuticle (EP) at the tips. Arrows point to vesicles in the cell A (cA) cytoplasm, releasing into the reservoir.R - reservoir, s - septate junction, cB - cell B. Karnovsky's. 15,380 X.

Inset. Semi-thin section of day 17 distal gland with long microvilli and forming end apparatus. Karnovsky's. Toluidine blue. 1,230 X.

Figure 111. Higher magnification of cell A, showing the epicuticle (EP) at the tips of filament-containing microvilli. R - reservoir, RER - rough endoplasmic reticulum. Karnovsky's. 30,540 X.

Figure 112. Grazing section through a forming end apparatus with the microvillar (M) pattern mirroring the epicuticle (EP) of the forming end apparatus. Cell A (cA) is shown extending through cell B (cB) with microtubules (t) extending through the channel. Nu - nucleus. Karnovsky's. 14,210 X.

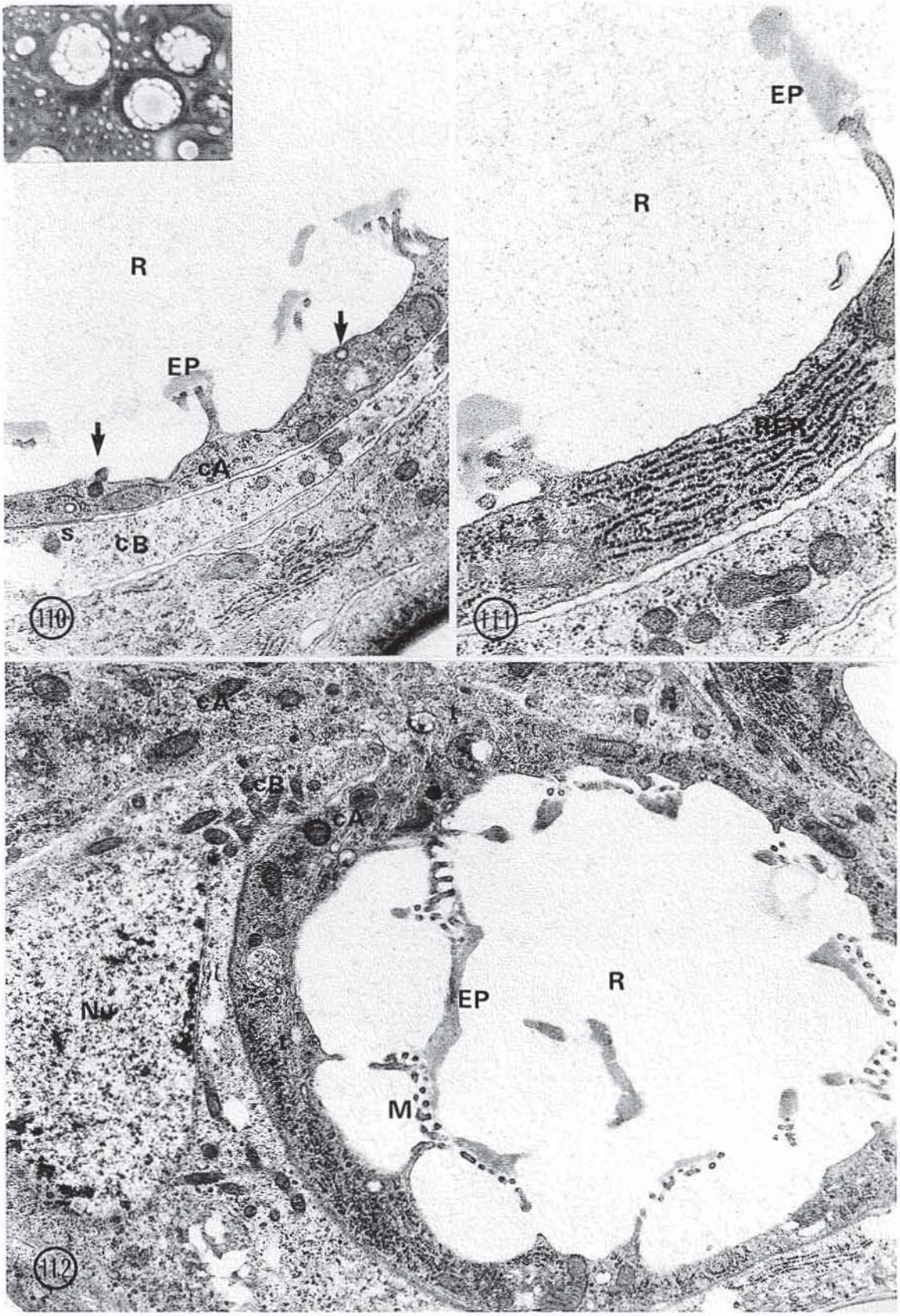
R
EP
cA
cB
S
110
EP
R
RER
111
cA
cB
cA
Nu
EP
R
M
112

Plate 27

Cell A Retraction

Figure 113. A reservoir (R) at early end apparatus deposition (day 16) with cell A's (cA) cytoplasm retracting through cell B (cB). Karnovsky's. 10,520 X.

Figure 114. High magnification of Figure 113 showing cross-sectional microtubules in the channel through cell B (cB). Cell A - cA. Karnovsky's. 16,000 X.

Figure 115. A day 17 reservoir (R) with advanced epicuticle deposition, clearly showing cell A's (cA) retraction through cell B (cB). Septate junctions (s) adhere cell A to cell B cover the full contact area, except adjacent to the microtubule (t) containing cytoplasmic channel. The rough endoplasmic reticulum in the extra-reservoir cytoplasm is vesiculated. 13,080 X.

Figure 116 and 117 Degenerating cell A within a reservoir. Karnovsky's Toluidine blue. 3,540 X and Karnovsky's 64,200 X.

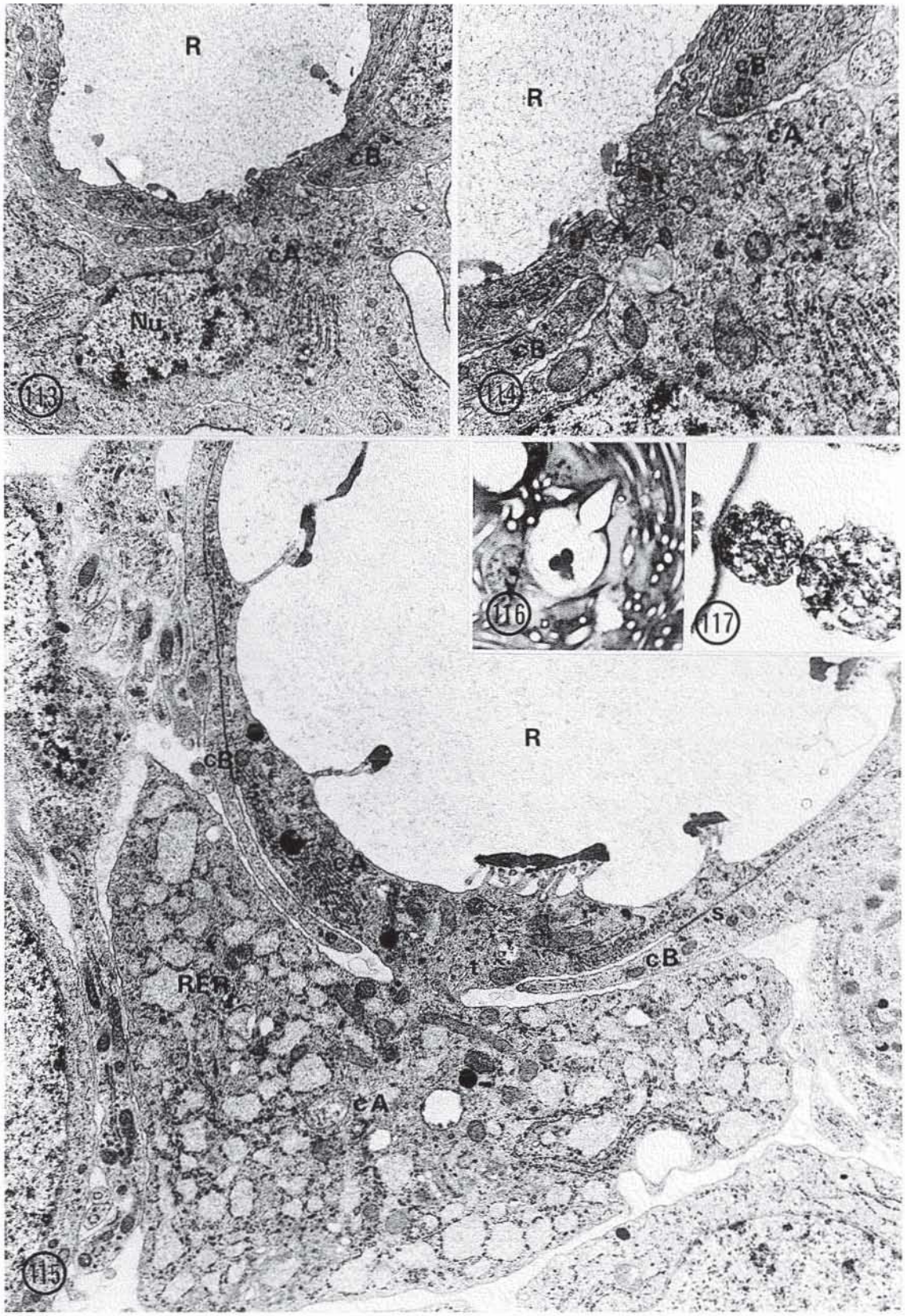
R
cB
cA
Nu
113
R
cB
cA
cB
114
116
117
R
cB
cA
RER
cA
S
cB
115

Plate 28

5th Instar Gland Secretion and Tracheoles

Figure 118 and 119. Day 21 and day 19 distal cement gland with orthochromatic secretion in reservoir. Karnovsky's.Toluidine blue. 1030 X and 2360 X.

Figure 120. Day 19 distal gland showing electron dense secretion in the reservoirs (R) ampullae (A) and ductules, with a different morphology that the adult secretion. Karnovsky's. 7,180 X.

Figure 121, 122 and Inset. Tracheoles in the distal gland (day 17, inset, day 0 adult). cD - cell D, d - ductule, Tr - trachea, T - tracheoles. Karnovsky's. 10,100 X, 16,150 X and 1,780 X respectively.

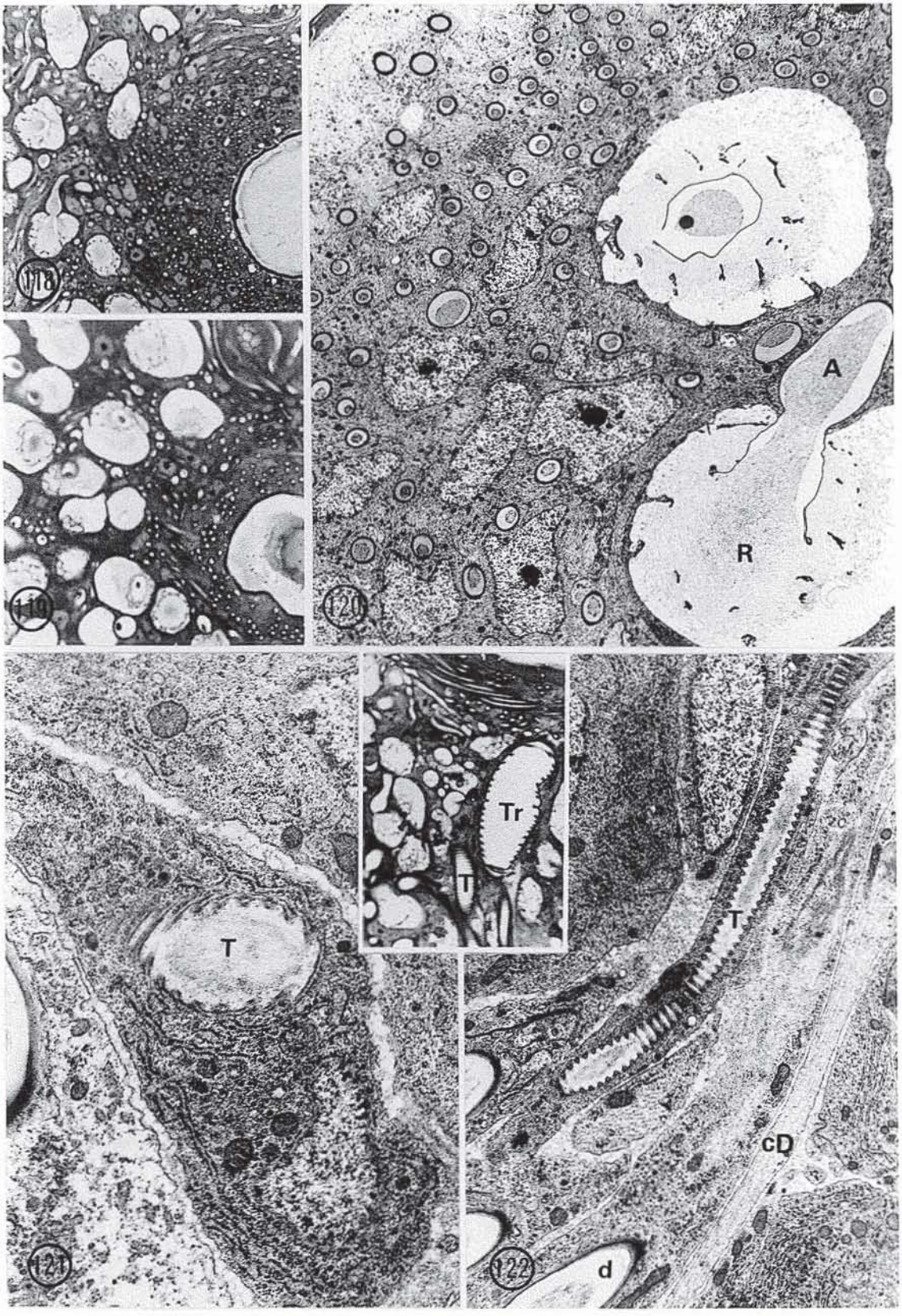
118
119
120
A
R
121
T
Tr
T
122
T
cD
d

Plate 29

Ductules and Cell D

Figure 123. Endocuticle deposition in the ampulla (A) with arrows pointing to vesicles. R - reservoir, Nu - nucleus. Karnovsky's. 12,060 X.

Figure 124, inset and 125. Cross-section of day 16 ductules showing cell D (cD) interspersed between cell C's (cC). Karnovsky's (Inset: Toluidine blue). 4,010 X, 1,760 X and 15,000 X.

Figure 126 and 127. Longitudinal sections of ductules (d) with associated cell D (cD) in day 17 ductules. Karnovsky's. (Toluidine blue). 2,320 X, 9,450 X.

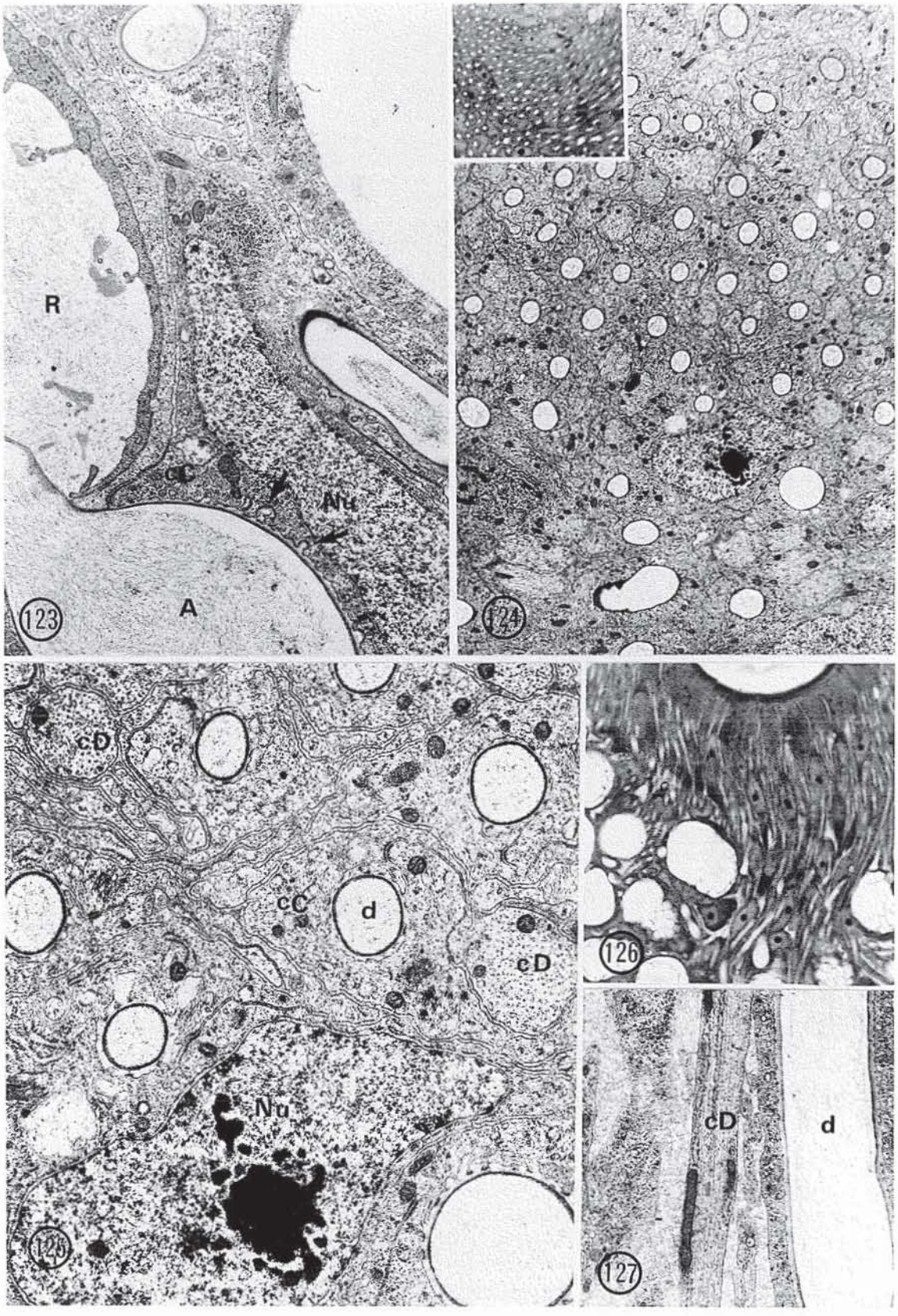
R
cC
Nu
A
123
124
cD
cC
d
cD
Nu
125
126
cD
d
127

Plate 30

Ductules and Cuticle Deposition

Figure 128. Cross-section through an unusually shaped ampulla with indicated centriole. Day 17. Karnovsky's. 14,970 X.

Figure 129. Ductules on day 18, with intercellular spaces developing between them. Karnovsky's. 7,350 X.

Figure 130. Detail of a day 19 ductule, with a nucleus (Nu) and an elaborate septate (s) junction. Karnovsky's. 14,980 X.

Figure 131. High magnification of a day 11 ampulla with indicated membrane vesicle. Karnovsky's. 20,700 X.

Figure 132. Ductules (d) in a day 20 distal gland, showing the ductule cuticle almost complete, with the cell C cytoplasm extending projections across the intercellular space. Cell D's are still observed. Karnovsky's. 15,380 X.

Inset. Semi-thick section of a day 20 distal gland, showing the developing intercellular space between the ductules. Karnovsky's. 1,850 X.

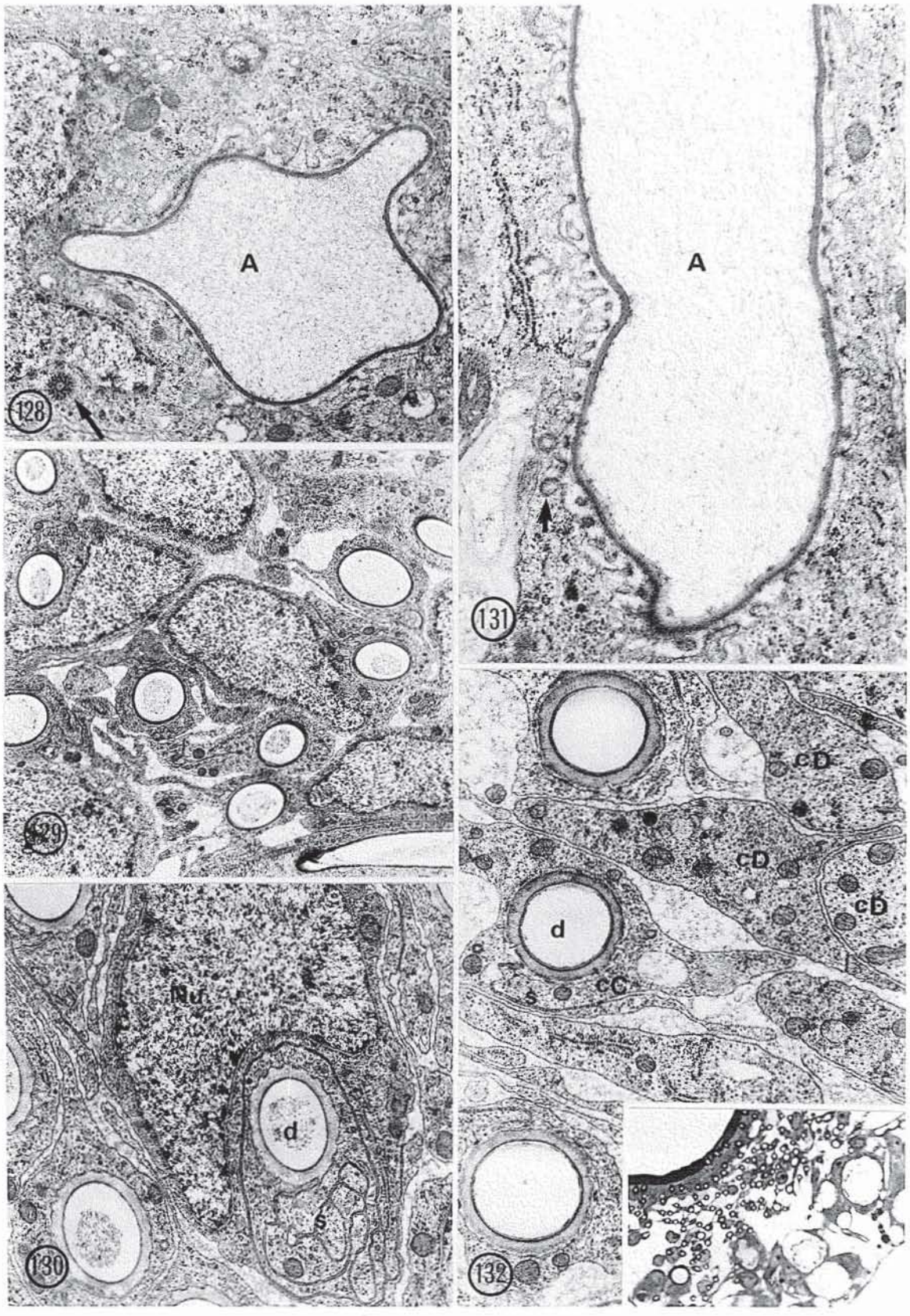
A
128
A
131
129
cD
cD
cD
d
s
cC
Nu
d
s
130
132

Plate 31

Duct Cuticle Deposition

Figure 133 and 134. Cuticulin deposition in the ductules and main duct. Arrow - vesicles. Karnovsky's. 13,590 X and 13,850 X.

Figure 135. Semi-thin section of a day 20 distal gland showing the fully formed duct cuticle. L - lumen. Karnovsky's. Toluidine blue. 2,640 X.

Figure 136 and 137. High magnification of a day 19 distal gland showing endocuticle deposition at the tips of microvilli. Ct - cuticulin, EP - inner epicuticle, EN - endocuticle, M - microvilli, cC - cell C, cE - cell E, d - ductule, L - lumen. Karnovsky's. 9,515 X and 18,460 X.

Figure 138. Day 20 duct cuticle showing the cuticulin-epicuticle layer (arrow) and the three layers of endocuticle (EN). Karnovsky's. 18,880 X.

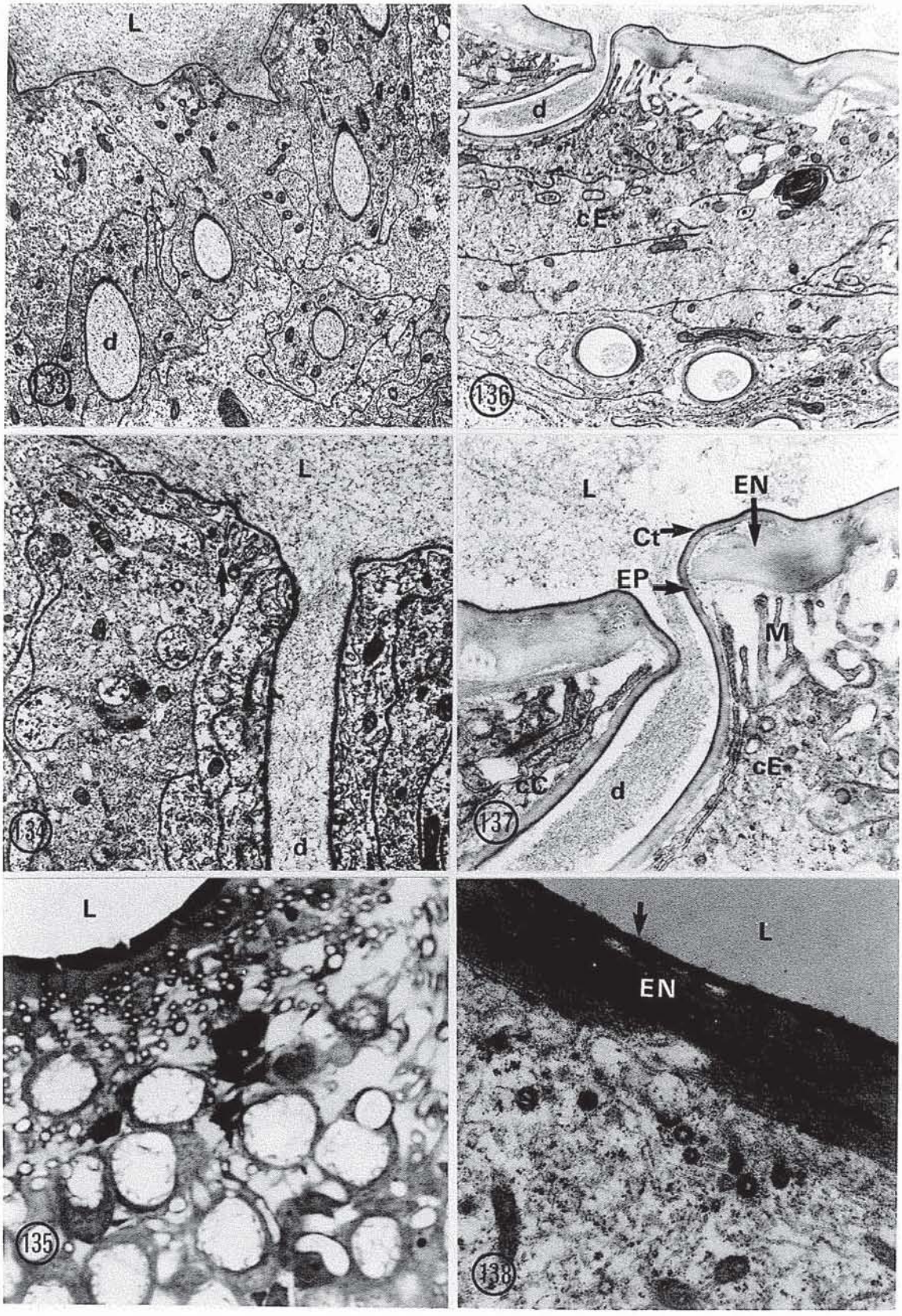
L
d
133
d
cE
136
L
d
134
L
EN
Ct
EP
M
cE
cC
d
137
L
135
EN
L
138

Plate 32

Proximal Gland

Figure 134. Semi-thin section of the transition between a proximal and distal day 20 cement gland. The distal duct cuticle (DDC) stains orthochromatically and the proximal duct cuticle (PDC) stains metachromatically. S - secretion. Karnovsky's Toluidine blue. 1,615 X.

Figure 140. Day 10 proximal gland showing the epithelial (e) layer, with a mitotic figure, and the mesothelial (ms) developing muscle layer. 2,950 X.

Figure 141. Day 17 proximal duct with the flattening epithelial layer (e) and muscle layer (ms) showing clear striations. L - lumen. Notice the muscle layer ends as the duct corrugation becomes less regular. Karnovsky's. 1,550 X.

Figure 142. Thin section of a day 10 proximal gland epithelium showing apico-lateral interdigitation of the membranes. L - lumen, G - Golgi, Nu - nucleus, t - tubules. Karnovsky's. 6,090 X.

Figure 143. Semi-thin section of a day 20 proximal gland showing well developed corrugated cuticle and epithelial (e) and muscle (ms) layer. Karnovsky's Toluidine blue. 1,615 X.

Figure 144. Zonular desmosomes (ds) at the lumen of a day 11 epithelial cell in the proximal gland. M - microvilli. Karnovsky's. 18,275 X.

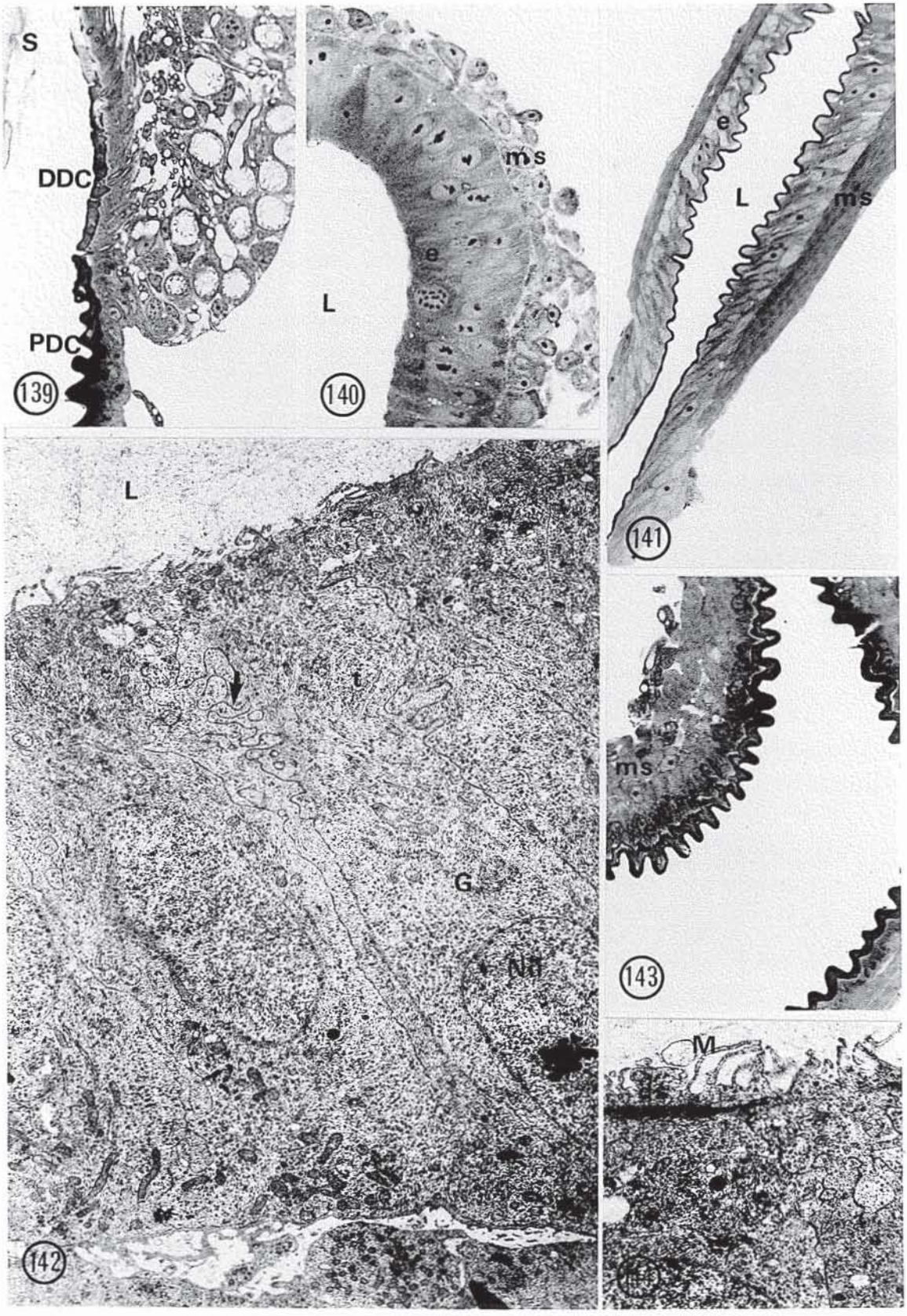
S
DDC
PDC
139
ms
e
L
140
e
L
ms
141
L
t
G
NT
142
ms
143
M

Plate 33

Proximal Gland - Desmosomes

Figure 145 and 146. Day 11 and day 8 epithelial layer with microtubules arranged longitudinally, with desmosomes (ds) along the lateral and apical membrane surfaces. The filaments of the apical desmosomes run parallel to the lumen. M - microvilli. Karnovsky's. 9,430 X and 34,560 X.

Figure 147 and 148. Epithelial (e) and mesothelial (ms) cell layers with intercellular space (IS) between them and between mesothelial cells. Mesothelial cells connect to the epithelium via macular desmosomes (ds). Nu - nucleus, BL - basal lamina. Karnovsky's. 5,220 X and 11,120 X.

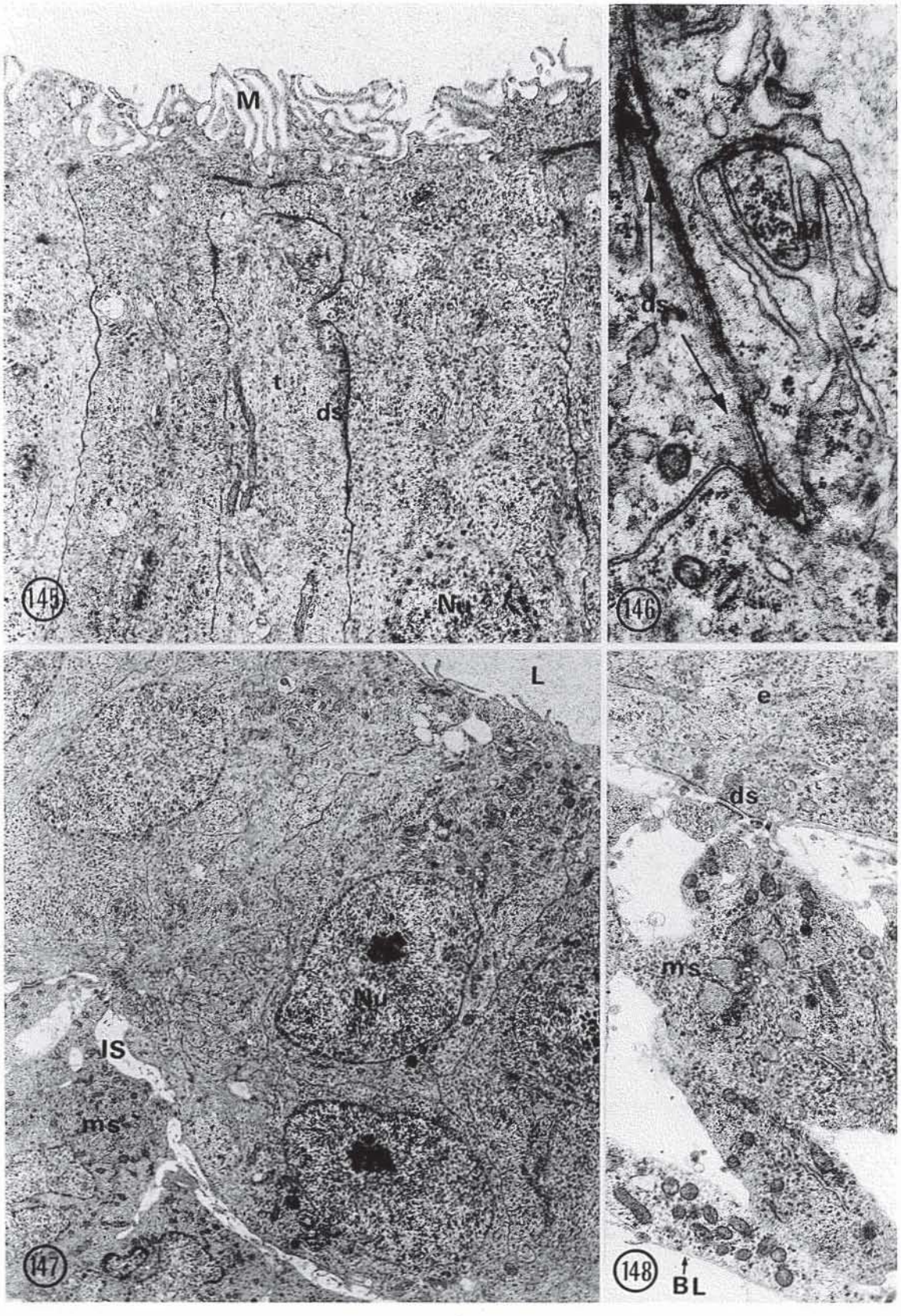
M
t
ds
Nu
145
ds
146
L
Nu
IS
ms
147
e
ds
ms
148
BL

Plate 34

Desmosomes - Fine Structure

Figure 149. Mesothelium of a day 14 gland showing flocculent material in the intercellular space (IS). NR - nerve, ds - desmosome, m - mitochondria. Microtubule fixative. 22,360 X.

Figure 150. Mesothelium (ms) of a day 11 proximal gland showing parallel microtubules (t) and macular desmosomes (arrows). Nu - nucleus, e - epithelium. Karnovsky's. 7,660 X.

Figure 151. High magnification of Figure 150 showing the microtubules (t) elongate mitochondria (m), desmosomes (ds) and centriole (c). Karnovsky's. 17,080 X.

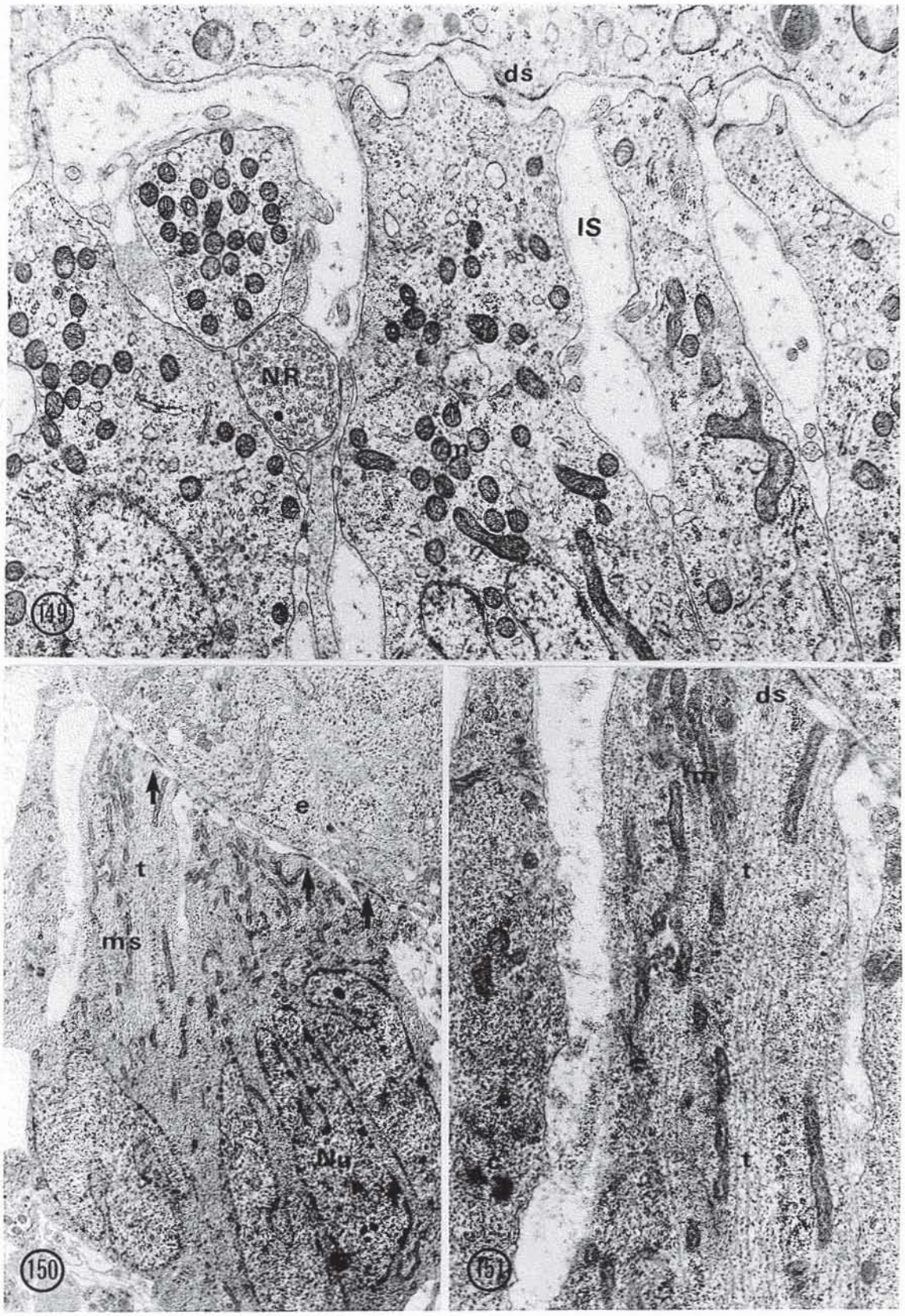
ds
IS
NR
m
149
e
t
ms
Nu
150
ds
m
t
t
151